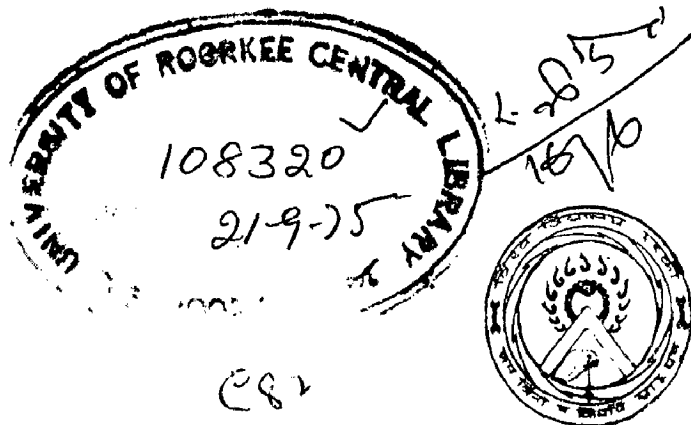


DESIGN OF HYDRAULIC STRUCTURES  
ON  
NON-HOMOGENEOUS FOUNDATIONS

A DISSERTATION  
submitted in partial fulfilment of the  
requirements for the Degree  
of  
MASTER OF ENGINEERING  
in  
WATER RESOURCES DEVELOPMENT

By

H. C. HEMANTHA KUMAR



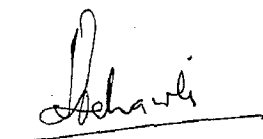
WATER RESOURCES DEVELOPMENT TRAINING CENTRE  
UNIVERSITY OF ROORKEE  
ROORKEE U.P. (INDIA)

1975

C E R T I F I C A T E

Certified that the dissertation entitled " Design of Hydraulic Structures on Non-homogeneous Foundations" which is being submitted by Sri H.C.Hemantha Kumar in partial fulfilment of the requirements for award of the Degree of Master of Engineering in Water Resources Development of University of Roorkee is a record of the Candidate's own work carried out by him under my supervision and guidance. The matter embodied in this dissertation has not been submitted for the award of any other degree or diploma.

This is further to certify that Sri H.C.Hemantha Kumar has worked for a period of 8 months since October, 1974 to May, 1975 staying at Roorkee, in the preparation of this dissertation.



Roorkee  
May, 29, 1975.

( A.S. CHAWLA )  
Research Officer  
U.P. Irrigation Research Institute  
Roorkee.

## A C K N O W L E D G E M E N T S

The author gratefully acknowledges the valuable guidance offered and the encouragement given by Dr. A.S.Chawla, Research Officer, Uttar Pradesh Irrigation Research Institute, Roorkee, under whose supervision and guidance the present dissertation has been prepared.

The author is grateful to Prof. Prahlad Das, Professor and Head, W.R.D.T.C., University of Roorkee, Roorkee for extending various facilities for the preparation of this work.

Grateful thanks are also due to various authors and agencies whose literature has been of help in bringing out this review.

*H. C. Hemantha Kumar*  
H.C.Hemantha Kumar

# C O N T E N T S

CHAPTER		PAGE
I	INTRODUCTION	1
	1.1 Historical background	1
II	PERVIOUS MEDIUM OF FINITE DEPTH	4
	2.1 General	4
	2.2 Stepped apron with a cutoff	5
	2.2.1 Calculation of uplift pressures	9
	2.2.2 Exit gradient	10
	2.2.3 Charts	11
	2.2.4 Mutual Interference of piles	17
	2.2.5 Safety against piping failures	18
	2.3 Flat Apron (without a step) with an Intermediate cutoff	18
	2.4 Effect of Impermeable layer on uplift pressures	22
	2.5 Flat apron with Downstream Cutoff under Scoured conditions	26
	2.5.1 Uplift pressures	26
	2.5.2 Exit gradient	31
3		
III	STRATIFIED FOUNDATIONS	35
	3.1 Floor on two strata of equal thickness	36
	3.1.1 Uplift pressures	39
	3.1.2 Seepage discharge	40
	3.2 Cutoff in two strata of equal thickness	41
	3.3 Floor on two strata of unequal thickness	44
	3.4 Floor with end cut off on two strata	47
	3.5 Floor with intermediate cutoff on two strata (of equal thickness)	59
	3.6 Two layered media (Foundation) with a cut off at upstream end	61
	3.7 Two layered media (Foundation) with two cut offs	65
IV	ANISOTROPIC FOUNDATION	68
	4.1 Equations of motion in homogeneous anisotropic medium	72
	4.2 Floor with a cut off	78
	4.3 Floor with a cutoff founded on anisotro- pic soil of finite depth	92
	4.4 Experimental studies	97

## Contents (Contd..)

V	NUMERICAL METHODS FOR SOLUTION OF NON HOMOGENEOUS FOUNDATIONS	105
5.1	General	105
5.2	Solution of Anisotropic Seepage by Finite difference method	105
5.2.1	Outline of the method	107
5.2.2	Application	108
5.3	Solution of Anisotropic seepage by Finite element method	109
5.3.1	Theory of flow in Anisotropic media	109
5.3.2	Two dimensional seepage in Anisotropic medium	111
5.3.3	Application	112
VI	CONCLUSIONS	115
	APPENDIX I	118
	APPENDIX II	121
	REFERENCES	127

## NOTATIONS

- a =  $\tanh^2 \frac{\pi b}{2T}$  = A constant in  $\xi$  plane
- b = Width (or half width) of floor
- $b_1$  and  $b_2$  = Widths of floor at upstream and downstream of cut off.
- $b'_1$  and  $b'_2$  = Widths of floor at upstream and downstream of cutoff in transformed plane.
- $b'$  = Distance between two cut offs.
- C = Correction factor for mutual interference of piles
- d = Depth of cut off
- $d_1$  = Depth of cut off measured along its upstream face
- $d_2$  = Downstream scour depth
- $d'$  = Depth of cut off in transformed plane
- $G_E$  = Exit gradient
- g = Gravitational constant
- H = Difference in (Head) upstream and downstream water levels.
- h = The head at any point
- $h_0, h_1, h_2, h_3, h_4$  = Heads at nodes 0, 1, 2, 3, 4
- {grad H} = Head gradient (vector) in original and changed  
{grad H'} (new) principal axes of anisotropy respectively
- K and K' = Complete elliptic integrals

$[K]$  and  $[K']$  = Permeability matrices in original and new principal axes of anisotropy respectively

$\left. \begin{array}{l} K_{xx}, K_{yy} \\ k_{x1}, k_{y1} \\ k_x, k_y \end{array} \right\}$  = Seepage coefficients in the directions of principal axes of anisotropy

$K_{x'x'}, K_{y'y'}$  = Seepage coefficients in new principal axes of anisotropy

$k$  = Seepage coefficient

$k_1, k_2$  = Coefficients of permeability in top and bottom layers respectively.

$L_1$  and  $L_2$  = Lengths of floor in semi-infinite plane

$M$  =  $T/\pi$  = Transformation parameter

$M' = \frac{k_1 H}{2T}$  = Transformation parameter

$m = d/b$  = Ratio of depth of central cut off to half width of floor.

$m'$  and  $m$  = Moduli

$N$  = Constant of Integration.

$n = T/b$  = Ratio of depth of pervious medium to half width of floor.

$P$  = Argument of  $\text{Sn}^{-1}(P, m)$

$p$  = Pressure at any point on seepage fluid

$q$  = Discharge (seepage) per unit length.

$\text{Sn}^{-1}(P, m)$  = Elliptic integral of I kind

$\text{Sn}(U, m) = P$  = Elliptic function

- $s$  = Length of seepage segment  
 $T$  = Depth of pervious medium  
 $T_1, T_2$  = Depths of upper and lower stratum (pervious) respectively.  
 $t$  = Auxiliary semi-infinite plane.  
 $U$  ( $=\text{Sn}^{-1}(P.m)$ ) = Inverse of Elliptic function  $\text{Sn}(U,m)=P$   
 $u$  and  $v$  = Components of fictitious dimensionless velocity  
 $v_x, v_y, v_z$  = Seepage velocities in principal directions of anisotropy.  
 $\{v\}, \{v'\}$  = Velocity vectors in original and new principal directions (axes) of anisotropy.  
 $w = (\phi + i\psi)$  = Rectangular flow fields.  
 $w' = (\phi' + i\psi')$   
 $w_1 = (\phi_1 + i\psi_1)$  = Complex potentials in upper and lower stratum  
 $w_2 = (\phi_2 + i\psi_2)$  respectively  
 $X, Y$  = Horizontal and vertical coordinate axes  
 $x, y, z$  = Spatial coordinates  
 $\bar{x}, \bar{y}, \bar{z}$  = Transformed coordinate axes in anisotropic medium.  
 $x', y', z'$  = New axes of principal directions of anisotropy  
 $\left. \begin{array}{l} x_1, y_1 \text{ or } \\ \mu, \nu \end{array} \right\}$  = Axes along principal directions of anisotropy  
 $z$  = Complex potential plane  
 $\alpha$  = Angle between  $\mu$  axis (principal axis of anisotropy) and horizontal.  
 $\alpha_1, \alpha_2$  = Transformation parameters.



- $\beta$  = Angle between transformed cut off with  $\mu$  axis.
- $\gamma$  = Angle between downstream floor and cut off in fictitious  $\mu - v$  plane
- $\delta$  = Angle between transformed straight line (floor line) to  $\mu$  axis.
- $\alpha_1$  and  $\alpha_2$  = Transformation parameters
- $\phi$  = Velocity potential (=  $kh\phi$ )
- $\phi_1, \phi_2$  = Velocity potentials in upper and lower stratum respectively,
- $\phi_x, \phi_D, \phi_B$  = Potentials under the floor and top of cut off.
- $\psi, \psi_1, \psi_2$  = Stream functions
- $\epsilon = \frac{1}{\pi} \tan^{-1} \sqrt{k_2/k_1}$  = Parameter depending on permeability coefficients of upper and lower stratum.
- $\rho = \sqrt{k_1/k_2}$  = Square root of ratio of permeability coefficients of upper and lower stratum
- $\mu = -\log m'$  = Negative logarithm of complementary modulus.
- $\lambda = v^2 = k_{y1} / k_{x1}$  = Ratio of permeability coefficients of in principal directions of anisotropy
- $\zeta$  = Auxiliary semi infinite plane.
- $\pi$  = Constant.

-----

## S Y N O P S I S

Approximate or closed - form solutions are available for the problem of seepage below the hydraulic structures founded on homogeneous and isotropic medium with various boundary conditions. But mostly the foundation met with below hydraulic structure is rarely homogeneous and isotropic. Anisotropy , stratification and non homogeneity to some degree or the other are common characters of foundation below hydraulic structures . The occurrence of pervious foundations of finite depth is also a common feature.

In this dissertation an attempt has been made to review critically the effect of (1) finite depth of pervious medium (2) stratification (3) Anisotropy and (4) Non-homogeneity on the uplift pressures below the structure, exit gradient and seepage discharges.

The effect of finite depth of pervious medium on uplift pressures (1) below the floor (2) at junction of floor<sup>and</sup> cut off and (3) at tip of cut off has been reviewed. Also the effect of downstream scour depth on uplift pressures and exit gradient in the case of an apron (floor) with downstream end cut off has been studied .

In the case of structure on two strata of equal thickness and of different permeabilities, general formulae are given based on solution obtained by Polubarinova-Kochina, to calculate uplift pressures below the floor and also to find seepage discharge.

An attempt has also been made to study the effect of anisotropy of foundation soil (with principal directions of permeability not coinciding with coordinate axis of physical plane) on the pressures (1) at junction of cut off and floor and (2) at tip of cutoff, in the case of a floor with a downstream end cut off. A vertical cutoff in an anisotropic medium, will, after suitable transformation become an inclined one in the transformed plane. The effect of both finite depth of pervious medium and the depth of inclined cut off on pressures at tip of cut off and exit gradient, in the case of a stepped floor, has been briefly reviewed.

Finally, the versatility and wide range of applicability of finite element method for solution of seepage in Non-homogeneous foundations has been reviewed.

# CHAPTER I

## INTRODUCTION

### 1.1 HISTORICAL BACKGROUND

Design of Hydraulic structure requires testing their stability against forces due to surface flow and against forces caused by seepage water. The water seeps under the foundations of such structures and exerts pressures on the bottom and tends to wash away the soil under it. The structure has to be made heavy enough to withstand the uplift pressures and the value of the exit gradient of the first streamline has to be kept within safe value by providing end cutoff.

The application of conformal mapping to the solution of confined flow below the foundations of hydraulic structures was for the first time indicated by Pavlovsky (14) and Khosla(7). Based on conformal transformation, general solutions for the various boundaries have been given by Muskat (12), Harr (6) and Pollubarinova-Kochina (15) and Arvin and Numerov (3). These solutions are applicable for the seepage below hydraulic structures founded on homogeneous and isotropic permeable soil with various boundary conditions. In practice, the homogeneous and isotropic soil extending upto infinite depth is seldom encountered. The homogeneous permeable soil may be underlain by a homogeneous stratum of hydraulic conductivity higher or smaller than that of upper stratum. On the other hand, the hydraulic structure may be underlain by homogeneous but anisotropic stratum extending upto finite or infinite depth.

The solutions of seepage below hydraulic structures founded on homogeneous isotropic soil extending upto finite depth and underlain by impermeable or highly permeable layer were obtained by Pavlovskii (14) . Kulandaiswamy (8) and Muthukumaran (13) have prepared design charts for determining exit gradient and uplift pressures below the foundation of the structure founded on soil underlain by an impervious layer.

The solution of the seepage below structures with a flat bottom founded on two layers of equal thickness is given by polubarinova - Kochina (15) and that for two layers of unequal thickness has been obtained by Lenau C.W. (9). The uplift pressures below flat floor with end cut off founded on two layers, upper layer being of higher permeability has been studied by Alamsingh and Punmia (1). The effect of higher permeability of lower layer has been determined by Sharma et. al. (22). They have combined analytical and experimental results to provide design curves for determining exit gradient and uplift pressures, covering the complete range of the values of  $k_2/k_1$  from 0 to infinity.

The effect of anisotropic media on the uplift pressures has been studied experimentally by P.V.Rao (19), Alamsingh and Punmia (2) and by Punmia and Patwa (18).

In the present dissertation an attempt has been made to study the effect of non homogeneity of the foundation on the stability of the structures. The cases with the following boundary conditions have been reviewed critically.

- (1) Hydraulic structures founded on permeable soil of finite depth underlain by impermeable or very pervious layer (Chapter II)
- (2) Structures founded on stratified foundations (Chapter III)
- (3) Structures founded on homogeneous but anisotropic soil (Chapter IV)
- (4) Application of Numerical methods for the solution of problem of seepage below hydraulic structures founded on nonhomogeneous soil (Chapter V).

## C H A P T E R    I I

### P E R V I O U S    F O U N D A T I O N    O F    F I N I T E    D E P T H

#### 2.1 GENERAL

The solution of seepage below hydraulic structure founded on finite depth of permeable soil could be obtained by conformal mapping, approximate methods such as method of fragment, or by experimental methods. Pavlovskii (14) was the first to treat the problem of seepage as a problem of mathematical physics and used the method of conformal transformation for its solution. He obtained the solution of seepage below a flat apron with a central cut off on limited depth of pervious foundation. Muskat (12) analysed the case of flat floor with sheet piling anywhere on finite depth of permeable soil. Pollubarinova. Kochina(15) gave analytical solutions by the method of conformal mapping for seepage below flat bottomed structures with single and two cut offs founded on permeable foundation of finite depth. Chugaev (4) while finding a method of determining the underground profile of a structure which is safe in regard to percolation introduced a method called the "method of resistive coefficients" (method of fragments) where in the underground profile was divided into separate elements resistive coefficient for each separate element determined, and hydraulic head distributed in proportion to these

coefficients. The uplift diagram could thus be drawn. The method is suitable for any complicated weir profile with number of cut-offs on pervious foundations of finite depth.

## 2.2. STEPPED APRON WITH A CUT OFF

The general case of a stepped apron with a cut off founded on pervious foundation of finite depth has been dealt by Sri MuthuKumaran (13). He has given the design procedure and provided charts for determining the exit gradients and uplift pressures at salient points of weir profile.

The weir profile is shown in Fig. 2.1. An impervious floor AECB of length  $b_1 + b_2$  located on a permeable soil of stratum depth  $T$  has been considered. The floor has a step of depth,  $d_2$  at E and a sheet pile of depth  $(d_1 - d_2)$  at the step. The downstream pervious bed is at the same level as the down stream impervious bed. The differential equation governing seepage phenomenon is

$$\frac{\partial^2 \phi}{\partial x^2} + \frac{\partial^2 \phi}{\partial y^2} = 0 \quad \dots(2.1)$$

where  $\phi$  = velocity potential equivalent to 'kh',

$h$  = the head,  $k$ =the coefficient of percolation, and  $x$  and  $y$  are spatial coordinates.

The foundation profile AEDCB forms the inner boundary of flow and represents streamline  $\Psi = 0$ , in which  $\Psi$  = stream





function. The lower impervious boundary FHG represents the streamline  $\Psi = q$ , where  $q$  = the total discharge per unit width percolating through the foundation. Along the boundary AF at the upstream bed level potential  $\phi = kH$  i.e., the total head, and at the downstream bed, BG potential function,  $\phi = 0$ .

Both the profiles of the structure in the  $z$  plane and the rectangular flow field of the  $w$  plane can be transformed on to the lower half of the same semi-infinite  $p$ -plane. Thus

$$z = f(p) \quad \dots(2.2)$$

and  $w = F(p) \quad \dots(2.3)$

are obtained in which  $z = x+iy$ , representing physical plane,  $p = s+it$ , representing an auxiliary semi-infinite plane, and  $w = \phi + i\Psi$ , representing the rectangular flow field. For convenience, a new variable  $w' = \phi' + i\Psi'$  has been introduced which is defined as

$$\phi' = \frac{\phi}{kH} K \quad \dots(2.4)$$

$$\Psi' = \frac{\Psi}{q} K' \quad \dots(2.5)$$

where  $K$  and  $K'$  are complete elliptic integrals of the first kind with modulus ' $m$ ' and  $m'$  respectively and  $m' = 1-m$ . Combining equations 2.2 and 2.3 and replacing  $w$  by  $w'$ , we obtain

$$z = f(p) = fF^{-1}(w') \quad \dots(2.6)$$

and  $w' = F(p) = Ff^{-1}(z) \quad \dots(2.7)$

The relationship between z and p fields is given

by

$$z = \frac{2}{\pi} (T-d_2) \tanh^{-1} \sqrt{\frac{(\alpha_2 + 1)(p-1)}{(\alpha_2 - 1)(p+1)}} - \frac{2T}{\pi} \tanh^{-1} \sqrt{\frac{(\alpha_1 - 1)(p-1)}{(\alpha_1 + 1)(p+1)}} + id_2 \dots (2.8)$$

The transformation constants are given by

$$\alpha_i = \sec \alpha_i, \quad (i=1,2) \quad \dots (2.9)$$

$$\frac{\sin \alpha_1}{\sin \alpha_2} = 1 - \frac{d_2}{T} \quad \dots (2.10)$$

$$\alpha_2 = \frac{\pi \left(1 - \frac{d_1}{T}\right) - \alpha_1}{\left(1 - \frac{d_2}{T}\right)} \quad \dots (2.11)$$

$$b_1 = \frac{2T}{\pi} \tanh^{-1} \sqrt{\frac{(\alpha_1 + 1)(\beta_1 - 1)}{(\alpha_1 - 1)(\beta_1 + 1)}} - \frac{2}{\pi} (T-d_2) \tanh^{-1} \sqrt{\frac{(\alpha_2 - 1)(\beta_1 - 1)}{(\alpha_2 + 1)(\beta_1 + 1)}} \quad \dots (2.12)$$

$$b_2 = \frac{2}{\pi} (T-d_2) \tanh^{-1} \sqrt{\frac{(\alpha_2 + 1)(\beta_2 - 1)}{(\alpha_2 - 1)(\beta_2 + 1)}} - \frac{2T}{\pi} \tanh^{-1} \sqrt{\frac{(\alpha_1 - 1)(\beta_2 - 1)}{(\alpha_1 + 1)(\beta_2 + 1)}} \quad \dots (2.13)$$

where  $\beta_1, \beta_2, \alpha_1$  and  $\alpha_2$  are transformation parameters.

The relation between  $w'$  and p fields after transformatin is

$$w' = \text{Sn}^{-1}(P, m) \quad \dots(2.14)$$

where  $\text{Sn}^{-1}(P, m)$  is elliptic integral of first kind with  $P$  as argument and  $m$  as modulus.

$$m = \frac{(\beta_1 + \beta_2)(\alpha_1 + \alpha_2)}{(\beta_1 + \alpha_2)(\beta_2 + \alpha_1)} \quad \dots(2.15)$$

$$P = \sqrt{\frac{(\alpha_2 + \beta_1)(\beta_2 - p)}{(\alpha_2 - p)(\beta_1 + \beta_2)}} \quad \dots(2.16)$$

Potentials underside of floor and sides of sheet pile as a ratio of total differential head are given by

$$\phi = \frac{1}{K} \text{Sn}^{-1}(P, m) \quad \dots(2.17)$$

### 2.2.1 Calculation of uplift pressures

It is <sup>not</sup> convenient to use equation (2.17) when the width of weir is comparable to depth of pervious foundation. Under such circumstances  $m$  and  $P$  are close to unity, the elliptic integrals in equation (2.17) vary rapidly and the values of  $m$  and  $P$  have to be computed to many significant places to get accurate results. It is therefore, necessary to rewrite the solution in some other form and express the elliptic integrals in terms of some other parameters.

From equations (2.15) and (2.16)

$$m' = 1-m = \frac{(\alpha_1 - \beta_1)(\alpha_2 - \beta_2)}{(\alpha_2 + \beta_1)(\alpha_1 + \beta_2)} \quad \dots(2.18)$$

$$1 - mP^2 = \frac{(\alpha_2 - \beta_2)(\alpha_4 + p)}{(\alpha_1 + \beta_2)(\alpha_2 - p)} \quad \dots(2.19)$$

Equation (2.17) is modified as

$$\phi = \frac{1}{K} \operatorname{dn}^{-1} \left[ \sqrt{(1-mP^2)}, m \right] \quad \dots(2.20)$$

or  $\operatorname{dn}^2(\phi K, m) = 1 - mP^2$

where  $\operatorname{dn}(\phi K, m)$  is an elliptic function given by  $\operatorname{dn}^2(U, m) = 1 - m \operatorname{sn}^2(U, m)$ ,  $\operatorname{sn}(U, m) = P$ , is an elliptic function whose inverse is the elliptic integral of the first kind,  $U = \operatorname{sn}^{-1}(P, m)$

The elliptic function  $\operatorname{dn}$ , can be evaluated by expanding it in an infinite series of functions of its argument and  $m'$ . The complete integral  $K$  can also be computed for given  $m'$ . Thus  $\phi$  can be computed for given values of  $(1-mP^2)$  and  $m'$ . The latter quantities can be computed from known values of  $d_1, d_2, T, b_1$  and  $b_2$ , by using equations (2.18), (2.19) and (2.8) to (2.13).

### 2.2.2 Exit Gradient

In addition to uplift pressures it is also important to find the hydraulic gradient at the downstream end of the percolation trajectory.

Gradient  $G$  at any point is given by

$$G = \frac{dh}{ds} \quad \dots(2.21)$$

where  $h$  = head at any point along the floor or cut off

$$= \frac{H}{K} \phi'$$

$s$  = distance along the streamline passing through the point.

Equation (2.21) can be rewritten as

$$G = \frac{H}{K} \frac{d\phi'}{ds} \quad \dots(2.22)$$

At the exit point B where  $w' = \phi'$ , exit gradient  $G_E$  is given by

$$G_E = \frac{H}{K} \left| \frac{dw'}{dz} \right|_{z = b_2 + id_2} \quad \dots(2.23)$$

$$= \text{infinity, if } b_2 > 0 .$$

The quantity of seepage is given by

$$q = kHK'/K \quad \dots(2.24)$$

where  $K'$  is the complete  $\int_{\Delta}^{\Delta} \frac{1}{\sqrt{1-m^2 \sin^2 \theta}}$  elliptic integral with modulus  $m'$ .

### 2.2.3 Charts

The potentials at salient points in the underprofile of the weir can be determined by the following steps

- (1)  $\alpha_1$  and  $\alpha_2$  are computed using equations (2.9) to (2.11) by trial and error.
- (2)  $\beta_1$  and  $\beta_2$  are obtained from equations (2.12) and (2.13) by trial and error.
- (3)  $(1-mP^2)$  is calculated from equation (2.19)

(Note:- p takes values -1,0,1 at E,D,C respectively)

- (4)  $m'$  is determined from equation (2.18)
- (5) Using equation (2.20) and steps (3) and (4)  $\phi$  is computed.

The values of  $\alpha_i$  and  $\beta_i (i=1,2)$  in the equations for potentials are close to unity and hence  $\alpha_i - \beta_i$  is very small. But it cannot be neglected, since small variation in this leads to large variations in potential distribution under the floor. Therefore charts have been provided for facilitating the computations of  $\alpha_i$  and  $(\alpha_i - \beta_i)$  for  $i = 1,2$ . For finding  $\alpha_i$  two charts (Fig.2.2 and 2.3) are provided where  $\alpha_i$  can be read for given values of  $d_1/T$  and  $d_2/T$ . Once the value of  $\alpha_i$  is known  $\alpha_{-2}$  can be worked out using equations (2.10) and (2.11). For finding  $(\alpha_i - \beta_i)$  for  $i = 1,2$ , Using Figs. (2.4) and (2.5) the following trial and error procedure is adopted. First a suitable value for  $(\alpha_i - \beta_i)$  is assumed, based on experience. Using this value and known values of  $\alpha_i$ ,  $R_I$  and  $R_{II}$  are read from Figs. (2.4) and (2.5) respectively. Then from equation

$$b_1 \times \frac{\pi}{2T} = R_I - \left(1 - \frac{d_2}{T}\right) R_{II} \quad \dots(2.25)$$

$b_1/T$  is computed and compared with known value of  $b_1/T$ . If  $b_1/T$  is greater than the computed value, then  $(\alpha_i - \beta_i)$  must be reduced and vice versa.

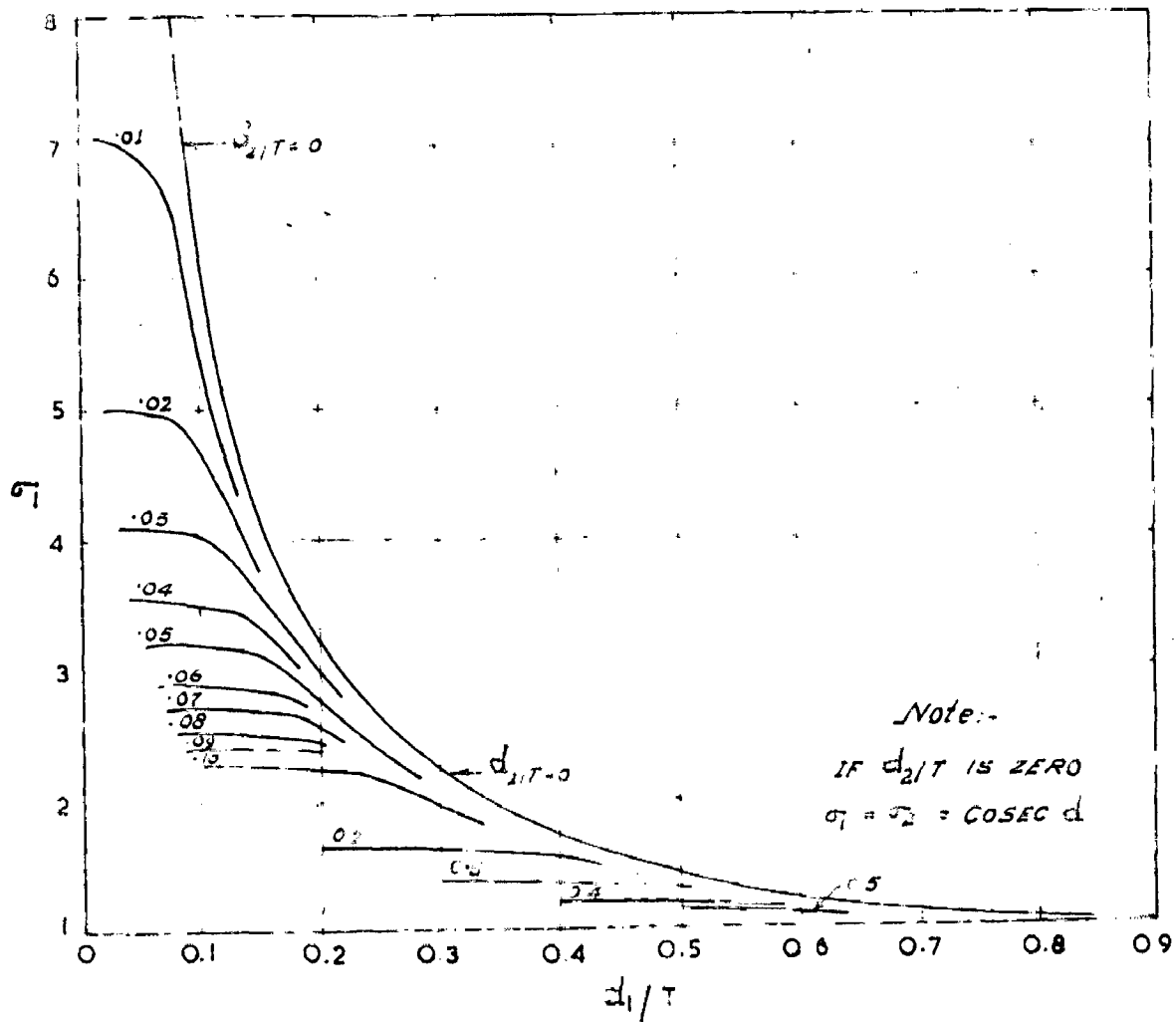


FIG 2.2 CHART FOR  $\sigma_1$ .

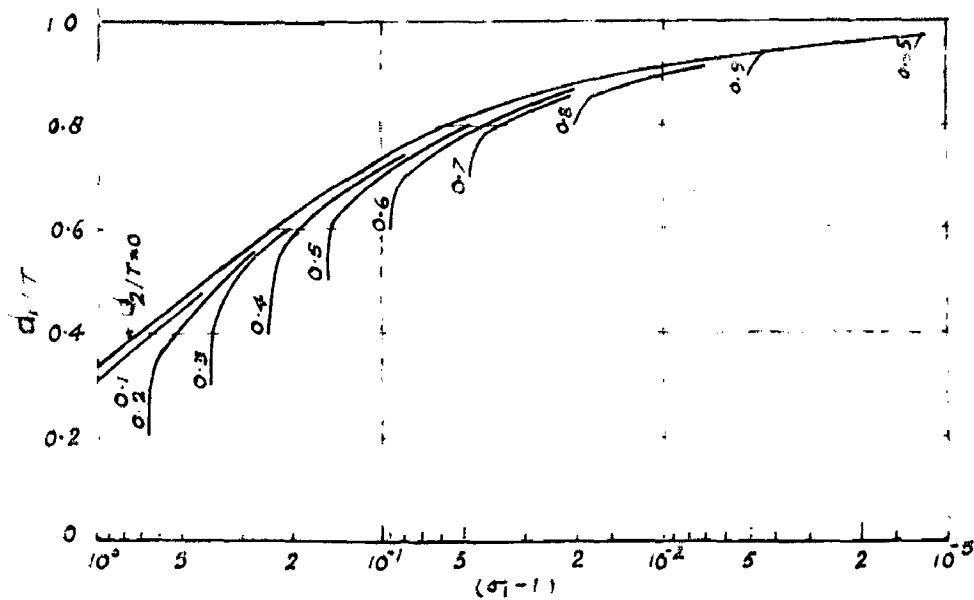


FIG 2.3 CHART FOR  $(\sigma_1 - 1)$



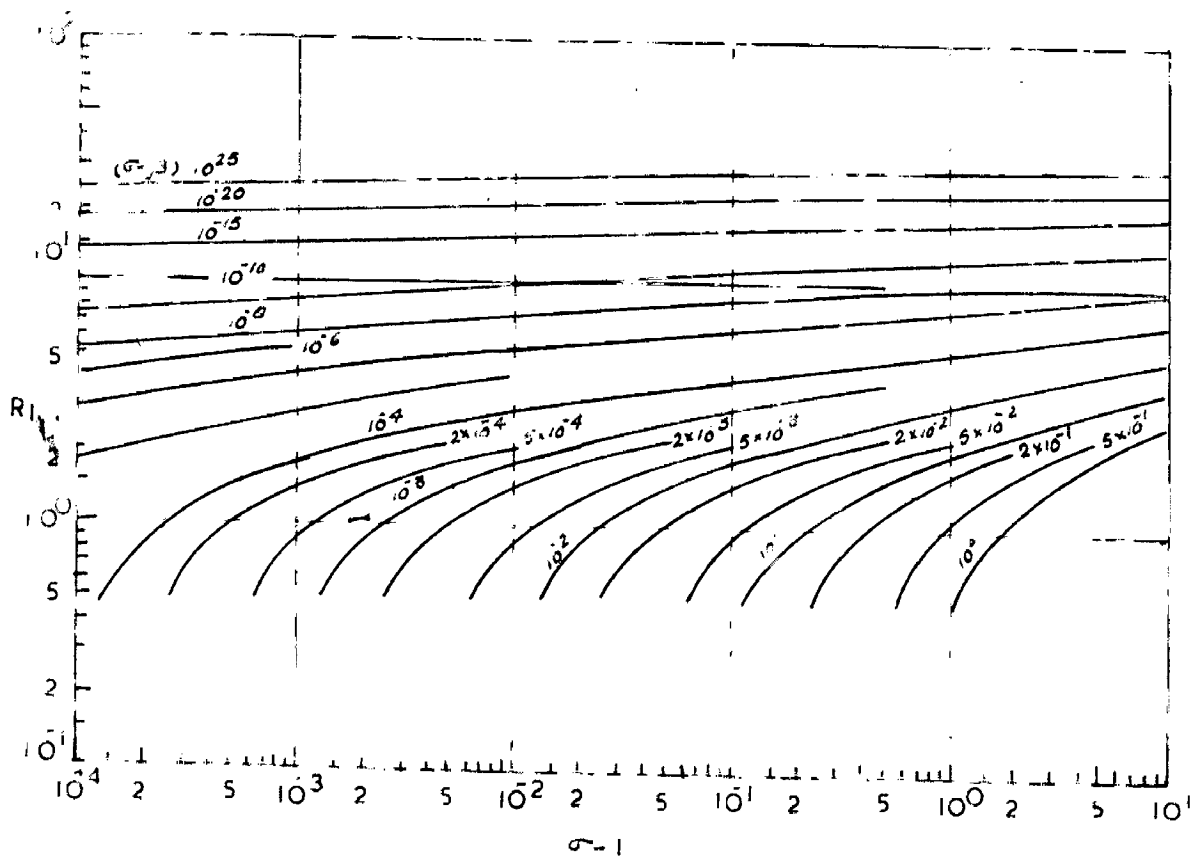


FIG 2.4 CHART FOR  $R_1$

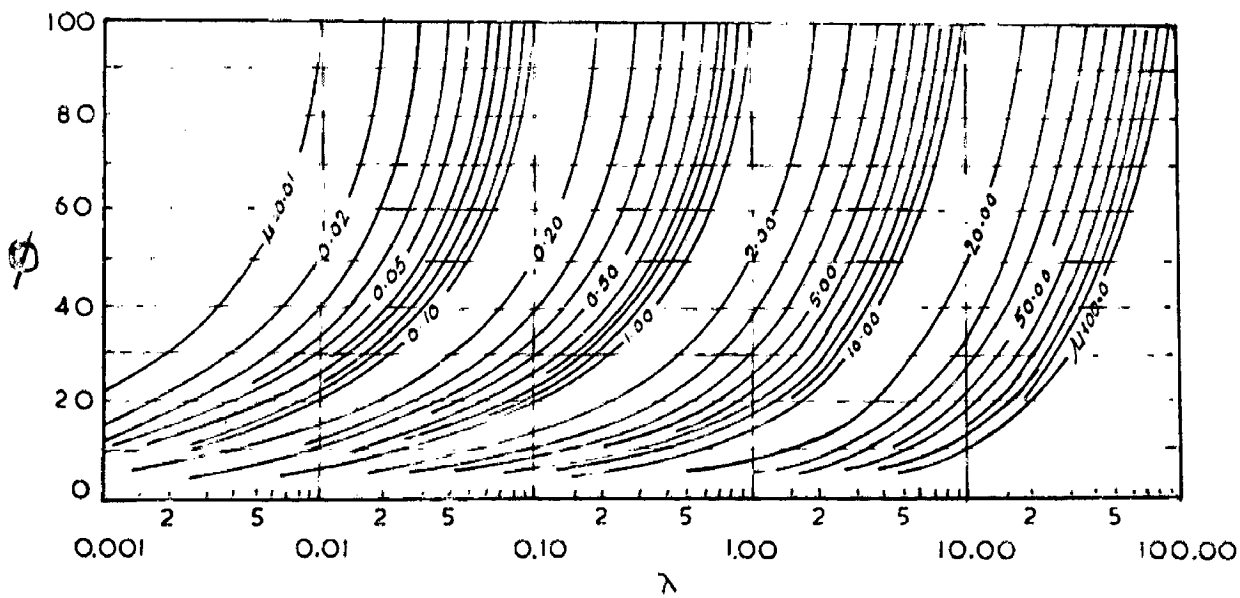


FIG 2.6 CHART FOR POTENTIAL

A Similar procedure and the use of equation,

$$\frac{b_2 \pi}{2T} = \left(1 - \frac{d_2}{T}\right) R_I - R_{II} \quad \dots(2.26)$$

will enable, determination of the value of  $(\sigma_2 - \beta_2)$

Since  $(\sigma_1 - \beta_1)$  is small in practical cases <sup>and</sup> since  $R_{II}$  does not contain  $(\sigma_1 - \beta_1)$ ,  $R_{II}$  can be read from Fig. (2.5), assuming  $\sigma_1 = \beta_1$  and  $R_I$  is then worked out by equation (2.25). Therefore in one single trial  $(\sigma_1 - \beta_1)$  can be read from figure (2.4) as  $R_I$  and  $\sigma_1$  are known.

Figure (2.6) shows the chart for reading  $m'$  and  $(1 - mP^2)$ . The following substitution is used since the values of  $m'$  and  $(1 - mP^2)$  are generally small.

$$\mu = - \log m' \quad \dots(2.27)$$

$$\lambda = - \log [1 - mP^2] \quad \dots(2.28)$$

All the charts prepared, cover the following ranges.

- (1)  $T/b$  varying from negligible values ~~to~~ about 2.5
- (2)  $T/d_1$  varying from negligible values to about 5.
- (3)  $b/d_1$  varying from about 0.5 to about 30.

The author observed by trial computations that when  $T/b = 2.5$  and  $T/d_1 = 5$ , the potentials at salient points were approximately equal to the corresponding values for infinite depth of pervious foundations.

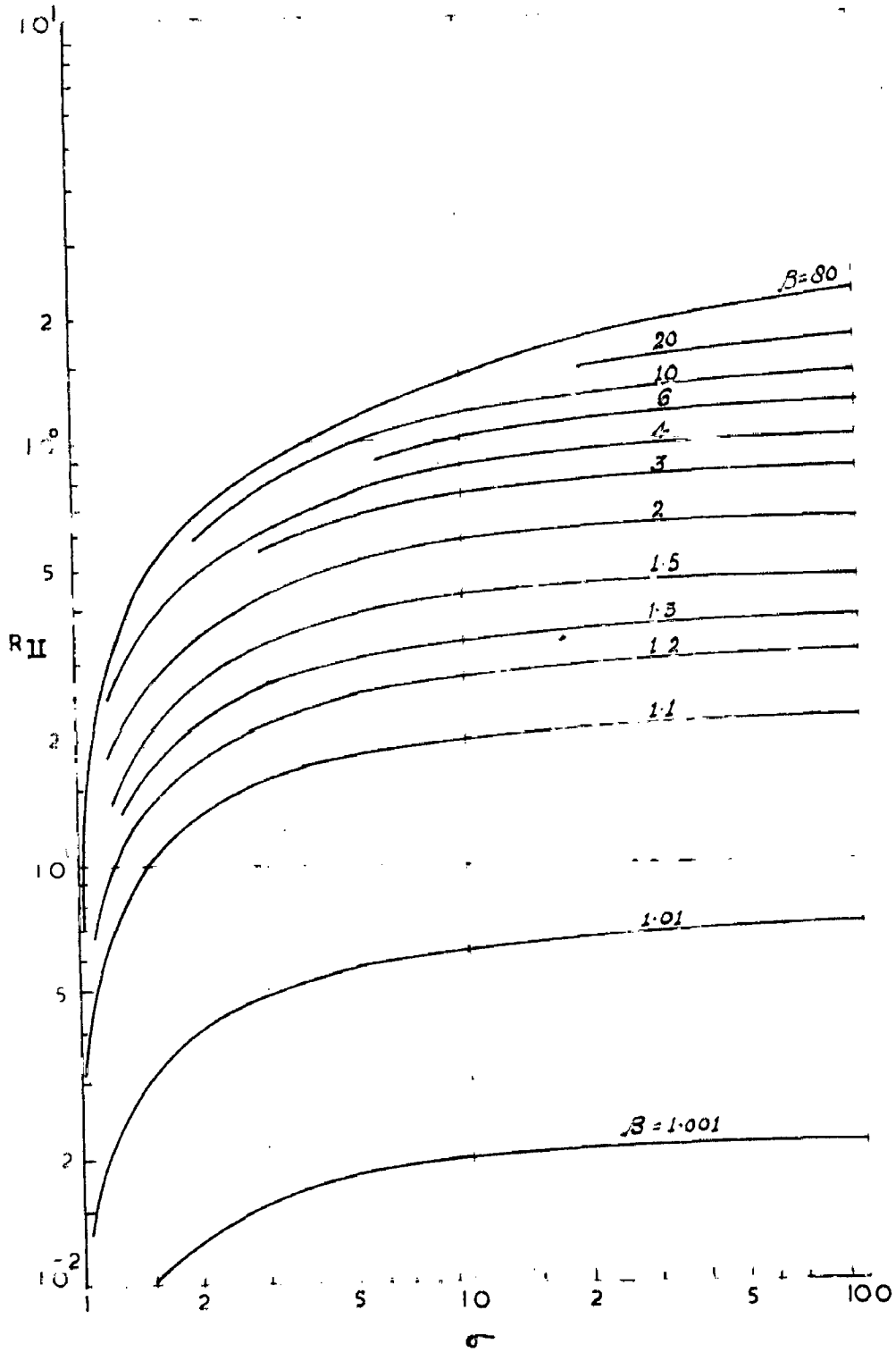


FIG. 2.5 CHART FOR  $R_{II}$ .

### 2.2.3 Mutual Interference of Piles

By improving the formula given by Khosla, the author gave after experimental verification, formula for mutual interference of piles for finite depth of pervious foundation, as follows:

$$C = 19 \sqrt{\frac{\sin \frac{\pi d_1}{2T}}{\sinh \frac{\pi b'}{2T}} \frac{\sin \frac{\pi d_1}{2T} + \sin \frac{\pi d_2}{2T}}{\tanh \frac{\pi b}{2T}}} \dots(2.29)$$

Where C = Correction at the corner where sheet pile of depth  $d_2$  meets the floor, due to the presence of sheet pile of depth  $d_1$ .

$b'$  = distance between piles

$b$  = width of floor.

It may be seen that equation (2.29) reduces to equation given by Khosla when  $T$  is large. The correction in equation (2.29) is additive if pile of depth  $d_1$  is on the downstream side of pile of depth  $d_2$  and subtractive if otherwise. The equation is valid for the following conditions-

- (1) The intermediate pile is longer or equal to outer pile.
- (2) The distance between the piles is more than twice the length of the outer pile.
- (3) The depth of the pervious stratum below the tip of the pile ( $t$ ) is greater than  $0.2b$  for  $b/T$  varying from negligible values to 2. When  $b/T$

equals 12, the minimum required value of  $t/b$  is negligible. For values of  $b/T$  between 2 and 12 minimum required value of  $t/b$  varies linearly from 0.2 to 0.

This equation was verified using both experimental and theoretical results and found to be valid.

#### 2.2.4 Safety Against Piping Failures

Piping failures are caused by seepage erosion or heaving. The seepage erosion, in potential theory is analysed on the basis of the exit gradient at the point on the pervious region nearest to the downstream end of the structure. Khosla, who has derived exit gradient for the general case and other simple weirs on infinite depth foundation (pervious) has shown that the result of the case of a floor with a sheet pile at end is adequate for practical purposes.

#### 2.3 FLAT APRON (WITHOUT A STEP) WITH AN INTERMEDIATE CUT OFF

This case is a particular form of general case discussed in previous section where a floor with a step and an intermediate cut off was considered. By putting  $d_2 = 0$  and  $d_1 = d$ , we get the present case. The solution for this case was obtained by applying Schwarz-Christoffel transformations successively twice, on the same principles

adopted in the previous case. Charts for finding potentials at salient points and for finding exit gradients were provided by V.C. Kulandaiswamy and Muthu Kumaran(8).

The uplift pressures and exit gradient are given by

$$\phi = \frac{1}{K} \operatorname{dn}^{-1} \left[ \sqrt{\frac{1-p_2}{1+\beta_2} \frac{1-p}{1+p}}, m \right] \dots(2.30)$$

$$G_E = \frac{H}{K \sqrt{m \sin \frac{\pi d}{2T}}} \dots(2.31)$$

where,

$$m = \frac{2(\beta_1 + \beta_2)}{(1 + \beta_1)(1 + \beta_2)} \dots(2.32)$$

The equation (2.31) for exit gradient applies only when the cut off is at the end of floor, while the exit gradient for an intermediate cut off is infinity. As the quantities to be used as variables in the chart namely  $m'$  and  $(1-mp^2)$  are generally small, their negative logarithms have been used i.e.,

$$\mu = -\log m' \dots(2.33)$$

$$\lambda = -\log \left[ \frac{1-\beta_2}{1+\beta_2} \frac{1-p}{1+p} \right] \dots(2.34)$$

where,  $m' = 1-m$  and

where  $p = -\alpha = -\sin \frac{\pi d}{2T}$  for point E (Refer Fig.2.1a)

$p = 0$  for point D and  $p = \alpha = \sin \frac{\pi d}{2T}$  for point C.

The charts for potentials (Fig. 2.7) are prepared using  $\mu$  and  $\lambda$  as variables. The chart for the exit gradient (Fig. 2.8) is computed using  $\mu$  and  $d/T$  as variables. The values of  $\mu$  and  $\lambda$  can be computed using the available data namely  $b_1, b_2, d$  and  $T$ .

The use of charts to find (1) potentials at points E, D and C (Fig. 2.1a) and (2) exit gradient is explained in the following steps.

(i) The values of  $\frac{1 - \beta_1}{1 + \beta_1}$  and  $\frac{1 - \beta_2}{1 + \beta_2}$  are computed

from the equation,

$$\sqrt{\frac{1 - \beta_i}{1 + \beta_i}} = \frac{\cos \frac{\pi d}{2T} \operatorname{sech} \frac{\pi b_i}{2T}}{1 + \sqrt{1 - \cos^2 \frac{\pi d}{2T} \operatorname{sech}^2 \frac{\pi b_i}{2T}}} \quad \dots(2.35)$$

(ii)  $m' (= 1-m)$  is computed from

$$m' = \frac{1 - \beta_1}{1 + \beta_1} \times \frac{1 - \beta_2}{1 + \beta_2} \quad \dots(2.36)$$

(iii)  $\mu$  is computed from equation (2.33).

(iv)  $\frac{1 - \sin \frac{\pi d}{2T}}{1 + \sin \frac{\pi d}{2T}}$  is computed and using equation (2.34)  $\lambda$  is determined.

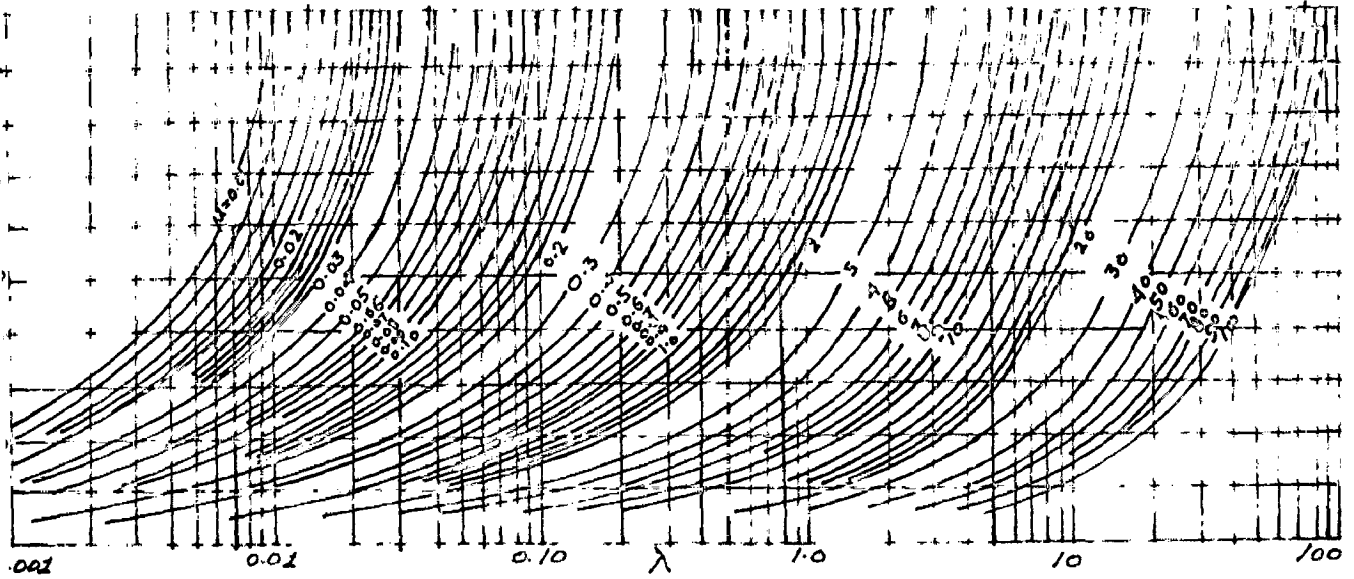


FIG. 2.7 CHART FOR POTENTIALS.

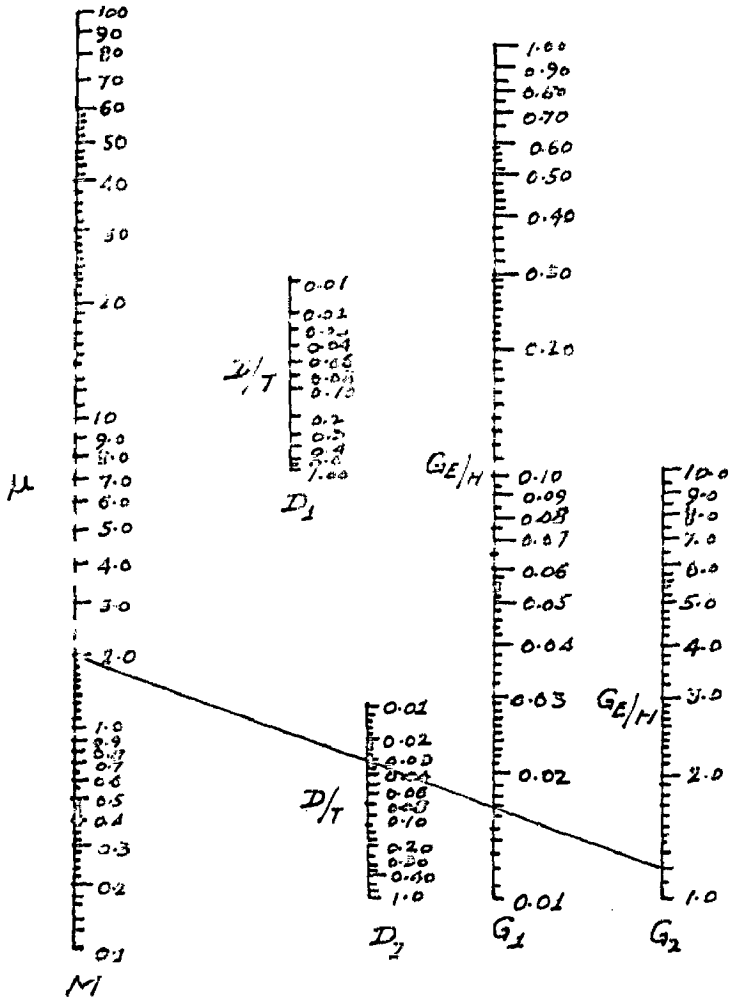


FIG. 2.8 CHART FOR EXIT GRADIENT.



- (v) With the values of  $\mu$  and  $\lambda$ , the value of  $\phi$  is read from Fig. (2.7)
- (vi) From Fig. (2.8) with the known value of  $\mu$  on line M proceed through the  $d/T$  value in line  $D_1$  or  $D_2$  straight to the corresponding line G i.e., from  $D_1$  to  $G_1$  or  $D_2$  to  $G_2$  and read the value of  $G_E / H$  i.e.,  $\frac{1}{K \sqrt{m \sin \frac{\pi d}{2T}}}$ .

- (vii) The exit gradient is computed using equation(2.31)

The formula for correction for mutual interference of piles (in case of weirs with more than one pile) and its limitations, is the same as given in previous section. The validity of this formula was checked by the authors by conducting experimental studies and found that the variation was within 5%.

The authors observed substantial variation in both potential at salient points and exit gradients ( $G_E$  increased) when the depth of pervious stratum below tip of sheet pile was increased from 0.20 to infinity, while studying a typical weir profile with two piles.

#### 2.4 EFFECT OF IMPERMEABLE LAYER ON UPLIFT PRESSURES

Based on the results of conformal mapping Pavlousky (14) studied the effect of lower impermeable layer on the uplift pressures. He carried out calculations for various combinations of the different parameters

to determine uplift pressures in the downstream portion of floor with central cut off. The parameters affecting the pressures are  $n = T/B$  and  $m = d/b$  where  $b =$  half width of floor,  $T =$  depth of impermeable boundary and  $d =$  depth of central cutoff. Following values of these parameters were considered .

$$n = 10.0 \text{ and } 1.0$$

$$d/T = 0.3, 0.5 \text{ and } 0.7$$

$$m = 3, 5 \text{ and } 7 \text{ for } n = 10.0$$

$$= 0.3, 0.5 \text{ and } 0.7 \text{ for } n=1.0$$

In addition the extreme case of  $n = \infty$  i.e., the depth of permeable stratum extending upto infinite depth was also considered.

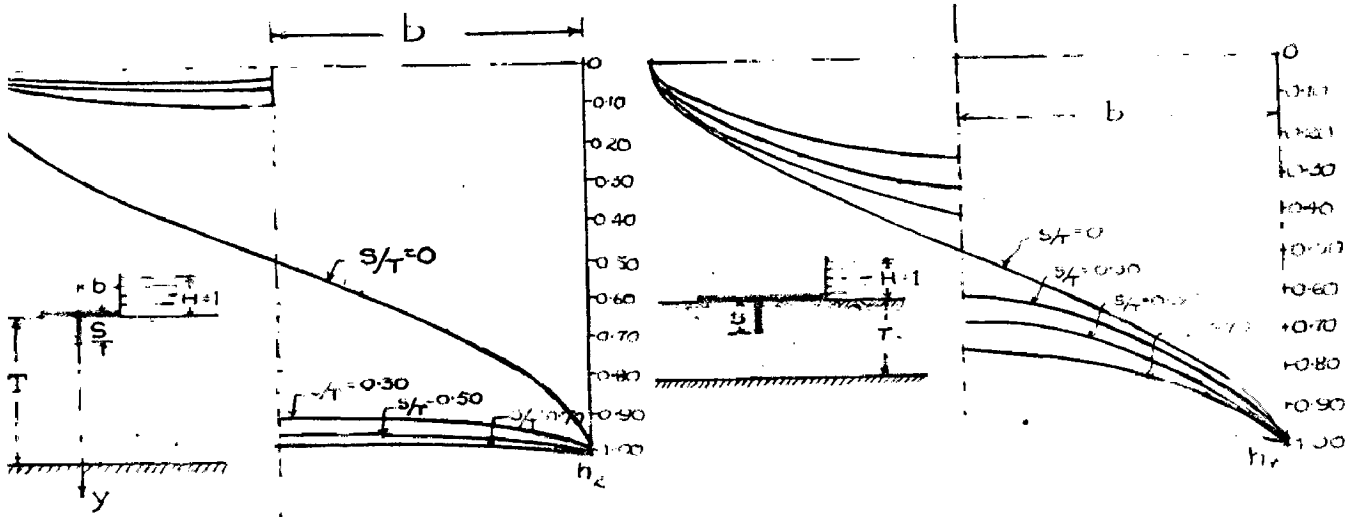
The effect of  $m$  and  $n$  on the uplift pressures was studied at two selected points i.e., the point A, immediately downstream of the piling and a point B, at the middistance between the piling and the downstream edge of the floor. The uplift pressures are given in Table 2.1 and plotted in Fig. 2.9. It is seen that-

- (a) The effect of impermeable layer is negligible for  $n \geq 5$  and  $m \leq 0.1$  . The difference in the uplift pressure calculated for  $n = \infty$  and for  $n = 5$  is less than 1% when the value of  $m \leq 0.1$  .

(b) The difference in uplift pressures calculated for  $n = \infty$  and  $n \geq 3$  is less 10% when the value of  $m \leq 0.4$ .

Pavlovs ky investigated another problem of what depth should be given to the piling to make it reasonably effective. He gave two graphs drawn from theoretical calculations (Fig. 2.10) to show efficiency of piling of various depths. The efficiency ( $h_{eff}$ ) was presented as the ratio of head lost in between points namely upstream junction point of pile and floor and downstream junction point, expressed as a percentage of total head. The interesting point in the graph is that line for  $T/b = 2$  for case of central pile is a straight line. The curves on one side of it are concave while those on otherside are convex. So if  $T/b = 2$  is taken as critical value it follows, from diagram that for  $T/b < 2$  specific efficiency rises with increase in depth of pile while for  $T/b > 2$  it drops with increase in depth of pile.

Thus whilst for infra critical values of  $T/b$  the piling should be as deep as technically possible, no material advantage is gained in the case of hyper critical values of  $T/b$ , by increasing the piling beyond a certain limit.



Thrust Curves for  $T/b = 10$

Upthrust curves for  $T/b = 1.0$

FIG:- 2.9

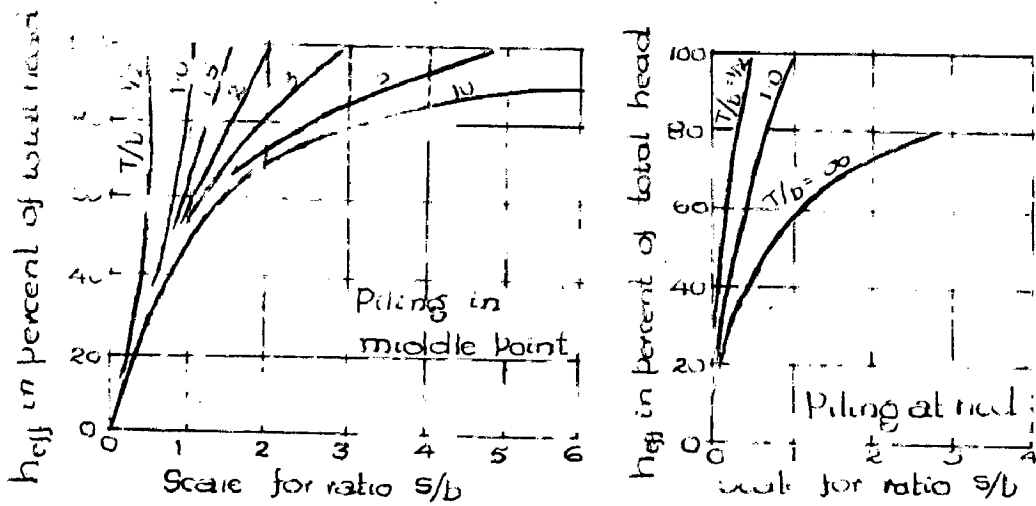


FIG:- 2.10

TABLE 2.1

(a) for  $T/b = 10.0$

Point	m = 3			m = 5			m = 7		
	n=10	n=∞	Bligh	n=10	n=∞	Bligh	n=10	n=∞	Bligh
A	0.099	0.101	0.125	0.060	0.063	0.083	0.039	0.045	0.062
B	0.085	0.088	0.061	0.048	0.054	0.042	0.031	0.039	0.031

TABLE 2.1

(b) for  $T/b = 1.0$

Point	m=0.3			m=0.5			m=0.7		
	n=1.0	n=∞	Bligh	n=1.0	n=∞	Bligh	n=1.0	n=∞	Bligh
A	0.394	0.406	0.385	0.328	0.353	0.333	0.256	0.306	0.295
B	0.288	0.310	0.192	0.249	0.282	0.167	0.198	0.251	0.147

2.5 FLAT APRON WITH DOWNSTREAM CUTOFF UNDER SCOURED  
CONDITIONS

2.5.1 Uplift Pressures

In the previous sections, determination of uplift pressures and exit gradients below apron with an intermediate cut off, either with or without a step, was discussed. Also the formula and chart for finding the exit gradient for the case of a floor with an end cut off were given. But when the apron is under scoured conditions, i.e., when

there is difference in levels between upstream and downstream of an apron (with a downstream end cut off), the pressure below it and the exit gradients differ from the case of apron having equal upstream and downstream elevations. One such case was investigated experimentally by B.C. Punmia et. al. (16) by electrical analogy method.

In the experimental study the authors studied the influence of parameters like  $b/T$ ,  $d_1/T$ , and  $d_2/T$  on pressures at (1) below the apron (2) at junction of floor and downstream end cutoff (3) at tip of cut off, where  $d_2$  is the downstream scour depth and other symbols have the usual notation. The sequence of their study was as follows . (a) the values of  $b/T$  were kept equal to  $1/2$ ,  $1$ ,  $2$  and  $4$  (b) For each  $b/T$  the value of  $d_1/T$  was taken as  $0.2$ ,  $0.4$ ,  $0.6$  and  $0.8$ , (c) For each  $b/T$  and  $d_1/T$  the value of  $d_2/T$  was taken as  $1/8$ ,  $2/8$ ,  $3/8$  and  $4/8$ .

The influence of the ratios of various parameters namely the width of apron, the depth of porous media, depth of cut off downstream scour depth on the pressures (i) below the apron ( $\phi_x$ ) (ii) at junction of apron and cut off ( $\phi_e$ ) (iii) at tip of cut off ( $\phi_D$ ) are shown in Figures (2.11) to (2.18)

From the results of the experiments the following conclusions have been drawn. (1) for a particular width of apron and depth of media, the pressures below apron increase

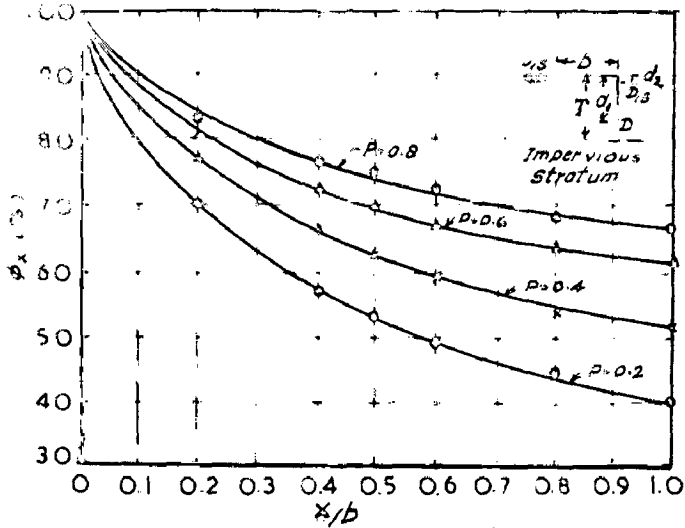


FIG.2-11 VARIATION OF  $\phi_x$  WITH  $\frac{d_1}{T}$ , FOR  $\frac{b}{T} = 1$  AND  $\frac{d_2}{d_1} = \frac{1}{8}$

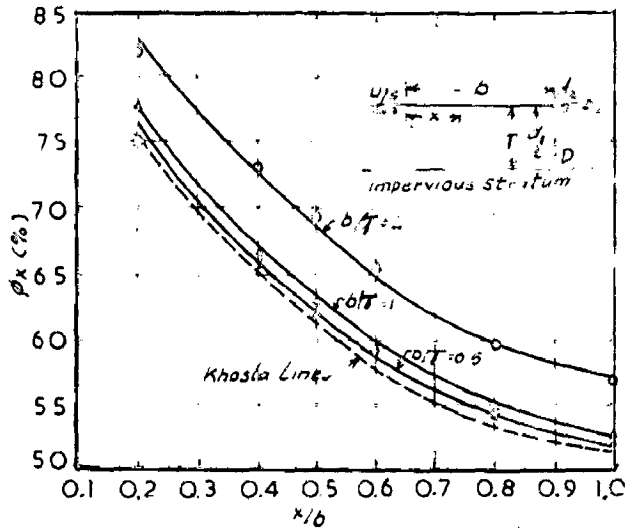


FIG.2-12 VARIATION OF  $\phi_x$  WITH  $\frac{b}{T}$ , FOR  $\frac{b}{d_1} = 2.5$  AND  $\frac{d_2}{d_1} = \frac{1}{8}$

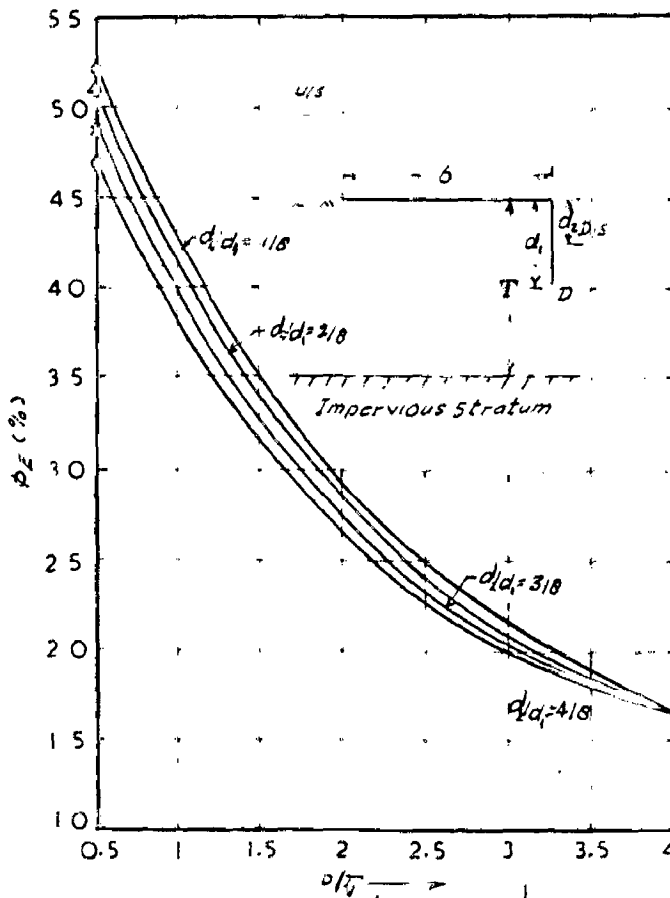


FIG.2-13 VARIATION OF  $\phi_E$  WITH  $\frac{b}{T}$  AND  $\frac{d_2}{d_1}$ , FOR  $\frac{d_1}{T} = 0.2$

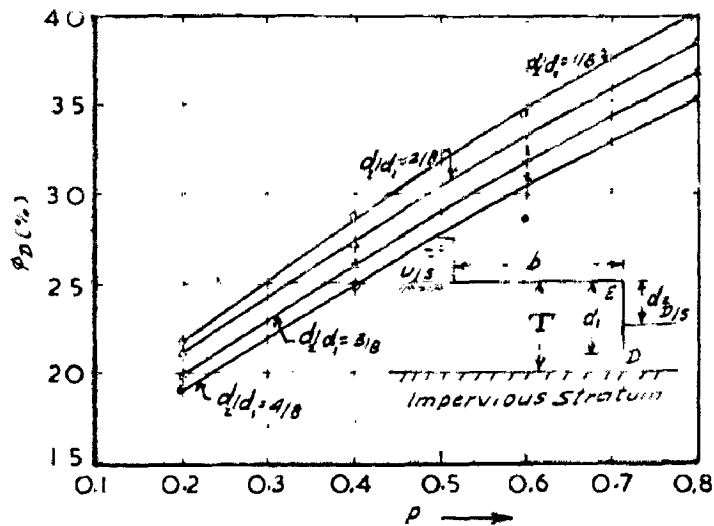


FIG 2-14 VARIATION OF  $\phi_D$  WITH  $\frac{d}{T}$  AND  $\frac{d_1}{d_1}$  FOR  $\frac{b}{T} = 2$

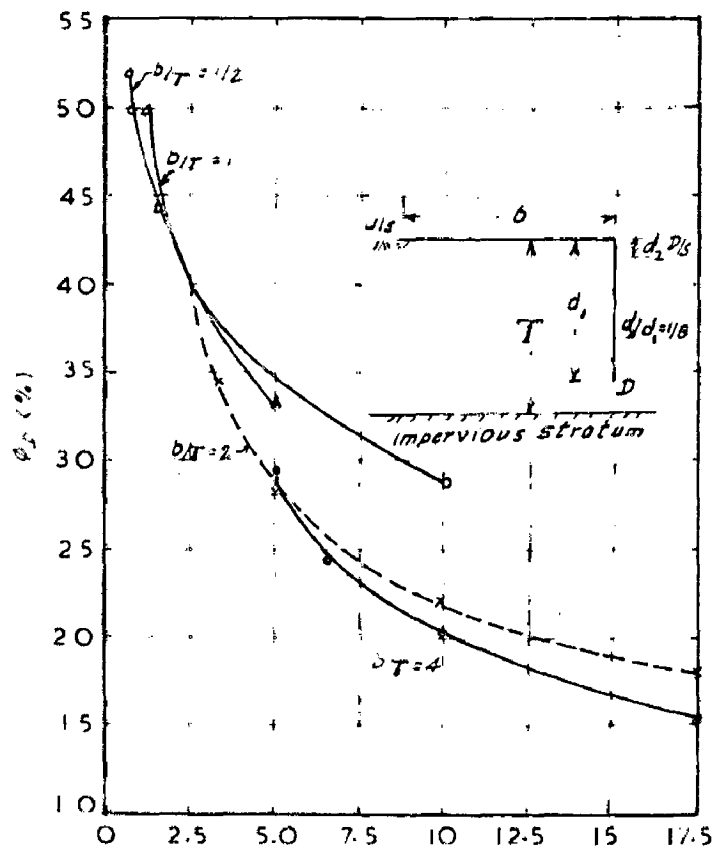


FIG 2-15 VARIATION OF  $\phi_D$  WITH  $\frac{b}{d_1}$  AND  $\frac{b}{T}$  FOR  $\frac{d_1}{d_1} = \frac{1}{8}$



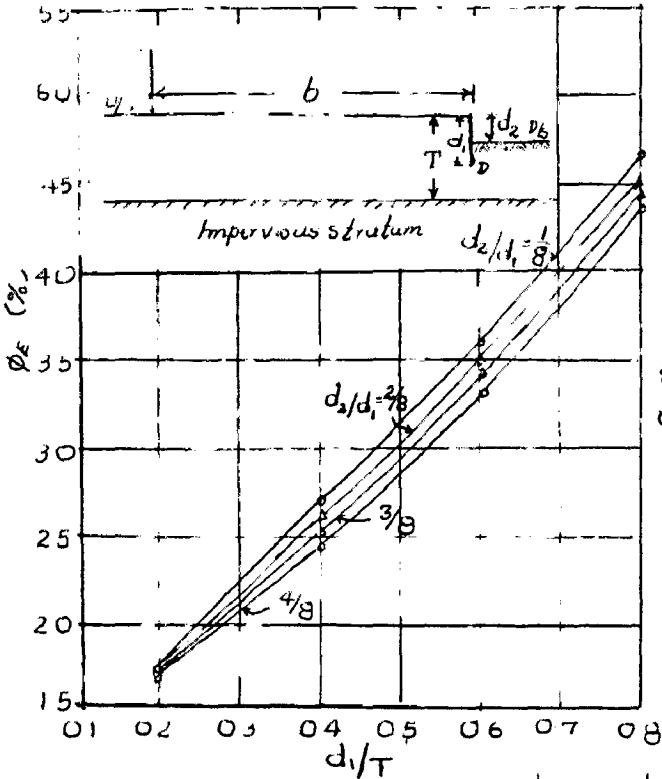


FIG 2.16 VARIATION OF  $\phi_E$  WITH  $\frac{d_1}{T}$  AND  $\frac{d_2}{d_1}$  FOR  $\frac{b}{T} = 4$

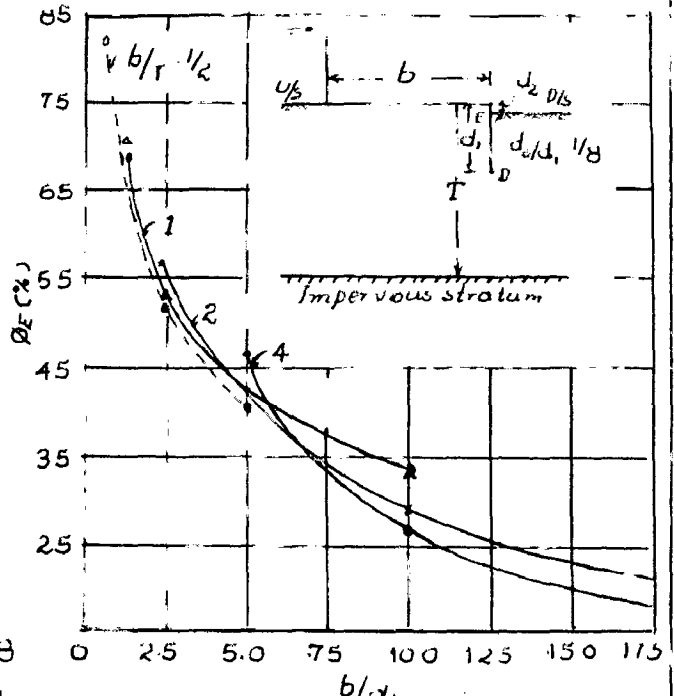


FIG 2.17 VARIATION OF  $\phi_E$  WITH  $\frac{b}{d_1}$  AND  $\frac{b}{T}$  FOR  $\frac{d_2}{d_1} = \frac{1}{8}$

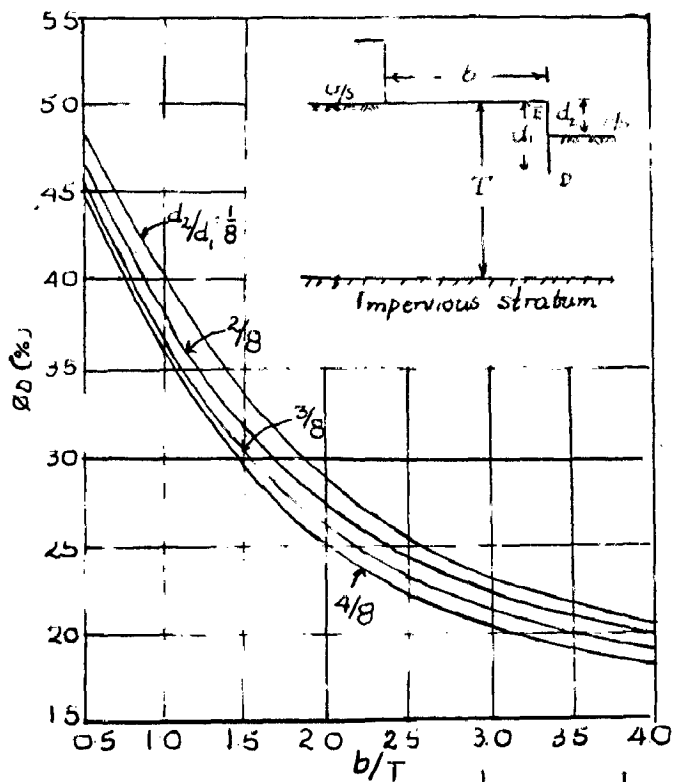


FIG 2.18 VARIATION OF  $\phi_D$  WITH  $\frac{b}{T}$  AND  $\frac{d_2}{d_1}$  FOR  $\frac{d_1}{T} = 0.4$

as depth of cut off increases. (2) The width of floor, the depth of cut off and the scour depth all being fixed, the pressures at any point below floor increase as the impervious layer comes nearer the floor (3) The pressure at junction point ( $\phi_E$ ) and that at tip of cut off ( $\phi_D$ ) increase when width of floor decreases (for constant depths of porous media, scour and cut off). But all the other parameters being fixed the pressures  $\phi_E$  and  $\phi_D$  slightly increase with decrease in scour depth (4) Pressures ( $\phi_D$ ) and ( $\phi_E$ ) increase rapidly with decrease in ratio of width of floor to depth of cut off. (5)  $\phi_D$  and  $\phi_E$  increase rapidly with increase in penetration ratio .

It can therefore be concluded that (i) the depth of the downstream cut off should be kept minimum required for safe value of exit gradient and also from scour considerations.

(ii) The width of floor downstream of the gate line should be kept minimum subject to the requirement from surface flow considerations, (iii) the depth of scour on the downstream, effects slightly reduction in uplift pressures, but at the same time would increase the value of exit gradient.

### 2.5.2 Exit Gradient

The effect of scour downstream of a structure can be studied from the expression for exit gradient at the end of floor with a step and downstream cut off. The

expression obtained by Muthukumaran is

$$G_E \frac{T}{H} = \frac{\pi \alpha_2 (1+\alpha_1) \sqrt{2(\beta_1 + \alpha_2)}}{2K (1 - \frac{d_2}{T})(\alpha_1 + \alpha_2) \sqrt{(1+\beta_1)(1+\alpha_2)}} \dots(2.37)$$

where the symbols have the notations as explained in earlier section. The values of  $G_E \frac{T}{H}$  have been evaluated for  $b/T = 1.0$  and for following values of  $d_1/T$  and  $d_2/T$ .

- |    |                       |                                      |
|----|-----------------------|--------------------------------------|
| 1) | $\frac{d_1}{T} = 0.2$ | $\frac{d_2}{T} = 0, 0.05, 0.1, 0.15$ |
| 2) | $\frac{d_1}{T} = 0.4$ | $\frac{d_2}{T} = 0, 0.1, 0.2, 0.30$  |
| 3) | $\frac{d_1}{T} = 0.6$ | $\frac{d_2}{T} = 0, 0.3, 0.4, 0.50$  |
| 4) | $\frac{d_1}{T} = 0.8$ | $\frac{d_2}{T} = 0, 0.5, 0.6, 0.70$  |

The values of  $\alpha_1$ ,  $\alpha_2$  and  $\beta_1$  were found using the charts given by Muthukumaran (13) the use of which was explained earlier.

The values of  $G_E \frac{T}{H}$  are plotted against  $\frac{d_2}{T}$  as abscissa for all the four values of  $d_1/T$  in Fig. 2.19.

A perusal of the figure indicates that the value of  $G_E \frac{T}{H}$  increases with increase in the value of  $\frac{d_1}{T}$  and  $\frac{d_2}{T}$ . However this rate of increase gradually increases as the value of  $d_2/T$  increases for a particular value

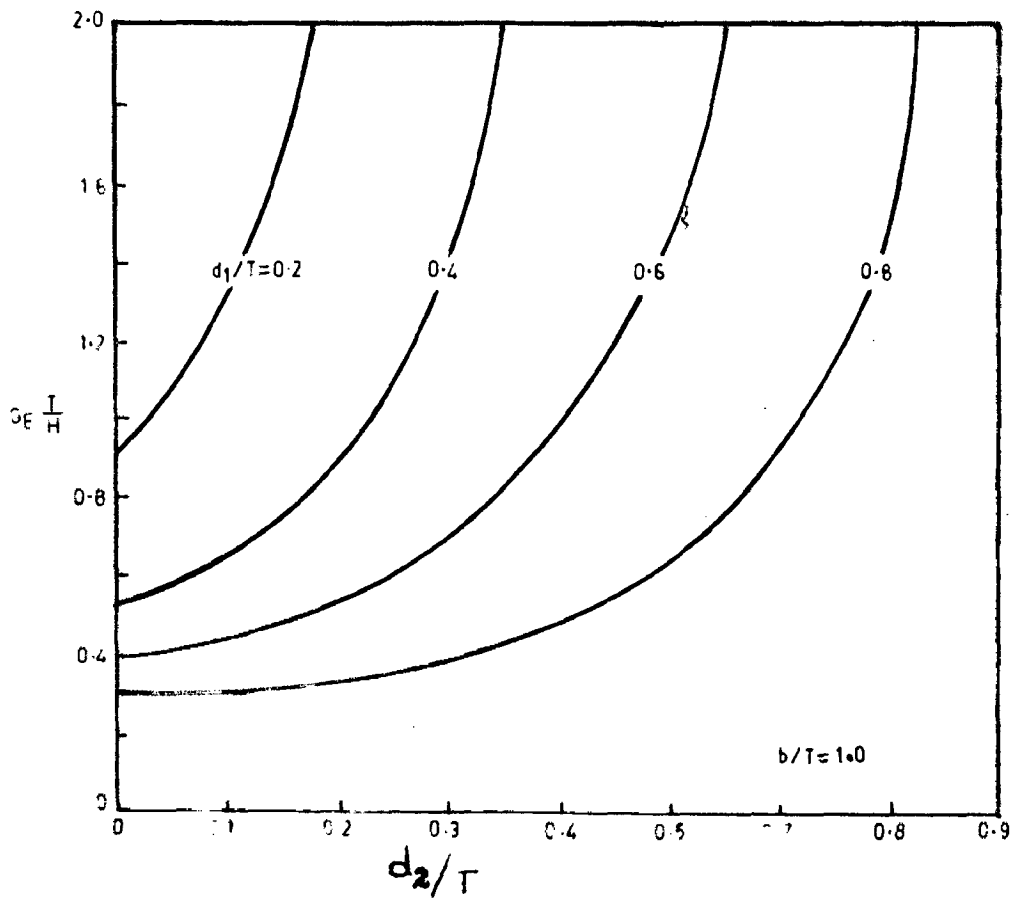
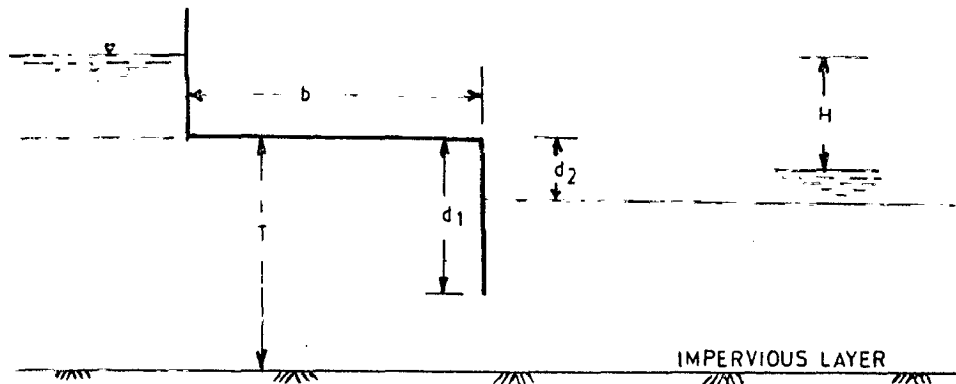


FIG. 2-19—EFFECT OF SCOUR ON EXIT GRADIENT.

of  $d_1/T$ . The rate of increase in the value of  $G_E \frac{T}{H}$  increases with decrease in the value of  $d_1/T$ . For example for  $d_1/T = 0.8$  the value of  $G_E \frac{T}{H}$  increases from 0.32 to 0.48 with increase in the value of  $d_2/T$  from 0.2 to 0.4. But for  $d_1/T = 0.6$  the value of  $G_E \frac{T}{H}$  increases from 0.55 to 1.00 with increase in the value of  $d_2/T$  from 0.2 to 0.4.

Since the value of  $G_E$  especially for deeper cut off i.e.  $d_1/T > 0.4$ , increases only gradually, limited scour downstream of the end cutoff without step may not result in significant increase in the value of exit gradient. However, excessive scour reduces the effectiveness of cut off in controlling the value of exit gradient. It is therefore seen that with downstream scour extending over large area, uplift pressure below the floor decreases whereas the value of  $G_E$  increases. This information would also help in determining the effect of the depth of filter on the downstream side of a structure.

## C H A P T E R   I I I

### S T R A T I F I E D   F O U N D A T I O N S

3.0        An exact solution has been obtained by Polubarinova-Kochina (15) for seepage below flat bottom weir or a cut off founded on soil consisting of two layers of equal thickness. Lenau (9) has obtained solution of flow below a flat bottomed structure founded on two strata of unequal thickness using perturbation technique. The effect of stratification on the seepage and uplift pressure below hydraulic structures with a flat floor only was also studied by Luthra (11) Gurudasram and Awade (5) on electrical analogy model.

Alamsingh and Punmia (1) conducted electrical analogy experiments to determine uplift pressures at key points of a floor with cut off at its downstream end founded on soil consisting of two layers of equal thickness. In these experiments the permeability of upper layer was taken to be higher than that of lower layer. Sharma et al (22) combined theoretical and model studies to determine the exit gradient and uplift pressures below a floor with an end cut off founded on two layered soil with permeability of upper layer being smaller than that of underlying layer. The ratio of the permeabilities of lower and upper layers have been varied between zero and infinity. The solutions obtained for various boundary conditions are given below.

### 3.1 FLOOR ON TWO STRATA OF EQUAL THICKNESS

Consider a flat floor AB(Fig.3.1) of length  $2b$  resting on a stratum of depth  $T$  with coefficient of permeability  $k_1$ . This stratum is resting on another stratum of thickness  $T$  with coefficient of permeability  $k_2$  underlain by an impervious layer. Since the structure is symmetrical about its centre line, only the right half is considered. Along the upstream bed  $AG_1$  ,  $\phi = -k_1H$  and along downstream bed  $BF_1$  ,  $\phi = 0$ . Due to the symmetry CDE is an equipotential surface where  $\phi = \frac{k_1H}{2}$  or  $\frac{k_2H}{2}$ . Along the lower impermeable boundary  $EF_2$ ,  $\psi = 0$ . The base of the structure CB is an impermeable boundary and may be taken as the stream line  $\psi = q$ .

$w_1 = \phi_1 + i\psi_1$  and  $w_2 = \phi_2 + i\psi_2$  represent the complex potentials in the upper and lower stratum. The boundary condition along the various surfaces are expressed in terms of  $w_1$  and  $w_2$  as follows.

$$BF_1 \quad \phi_1 = k_1H \text{ or } \text{Im}(iw_1) = k_1H$$

$$CB \quad \psi = q \text{ or } \text{Im}(w_1) = q$$

$$CD \quad \phi_1 = \frac{k_1H}{2} \text{ or } \text{Im}(iw_1) = \frac{k_1H}{2}$$

$$DE \quad \phi_2 = \frac{k_2H}{2} \text{ or } \text{Im}(iw_2) = \frac{k_2H}{2}$$

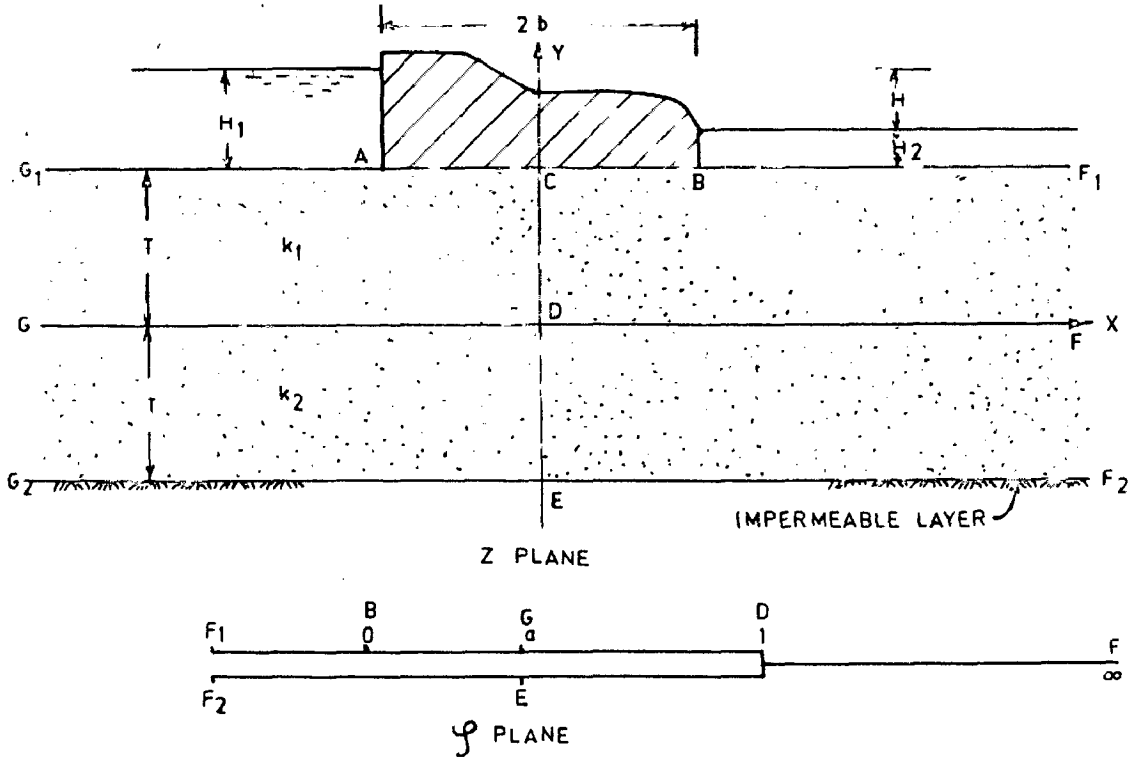


FIG.3-1-TRANSFORMATION LAYOUT.

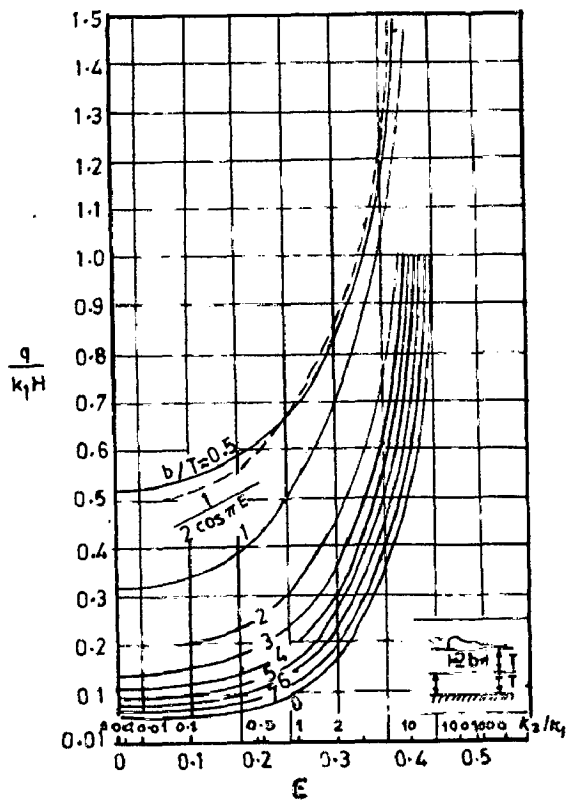


FIG.3-2-VARIATION OF SEEPAGE DISCHARGE WITH  $k_2/k_1$  AND  $2b$ .



$$EF_2 \quad \Psi_2 = 0 \quad \text{of} \quad \text{Im}(w_2) = 0$$

$$DF \quad \frac{\rho_1}{k_1} = \frac{\rho_2}{k_2} \quad \text{or} \quad \text{Im}\left(\frac{iw_1}{k_1} - \frac{iw_2}{k_2}\right) = 0$$

$$\Psi_1 = \Psi_2 \quad \text{or} \quad \text{Im}(w_1 - w_2) = 0$$

The region  $F_1BCDF$  and  $FDEF_2$  are mapped into the upper half and lower half of the complex  $\zeta$  plane. In mapping the region of upper stratum to the upper portion of the  $\zeta$ -plane, the points B, D and F are placed at 0, 1 and  $\infty$  along the real axis and point C lies at 'a'. The point E of the lower stratum is placed at  $\zeta = a$ .

The Schwartz - Christoffel, transformation equation that maps z- plane into  $\zeta$  plane is

$$\frac{dz}{d\zeta} = M (\zeta - a)^{-1/2} (\zeta - 1)^{-1/2} \quad \dots(3.1)$$

$$\begin{aligned} \text{or } z &= M \int \frac{d\zeta}{\sqrt{(\zeta - a)(\zeta - 1)}} + N \\ &= M \cosh^{-1} \left[ \frac{\zeta - \frac{1}{2}(1+a)}{\frac{1}{2}(1-a)} \right] + N \quad \dots(3.2) \end{aligned}$$

At point D,  $\zeta = 1$ , and  $z = 0$ . Therefore  $N = 0$ . At point C,  $\zeta = a$  and  $z = iT$ , Therefore

$$\begin{aligned} iT &= M \cosh^{-1} -1 \\ &= \bar{M} i \pi \end{aligned}$$

or  $M = T/\pi$

Eq. 3.2 reduces to

$$z = \frac{T}{\pi} \cosh^{-1} \left[ \frac{\zeta - \frac{1}{2}(1+a)}{\frac{1}{2}(1-a)} \right] \quad \dots(3.3)$$

$$\text{or } \zeta = \frac{1}{2}(1+a) + \frac{1}{2}(1-a) \cosh \frac{\pi z}{T} \quad \dots(3.4)$$

At point B,  $z = b+iT$  and  $\zeta = 0$ , therefore from Eq. 3.4

$$a = \tanh^2 \frac{\pi b}{2T} \quad \dots(3.5)$$

The potential functions  $w_1$  and  $w_2$  for the upper and lower layers are given by the following integrals

$$w_1 = \frac{M'_1}{2} \int \frac{(\sqrt{1-\zeta} + \sqrt{-\zeta})^{2\epsilon} + (\sqrt{1-\zeta} - \sqrt{-\zeta})^{2\epsilon}}{\sqrt{\zeta(1-\zeta)(\zeta-a)}} d\zeta + N' \quad \dots(3.6)$$

and

$$w_2 = -\frac{M'_1}{2} \tan \epsilon \pi \int \frac{(\sqrt{1-\zeta} + \sqrt{-\zeta})^{2\epsilon} - (\sqrt{1-\zeta} - \sqrt{-\zeta})^{2\epsilon}}{\sqrt{\zeta(1-\zeta)(\zeta-a)}} d\zeta + N' \quad \dots(3.7)$$

$$\text{where } \epsilon = \frac{1}{\pi} \tan^{-1} \sqrt{\frac{k_2}{k_1}} \quad \dots(3.8)$$

### Uplift Pressures

Substituting  $\zeta = \sin^2 \alpha$ , Eq. 3.6 reduces to

$$w_1 = \frac{M'_1}{2} \int \frac{(\cos \alpha + i \sin \alpha)^{2\epsilon} + (\cos \alpha - i \sin \alpha)^{2\epsilon}}{\sqrt{a - \sin^2 \alpha}} d\alpha + N' \quad \dots(3.9)$$

$$= M'_1 \int \frac{\cos (2\epsilon \alpha)}{\sqrt{a - \sin^2 \alpha}} d\alpha + N' \quad \dots(3.10)$$

At point B ,  $\zeta = 0$  and  $w = 0$  , therefore  $N' = 0$

At point C ,  $\zeta = a$  and  $w = \frac{k_1 H}{2}$  , therefore

$$\frac{k_1 H}{2} = M' \int_0^{\sin^{-1} \sqrt{a}} \frac{\cos(2\epsilon\alpha)}{\sqrt{a - \sin^2 \alpha}} d\alpha \quad \dots(3.11)$$

$$= M' J$$

Eq. 3.9 therefore reduces to

$$w_1 = \frac{k_1 H}{2J} \int_0^{\sin^{-1} \sqrt{\zeta}} \frac{\cos(2\epsilon\alpha)}{\sqrt{a - \sin^2 \alpha}} d\alpha \quad \dots(3.12)$$

Direct integration of Eq. 3.12 is not possible

It can however be integrated after expanding into an infinite series.

### Seepage Discharge

The seepage discharge can be determined by integrating Eq. 3.6 between limits  $\zeta = -\infty$  and  $\zeta = 0$  . The seepage flow can also be determined by adding the seepage discharge passing through upper layer at section CD and the seepage discharge passing through the lower layer at section DE. The flow rate through the upper layer can be obtained by integrating Eq. 3.6 between the limits  $\zeta = a$  and  $\zeta = 1$  and the flow rate through the lower layer can be obtained by integrating Eq. 3.7 between the limits  $\zeta = a$  and  $\zeta = 1$  . The total flow rate is given by

$$\frac{q}{k_1 H} = \frac{1}{2J \cos \epsilon \pi} \int_0^{\sin^{-1} k'} \frac{\cos (2\epsilon \alpha)}{\sqrt{k'^2 - \sin^2 \alpha}} d\alpha \quad \dots(3.13)$$

where  $q$  = seepage discharge per unit length of the structure. The values of  $q/k_1 H$  have been plotted against values of  $\epsilon$  and  $k_2/k_1$  for various values of  $b/T$  ranging between 0.5 and 8.0 (Fig.3.2). A perusal of the figure indicates that the seepage discharge increases with increase in the value of  $k_2/k_1$ . Also the seepage discharge reduces with the increase in the length of floor. This is also evident from Fig.3.2. It is seen that the discharge reduces rapidly for initial increase in the value of  $b/T$  and the rate of reduction reduces with increase in the value of  $b/T$ .

### 3.2 CUT OFF IN TWO STRATA OF EQUAL DEPTH

Pollubarinova - Kochina(15) has also obtained expression for seepage discharge below a cutoff penetrating to a depth 'd' in two layers of equal thickness  $T$  with coefficient of permeability being  $k_1$  and  $k_2$ .

$$\text{For } d < T$$

$$\frac{q}{k_1 H} = \frac{1}{J_1 + J_2} \left[ \frac{(\cos \frac{\pi d}{2T})^{2\epsilon}}{\cos \epsilon \pi} J_3 + \frac{J_1 - J_2}{2} \tan \epsilon \pi \right] \dots(3.14)$$

$$\text{For } d > T$$

$$\frac{q}{k_1 H} = \frac{J_1 + J_2}{2J_0} \tan \pi \epsilon \quad \dots(3.15)$$

where

$$J_1 = \int_0^{\pi/2} \frac{(\sqrt{1-\alpha^2 \sin^2 \phi} + \alpha \cos \phi)^{2\epsilon}}{\sqrt{1-\alpha^2 \sin^2 \phi}} d\phi \quad \dots(3.16)$$

$$J_2 = \int_0^{\pi/2} \frac{(\sqrt{1-\alpha^2 \sin^2 \phi} - \alpha \cos \phi)^{2\epsilon}}{\sqrt{1-\alpha^2 \sin^2 \phi}} d\phi \quad \dots(3.17)$$

$$J_3 = \int_0^{\pi/2} \frac{\cos 2\epsilon \phi d\phi}{\sqrt{1-\alpha'^2 \sin^2 \phi}} \quad \dots(3.18)$$

$$J_0 = J_1 - J_2 + \frac{2\alpha'^{2\epsilon}}{\sin \epsilon \pi} J_3 \quad \dots(3.19)$$

$$\phi = \sin^{-1} \sqrt{\frac{\zeta}{a}} \quad \dots(3.20)$$

$$\alpha = \sin \frac{\pi d}{2T} \quad \text{and} \quad \alpha' = \cos \frac{\pi d}{2T} \quad \dots(3.21)$$

$$a = -\tan^2 \frac{\pi d}{2T} \quad \dots(3.22)$$

for  $d = T$

$$\frac{q}{k_1 H} = \frac{1}{2} \tan \epsilon \pi = \frac{1}{2} \sqrt{\frac{k_2}{k_1}} \quad \dots(3.23)$$

The values of  $G_E \frac{T}{H}$  have been plotted, in Fig.3.3 against the values of  $d/T$  and  $k_2 / k_1$ . A perusal of the figure indicates that the value of  $G_E \frac{T}{H}$  decreases rapidly with increase in value of  $d/T = 3/4$ . The reduction in the value of  $G_E \frac{T}{H}$  with increase in the value of  $d/T$  beyond  $3/4$

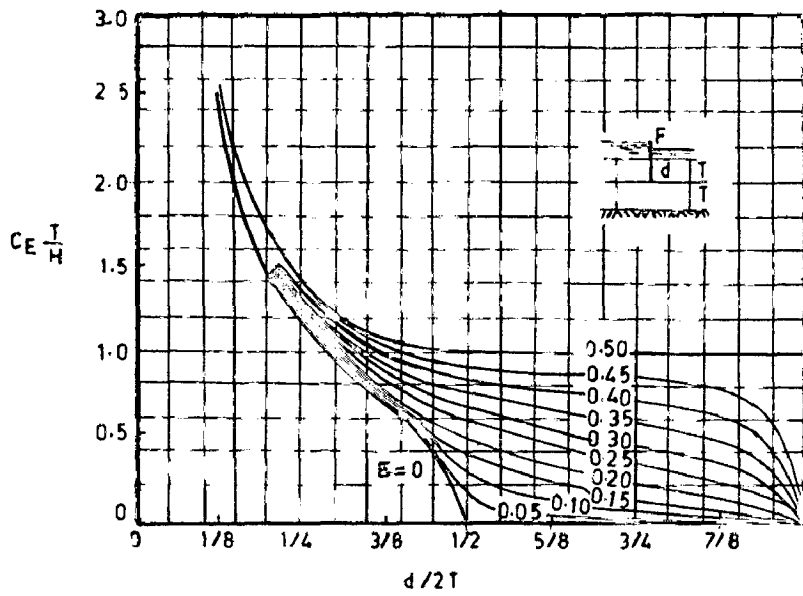


FIG.3-3-VARIATION OF EXIT GRADIENT WITH  $\epsilon$  &  $d$ .

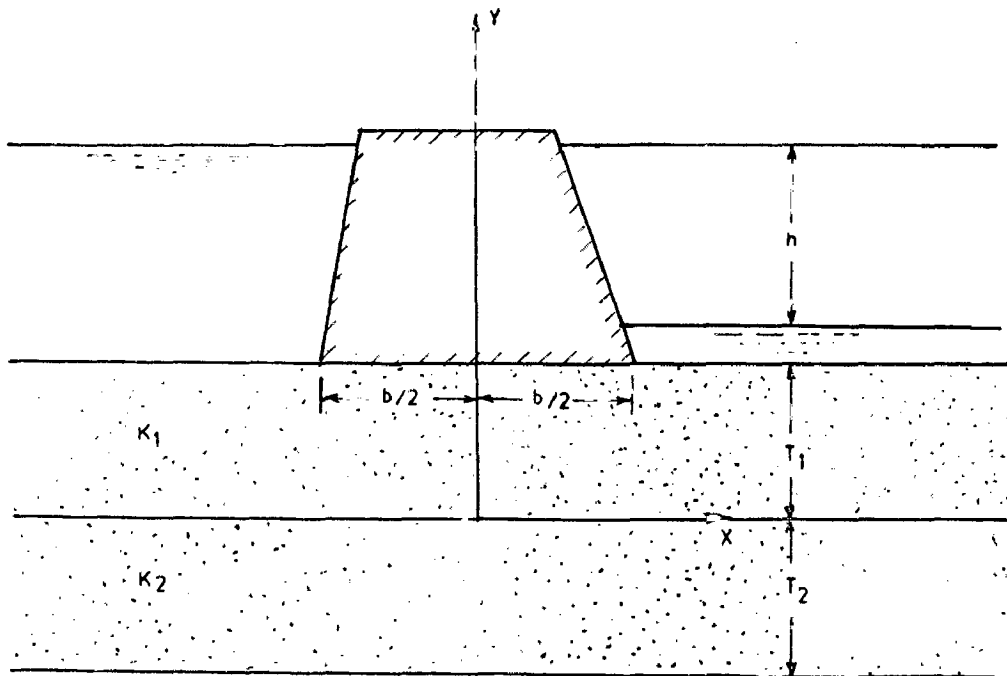


FIG.3-4-FLOOR ON TWO STRATA OF UNEQUAL THICKNESS.

is very small. The ratio of the permeability of lower layer to that of upper layer has very little effect on the value of  $G_{E-H}^T$  for  $d/T$  less than  $3/4$ .

### 3.3 FLOOR ON TWO STRATA ON UNEQUAL THICKNESS

Lenau (9) has obtained the solution of seepage below a flat floor founded on two strata of unequal thickness using "perturbation technique" Fig. (3.4), He has obtained expressions for the seepage discharge only and has not derived any relation for uplift pressures. Expression for discharge is

$$\frac{q}{k_1 H} = \frac{(1-p)^{2\rho} \sqrt{\gamma} / \pi}{2\rho \sqrt{\gamma}} + \frac{1}{\pi} \log \left( \frac{1+p}{2\rho} \right) + O(\rho) \dots (3.24)$$

where

$$p = \tanh \left( \frac{\pi b}{8T_1} \right) \dots (3.25)$$

$$\gamma = \frac{T_1}{T_2}$$

$$\rho = \sqrt{k_1/k_2}$$

Eq. 3.24 can give relatively accurate values for smaller values of  $\rho$  and  $\sqrt{\gamma}$ . The values of  $q/k_1 H$  have been plotted against  $b/T_1$  for different values of  $\sqrt{k_1 T_1/k_2 T_2}$  in Fig. 3.5. A perusal of the figure indicates that the length of the floor becomes unimportant as the value of  $\sqrt{k_1 T_1/k_2 T_2}$  approaches zero and the value of  $q/k_1 H$

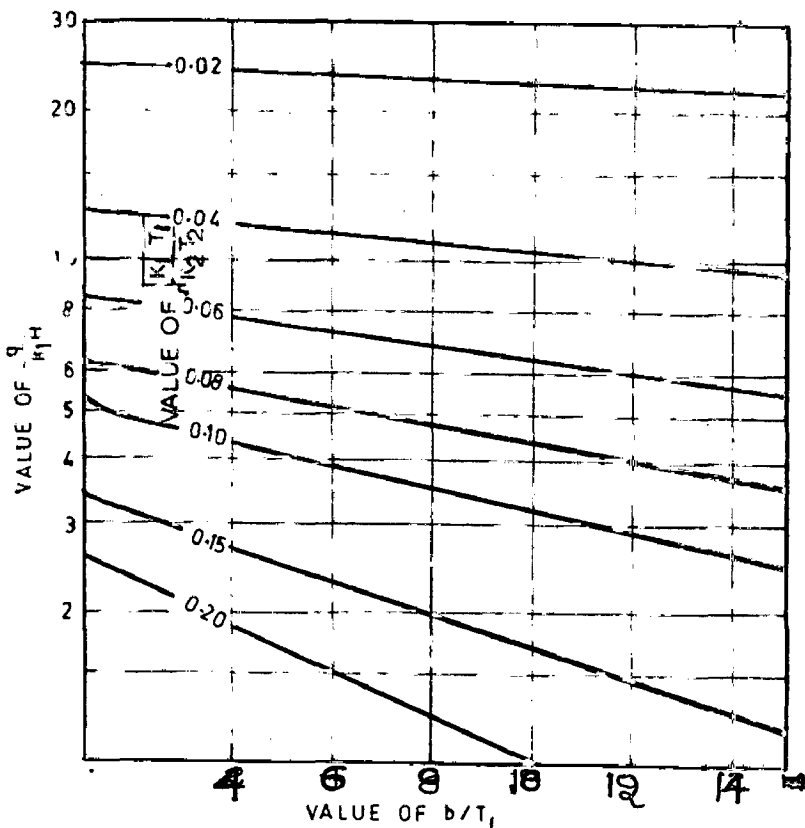


FIG.3.5- $q/k_1 H$  V/S  $b/T_1$

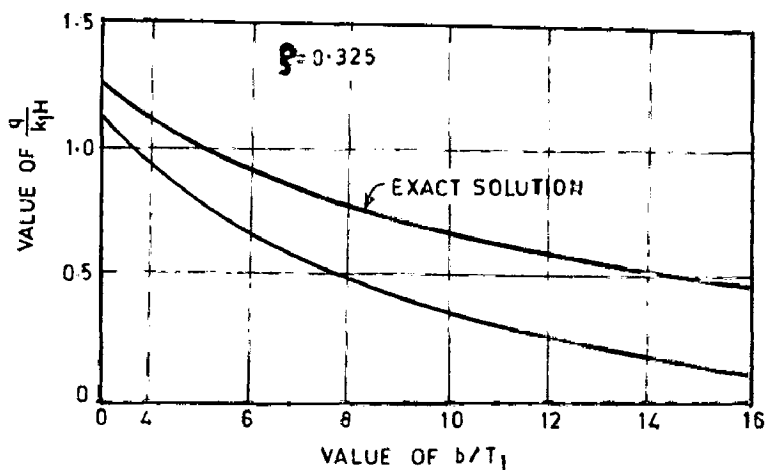


FIG.3.6-COMPARISON BETWEEN Eq3.24 AND EXACT SOLUTION GIVEN BY POLUBARINOVA KOCHINA.



approaches the value of  $\frac{1}{2} \sqrt{\frac{k_2 T_2}{k_1 T_1}}$  . A similar tendency

is seen from the results of the solution given by Polubarinova-Kochina for floor founded on two layers of equal thickness.

A comparison between the results obtained from Eq. 3.24 and exact solution given by Polubarinova-Kochina (15) is illustrated in Fig. 3.6 (for  $\xi = 0.325$ ) . The Eq. 3.24 is seen to under-estimate seepage discharge  $q/k_1 H$ , the accuracy decreasing with increase in  $b/T_1$  . For example when  $b/T_1 = 3$  the absolute and relative errors are 0.15 and 15% respectively, and when  $b/T_1 = 16$  the absolute and relative errors are 0.34 and several hundred percent. The Eq. 3.24 can be expected (From Fig. 3.6) to underestimate the total seepage to a maximum of  $1.0 \xi$  if  $b/T_1 \leq 16$  and  $\gamma \leq 1$ . For  $\gamma > 1$  ( $T_1/T_2 > 1$ ) the error will be somewhat larger but probably no more than  $\xi \sqrt{\gamma}$  .

Lenau (10) has also obtained an approximate solution of seepage below the foundation of a structure without cutoff resting on four layers of equal thicknesses. The approximate solution is accurate for very small values of  $b/T$  . However as  $b/T$  approaches zero the error approaches infinity. Hence the solution is recommended to be used only when  $b/T \geq 0.2$  .

### 3.4 FLOOR WITH END CUT OFF ON TWO STRATA

Alamsingh et. al (1) has studied on electrical analogy model the effect of stratified foundation on the uplift pressures below hydraulic structures with downstream end cut off . The permeability of upper layer was taken to be more than the lower layer. Sharma et. al (22) combined the theoretical and model studies to determine the exit gradient and uplift pressures below foundations of structures founded on two layers, with the permeability of upper layer being smaller than that of the underlying layer.

Alamsingh et al conducted experiments to determine uplift pressures only for  $k_1/k_2$  ratio as 1,4, 20 and 50,  $b/T$  ratio equal to 1,2,4 and 8 and  $d/T$  ratio as 0.25, 0.5 0.75 and practically 1.0 . The results indicate that uplift pressures increase with the increase in the permeability ratio  $k_1/k_2$  and penetration ratio  $d/T$  (Fig. 3.7 to 3.10). As expected the pressures at the corresponding points decrease with increase in the length of floor. The authors also found that for a given  $b/T$  ratio the uplift pressures at D and E decrease with increase in the value of  $\sqrt{k_1/k_2}$  for  $d/T < 0.5$  and increase with increase in the value of  $\sqrt{k_1/k_2}$  for  $d/T > 0.75$  (Fig. 3.11 and 3.12)

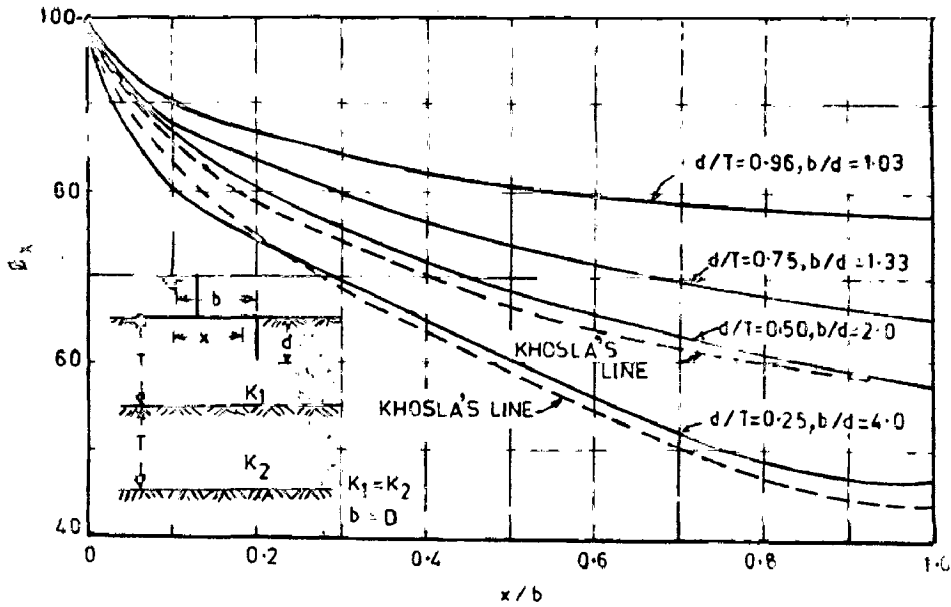


FIG.3.7-VARIATION OF  $\phi_x$  FOR VARIOUS VALUES OF  $d/T$  &  $b/d$ .  
 $b/T=1$  AND  $K_1/K_2=1$  FIXED.

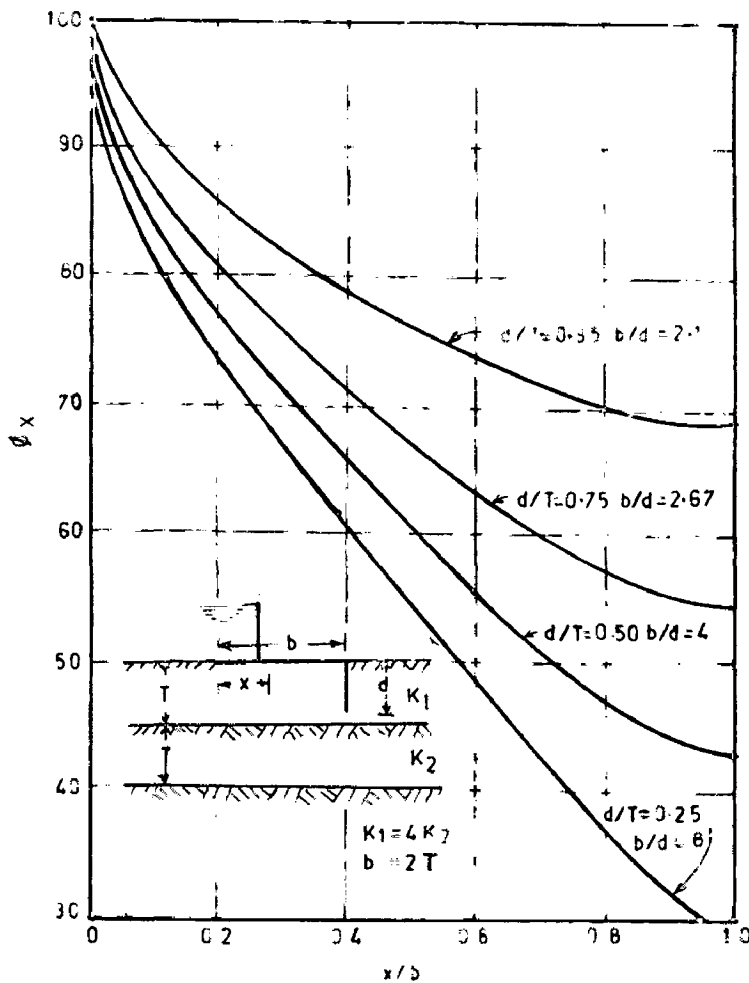


FIG.3.8-VARIATION OF  $\phi_x$  FOR VARIOUS VALUES OF  $d/T$  &  $b/d$ ,  
 $b/T=2$  AND  $K_1/K_2=4$  FIXED.

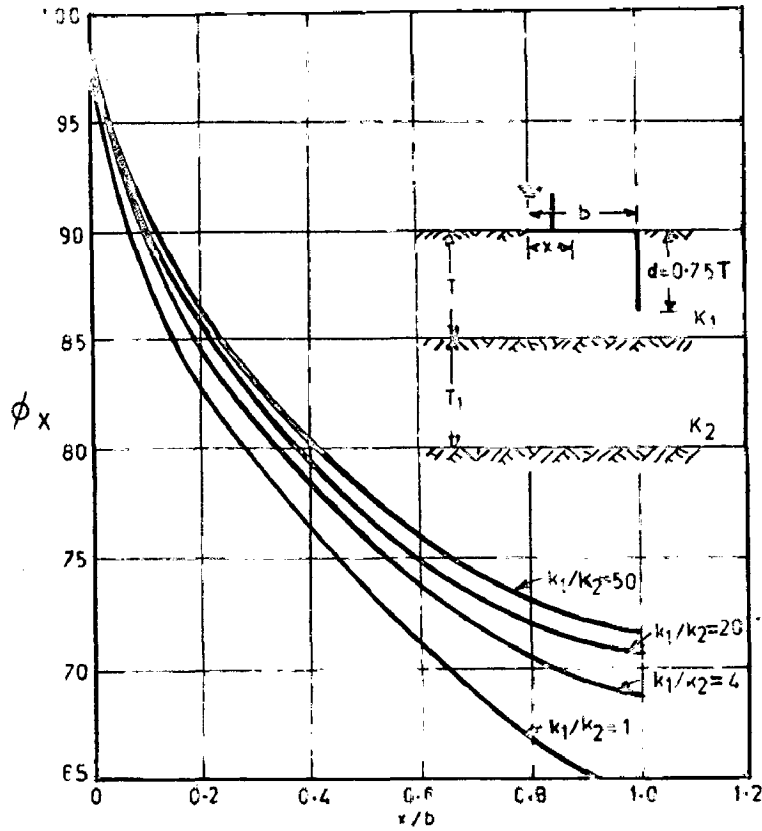


FIG.3.9-VARIATION OF  $\phi_x$  FOR VARIOUS VALUES OF  $k_1/k_2$   $b/T=1$ ,  $d/T=0.75$  AND  $b/l=1.33$  FIXED.

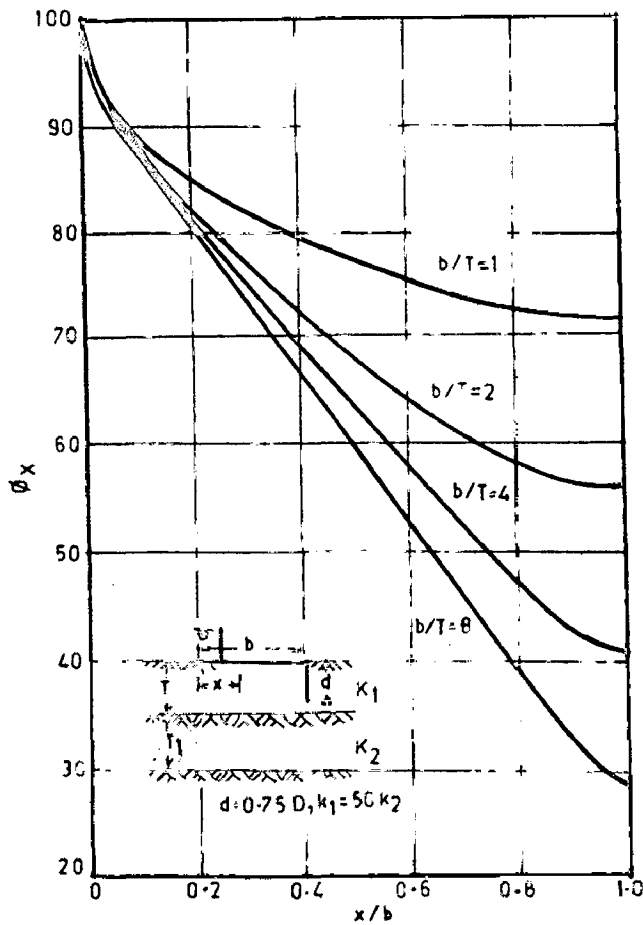


FIG.3.10-VARIATION OF  $\phi_x$  FOR VARIOUS VALUES OF  $b/T$ ,  $k_1/k_2=50$   $d/T=0.75$  FIXED.

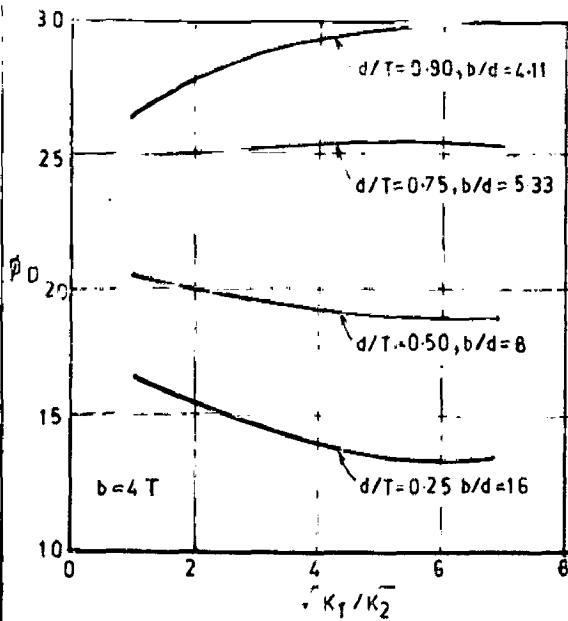


FIG.3.11-INFLUENCE OF  $K_1/K_2$   $d/T$  ON  $\phi_D$  FOR  $b/T=4$ .

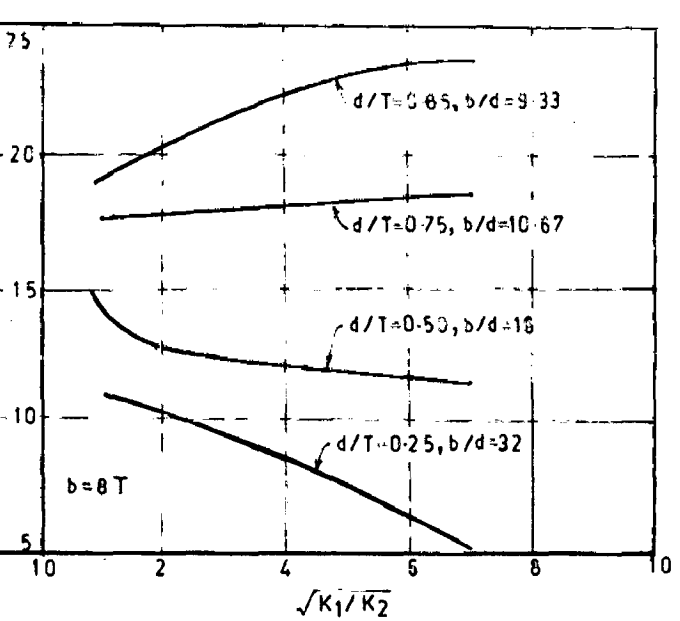


FIG.3.11(a)-INFLUENCE OF  $K_1/K_2$ ,  $d/T$ ,  $b/d$  ON  $\phi_D$  FOR  $b/T=8$ .

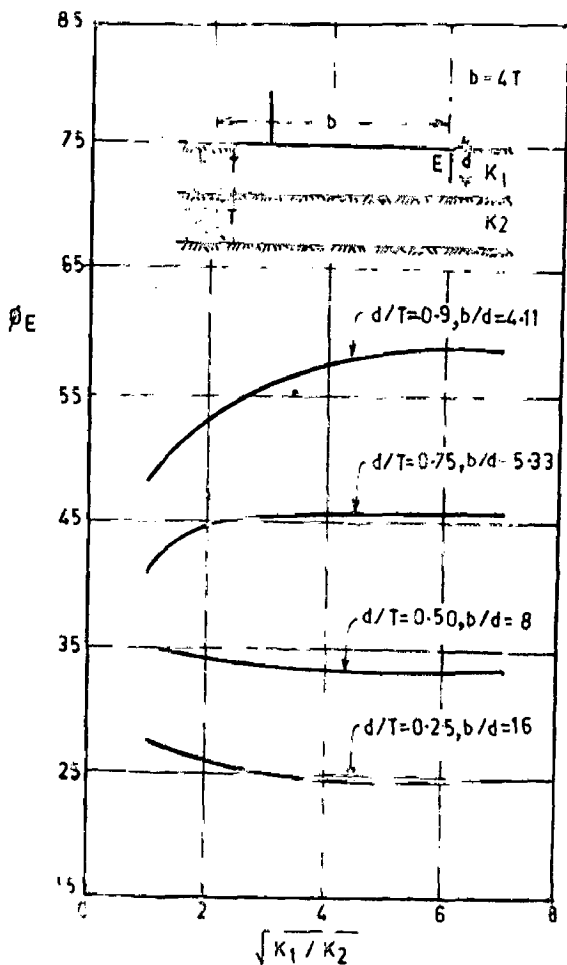


FIG.3.12-INFLUENCE OF  $K_1/K_2$ ,  $d/T$ ,  $b/d$  ON  $\phi_E$  FOR  $b/T=4$  FIXED

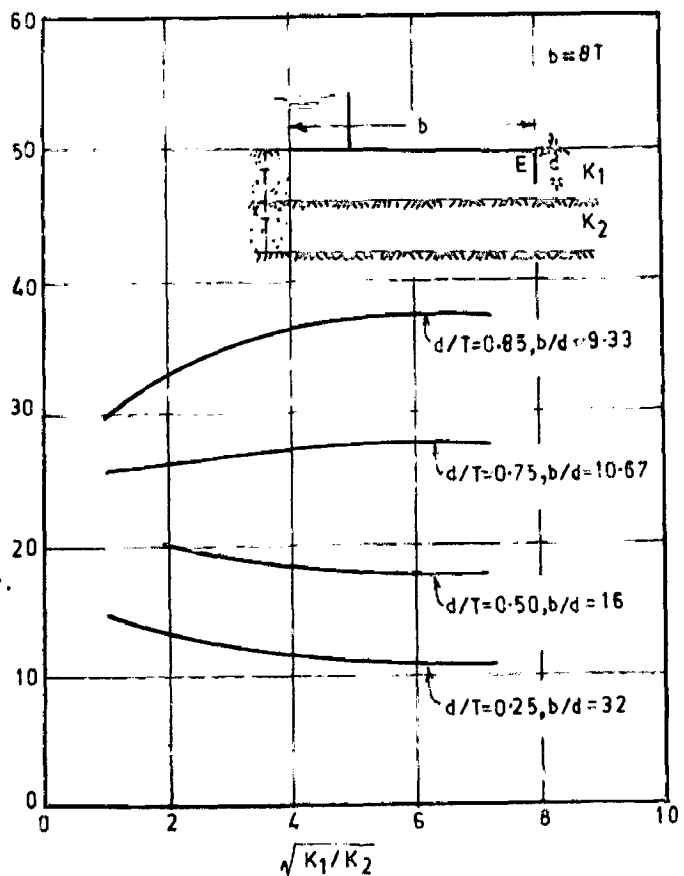


FIG.3.12(a)-INFLUENCE OF  $K_1/K_2$ ,  $d/T$ ,  $b/d$  ON  $\phi_E$  FOR  $b/T=8$  FIXED.

108320

Sharma et al have calculated exit gradient and uplift pressures below floor with end cut off from closed form solutions for  $k_2/k_1 = 0, 1$  and  $\infty$  and employed electrical analogy model for  $k_2/k_1 = 0, 1, 10$  and  $100$ . The theoretical and model test results for  $k_2/k_1 = 0$  and  $1$  were compared and found almost identical. The uplift pressures at the key points i.e., at the junction of the floor and cutoff, E and at the tip of the cut off, D for  $d/T_1 = 0.25, 0.5$  are shown in Figs. 3.13 to 3.16. The values of  $G_E \frac{T}{H}$  for various values of  $b/T_1$  and  $d/T_1$  are also shown in Fig. 3.17. Results of the studies indicate that

- (i) With the increase in the value of  $k_2/k_1$ , the uplift pressures increase in the portion of the floor where pressures are less than 50 per cent and decrease in the portion where pressures are more than 50 per cent (Fig. 3.18).
- (ii) As indicated by the studies conducted by Alamsingh the uplift pressures increase with increase in the penetration ratio and decrease at the corresponding point with increase in length of the floor (Fig. 3.20). However the pressures below floor are not affected by increase in length of the floor for large value of  $k_2/k_1$  i.e.,  $\geq 100$ .
- (iii) Thickness of lower stratum has insignificant effect on the uplift pressures (Fig. 3.19).
- (iv) The value of exit gradient, increases with increase in the permeability of lower layer (Fig. 3.17). Increase in the length of the floor has practically insignificant

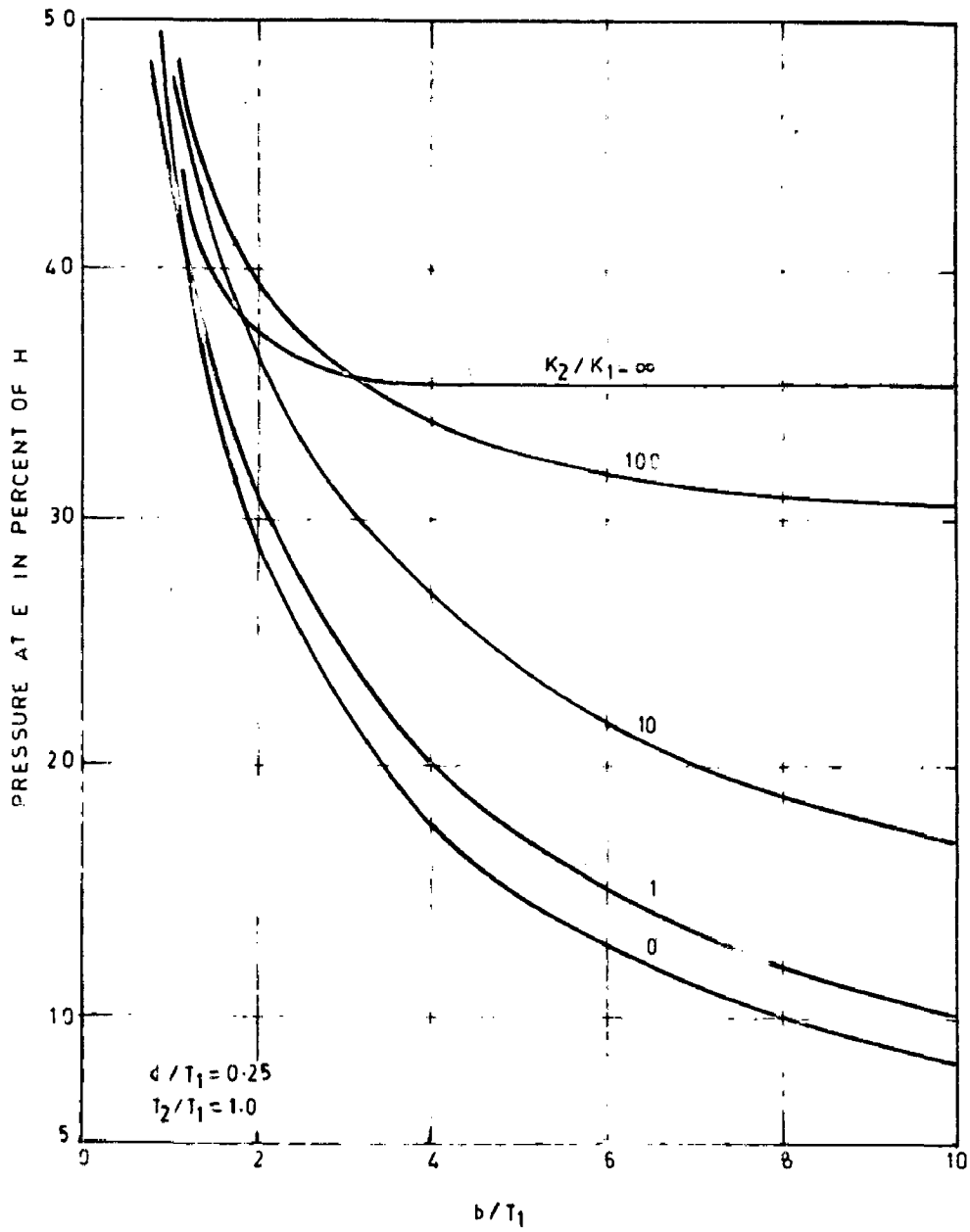
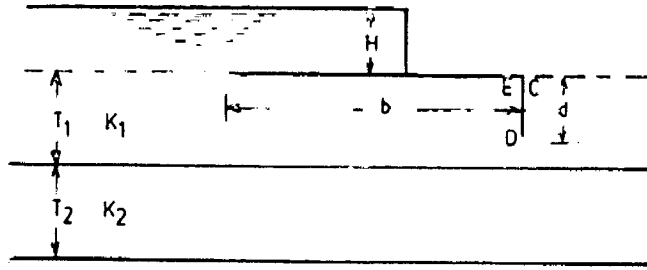


FIG 3-13-UPLIFT PRESSURES ON FLOOR.

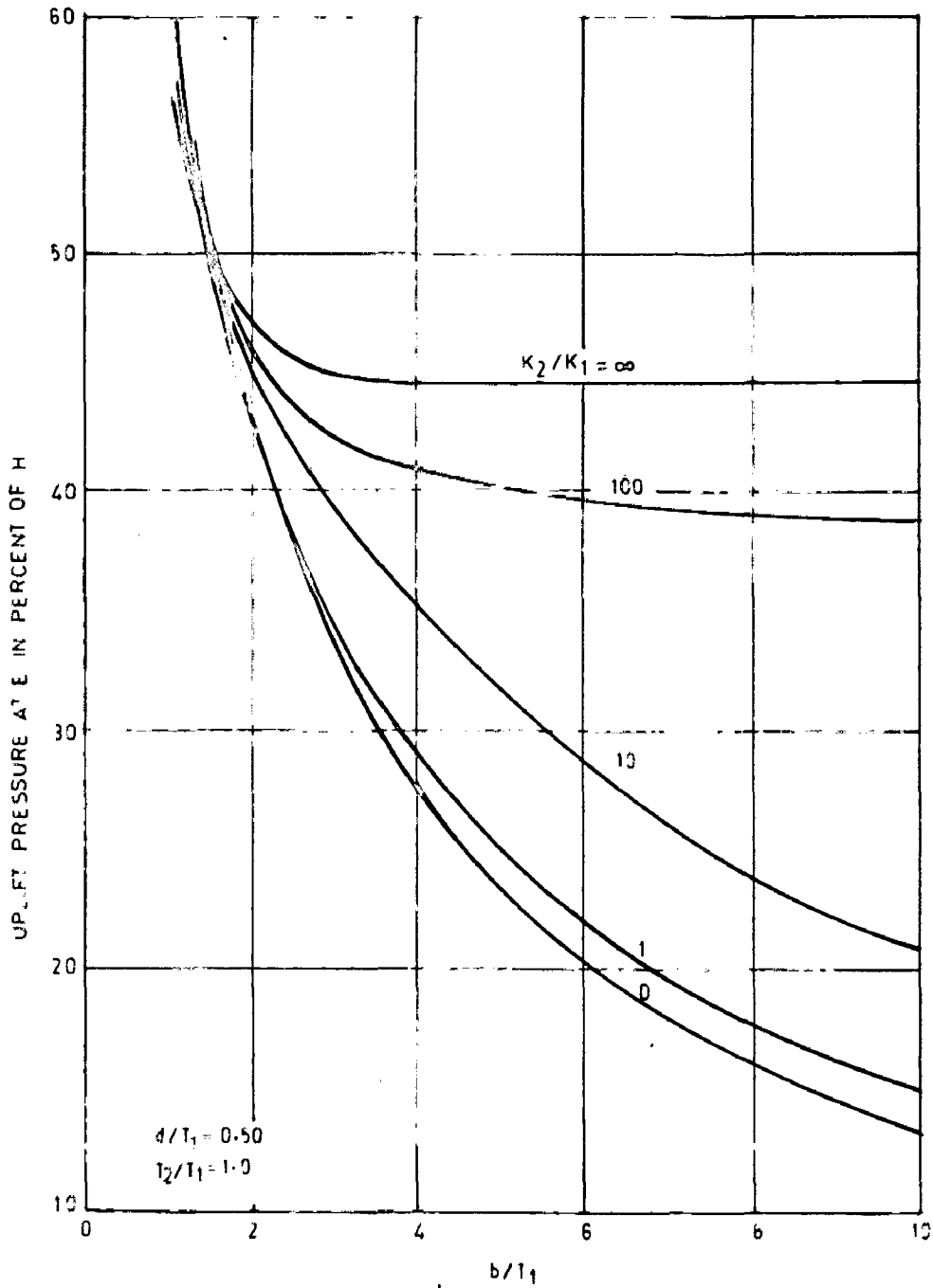
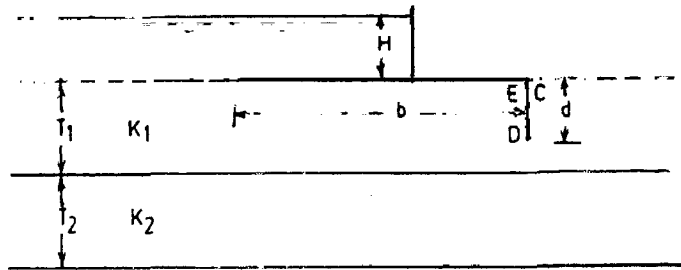


FIG 3.14-UPLIFT PRESSURES ON FLOOR



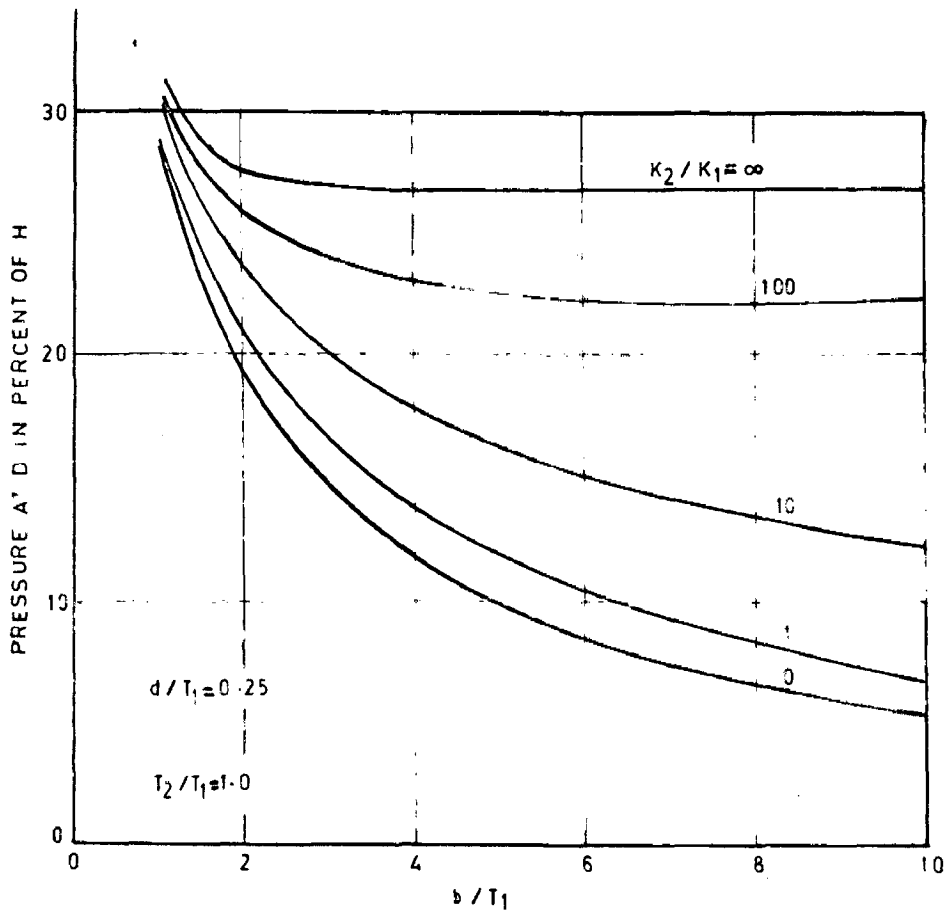
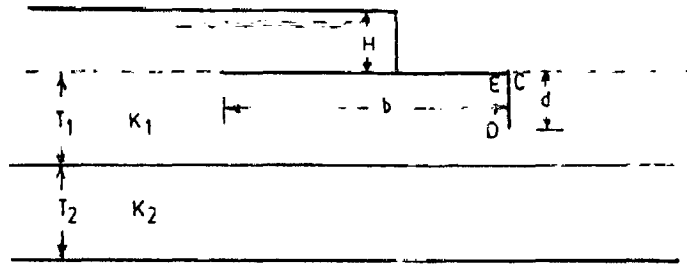


FIG. 3-15-UPLIFT PRESSURES AT BOTTOM OF CUTOFF.

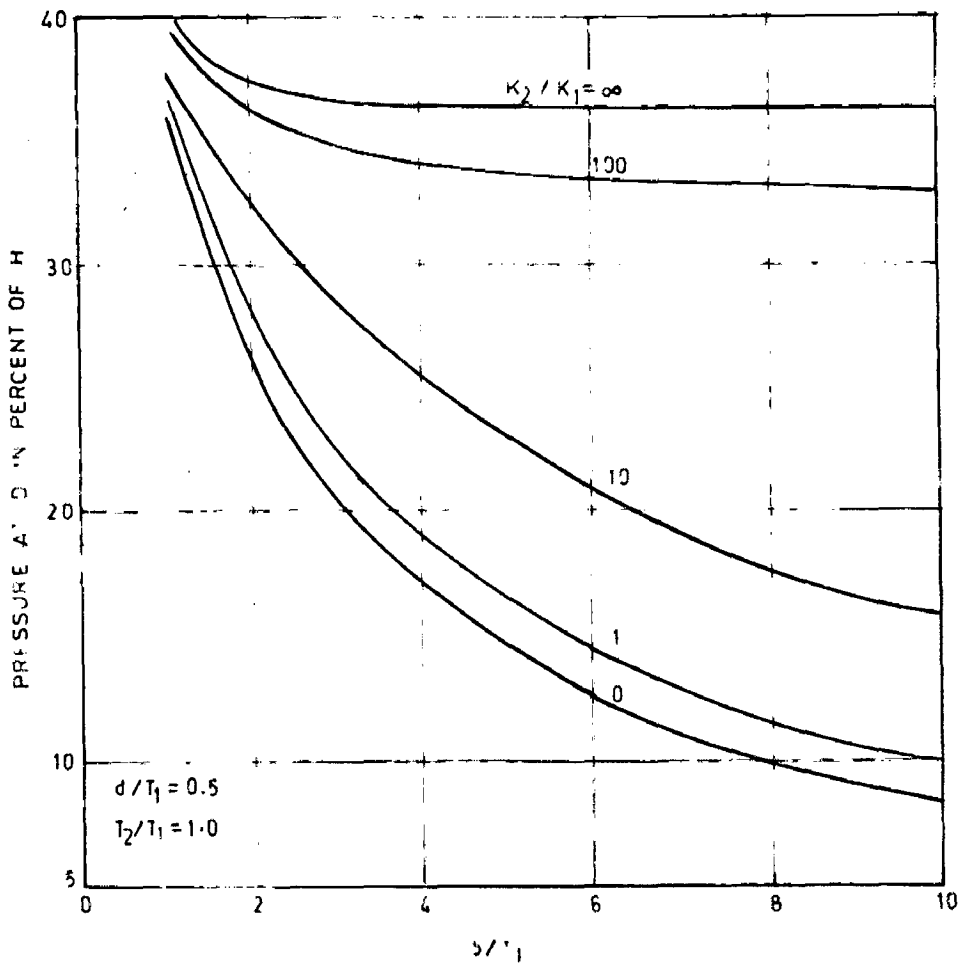
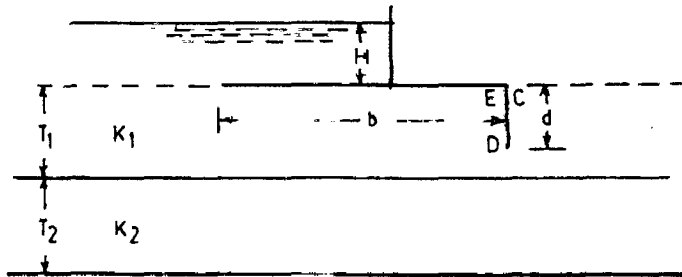


FIG 3-16-UPLIFT PRESSURES AT BOTTOM OF CUTOFF.

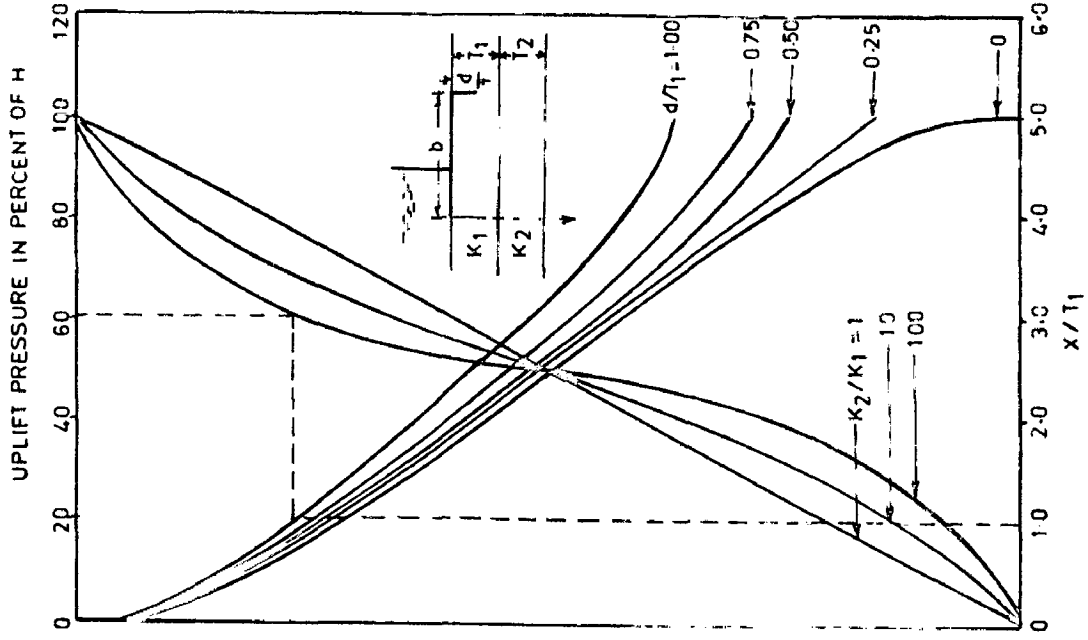


FIG.3-18-UPLIFT PRESSURE BELOW FLOOR  
 $T_2/T_1 = 1.0$ .

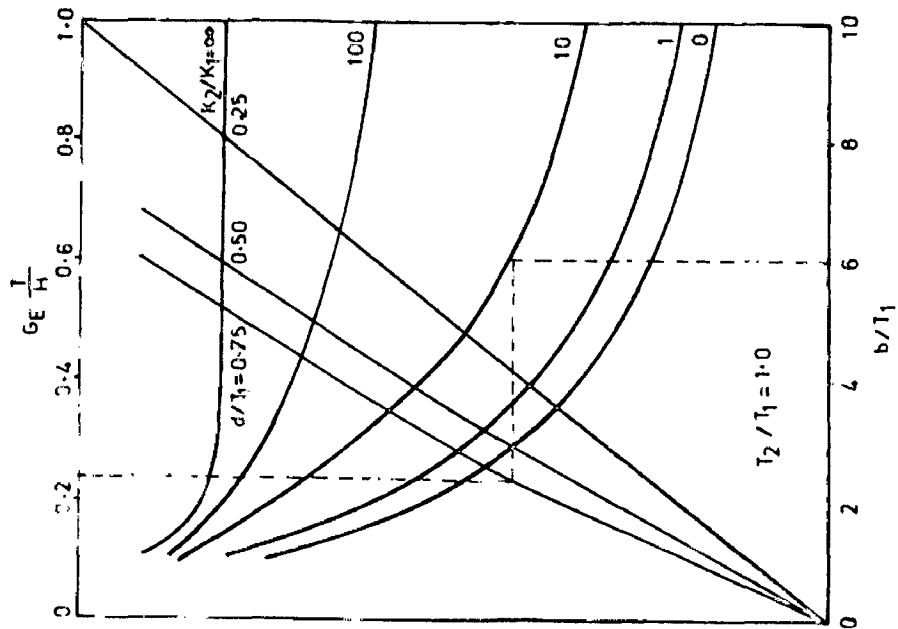
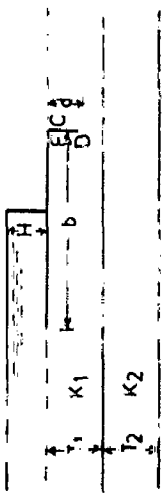


FIG.3-17-EXIT GRADIENT AT C.

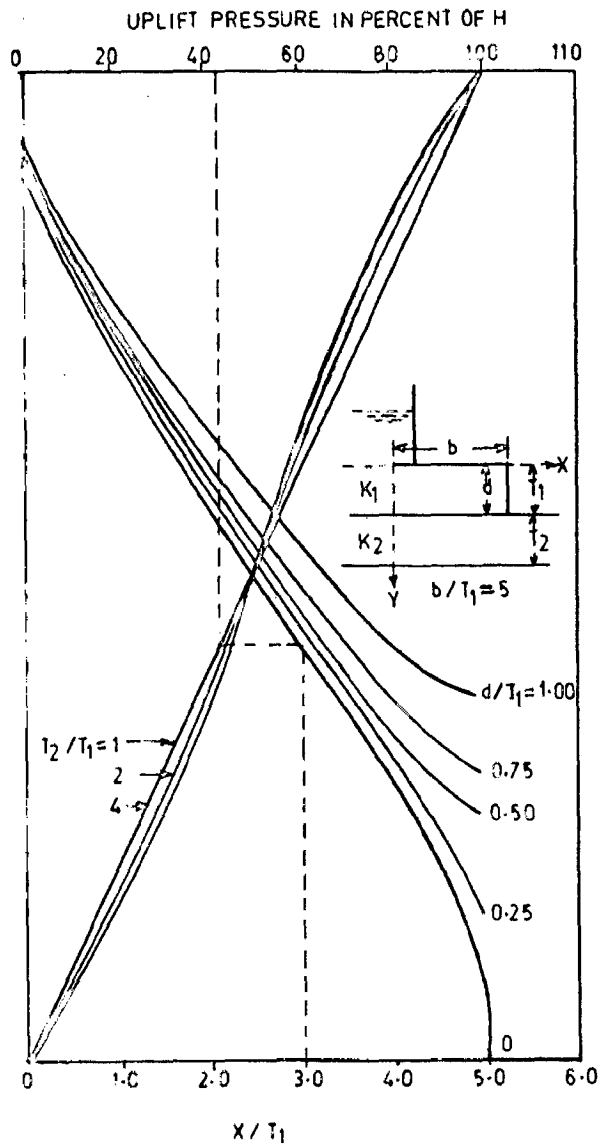


FIG. 3-19-UPLIFT PRESSURES BELOW FLOOR  $K_2/K_1=1$ .

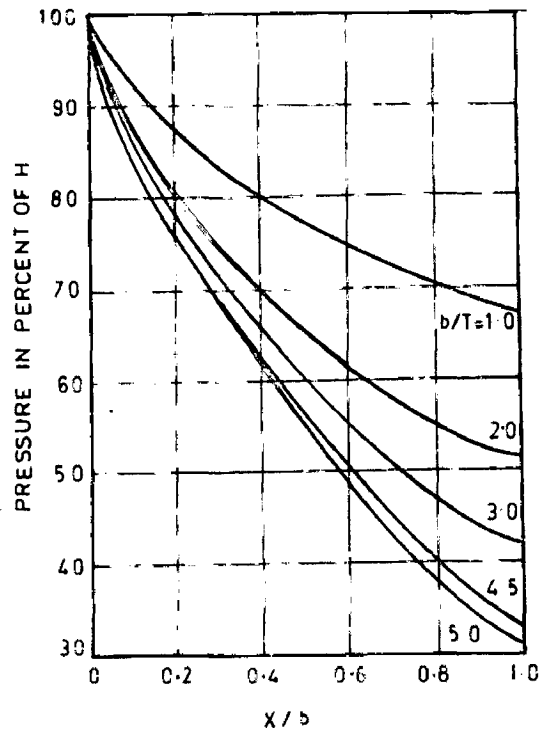


FIG. 3.20-UPLIFT PRESSURES BELOW FLOOR  $K_2/K_1=1$ ,  
 $d/T_1=0.75, T_2/T_1=1$ .

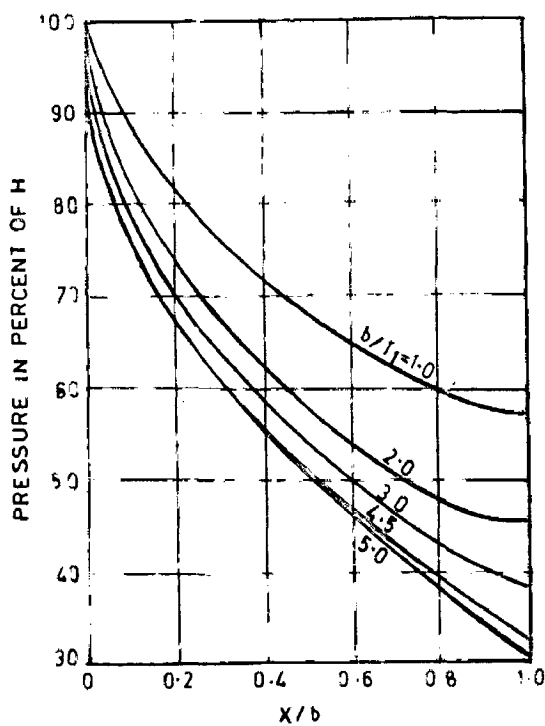


FIG. 3.20(a)-UPLIFT PRESSURE BELOW APRON  $K_2/K_1=10$ ,  
 $d/T_1=0.50, T_2/T_1=1$ .

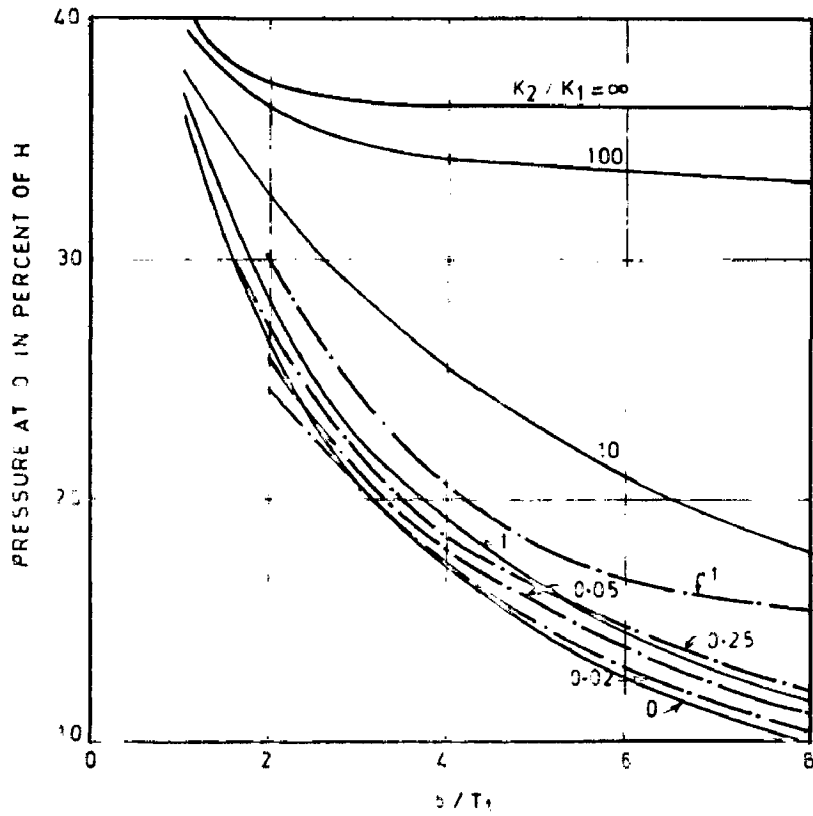
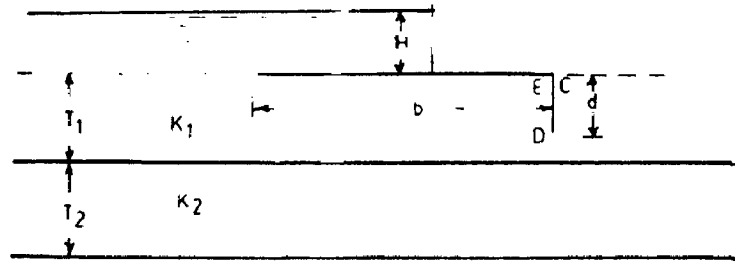
effect on the value of exit gradient for  $k_2/k_1 > 10$ .

(v) Increase in the depth of cut off has little effect in reducing the value of exit gradient when the permeability of the lower stratum is higher than the upper stratum.

The study conducted by Alamsingh et. al gives values of uplift pressures at D and E for  $k_2/k_1 = 1.0, 0.25, 0.05$  and  $0.02$ . The experimental values for  $k_2/k_1 = 1.0, 0.25, 0.05$  and  $0.02$  should fall along those for  $k_2/k_1 = 1.0$  and between those for  $k_2/k_1 = 1.0$  and  $k_2/k_1 = 0$  obtained theoretically by Sharma et. al. In order to compare these experimental results with those obtained by Sharma at al theoretically for  $k_2/k_1 = 0$  and  $1.0$  these were plotted on Fig. 3.21. However a perusal of this figure indicates that the pressures obtained experimentally by Alamsingh et al are higher than those calculated theoretically.

### 3.5 FLOOR WITH INTERMEDIATE CUT OFF ON TWO STRATA (OF EQUAL THICKNESS)

Punmia et al(17) conducted electrical analogy model studies to determine the uplift pressures below hydraulic structures with intermediate cut off founded on two layered media of equal thickness. The permeability of the upper layer was more than that of lower layer. Model tests were conducted with various combinations of  $b/T$ ,  $d/T$ ,  $b_1/b$  and  $k_1/k_2$  where  $b_1$  is the distance of cut off from upstream end of floor. The results of the studies indicate that -



LEGEND:-  
 CURVES OF SHARMA'S EXPERIMENTS ...  
 CURVES OF ALAM SINGH'S EXPERIMENTS ...

FIG.3-21-UPLIFT PRESSURES AT BOTTOM OF CUTOFF.

- (i) With increase in value of  $k_1/k_2$  the pressures on the floor on upstream side of cut off increase while the pressures decrease on down stream side.
- (ii) While the other parameters are not altered, the pressure at points on the upstream side of cut off increases with increase in depth of cut off or penetration ratio and the reverse is true for points on downstream of cutoff.
- (iii) With the other parameters being kept constant, the pressure at points on upstream side of cut off increases as the width of apron decreases and it decreases with decrease in width of apron on downstream side.
- (iv) The pressure on the floor on upstream side of cut-off decreases as the distance of cut off from upstream floor end increases.
- (v) Pressure at key points namely junction of floors cutoff ( $\phi_E$ ) and tip of cut off decreases as width of apron (floor) increases (keeping other parameters unchanged)
- (vi) Both  $\phi_E$  and  $\phi_D$  increase with increase in depth of cut off.
- (vii)  $\phi_E$  and  $\phi_D$  increase with increase in  $k_1/k_2$  while the other ratios are kept constant.

### 3.6 TWO LAYERED MEDIA (FOUNDATION ) WITH A CUT OFF AT UPSTREAM END

A study of two dimensional seepage under a flat bottomed structure with a cut off at upstream and resting



on two horizontal layers of different permeabilities and equal thicknesses (Fig.3.22) using a simple electrical analog was made by Stefan (23) .

By current measurements and by using the well known analog

$$q / k_1 H = i / \sigma_1 v$$

where

$q$  = total seepage discharge per unit length.

$k_1$  = permeability coefficient of upper layer.

$H$  = Difference in pressure head

$i$  = current

$\sigma_1$  = conductivity of upper layer

$v$  = voltage applied between electrodes.

the dimensionless flow rate is  $q / k_1 H$  was obtained and the results were plotted by the author (Fig.3.23) as a function of permeability ratio  $k_2 / k_1$  , given by a parameter  $\epsilon$  defined by

$$\tan \pi \epsilon = \sqrt{k_2 / k_1}$$

The lengths of the flat bottomed structure and sheet pile cut off (each relative to thickness of layers) and also the permeability ratio were varied.

The analytical solutions of pollubarinova-Kochina, which are special cases of boundary geometries, investigated using electrical analogy were also reproduced for completeness and reference.

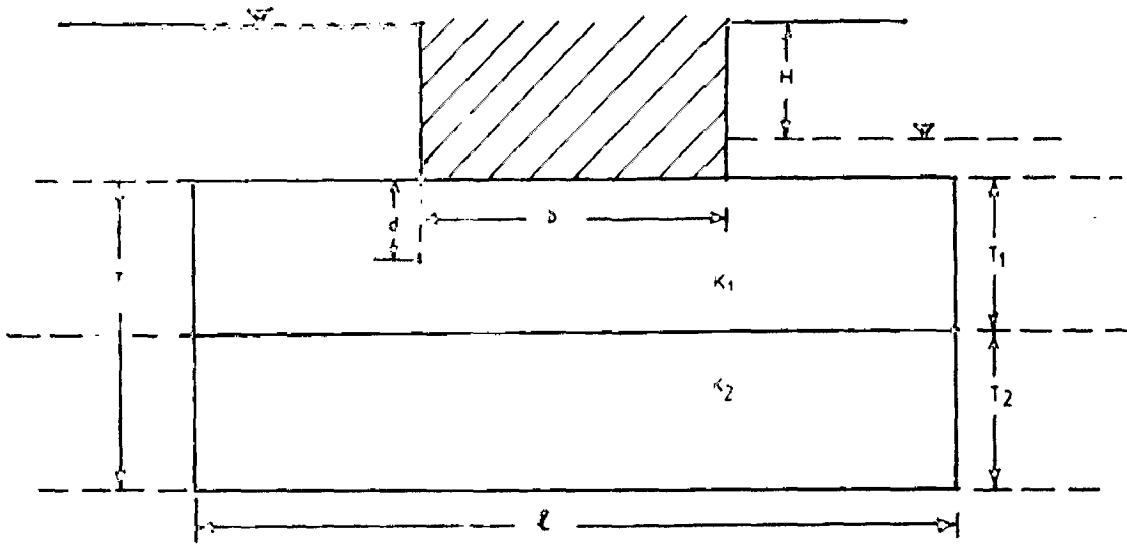


FIG.3.22-FLOOR ON TWO LAYERED MEDIA WITH UPSTREAM END CUTOFF

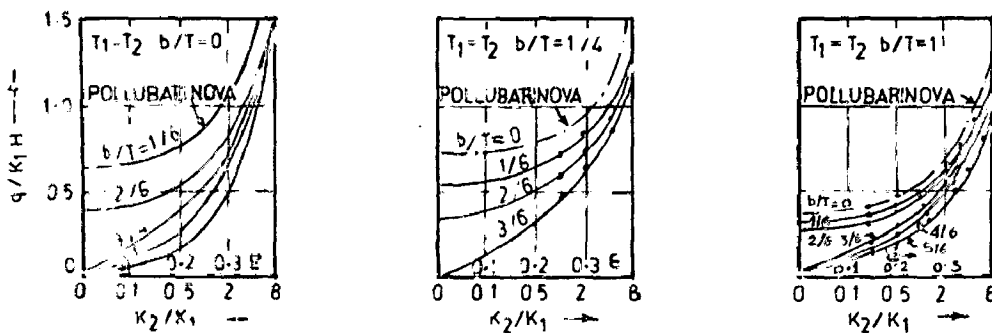


FIG.3.23-DIMENSIONLESS FLOW RATE THROUGH FOUNDATION AS FUNCTION OF LENGTH OF FLAT STRUCTURE DEPTH OF CUTOFF WALL AND PERMEABILITY RATIO OF TWO PERVIOUS LAYERS.

The author concluded praising the technique of investigation as very simple and easy. It may be helpful for those not experienced in seepage flow studies. The results of the study presented provide a basis for evaluating seepage flow through two layers of different permeabilities with upstream cut off.

### 3.7. TWO LAYERED MEDIA (FOUNDATION) WITH TWO CUT OFFS

The effect of foundation stratification on seepage under a hydraulic structure, on the underground contours and foundations of the spillways dams of the volga hydro electric stations named after V.I. Lenin was studied by Ronzhin (20). The foundation of the first dam was composed of three distinct layers and the second dam foundation of two layers. The underground contours comprised an upstream apron, two sheet piling walls and the spillway foundation slab.

The two layered foundation was tested by the electrical analogy method at different ratios of permeability coefficients of individual layers and at various permeabilities of sheet pile walls, but without considering the permeability of the upstream apron and that of concrete of body of dam. In the laboratory models, the upstream apron sheet piling and sheet piling under the dam were cut to the full depth of the first layer of the foundation like in the prototype. The test results showed that the diagram of

It is noteworthy that experimental curves fall well below theoretical ones in the range of high permeability ratios, the reason being limited length of model. The author indicated that errors in flow rate measurements were caused by limited length of analog paper.

A second point of investigation as observed by the author related to the pressure distribution along cutoff wall and base of structure. Local differential pressure heads with reference to downstream water level for various lengths of cut off and for various permeability ratios were shown. The author pointed out the permeability had no dramatic effect on pressures. However the pressure under the horizontal base of the structure increased with increase in permeability of lower layer.

Terming the ratio of difference in pressure head (at a point below the floor) to the distance of the point from downstream edge of the floor as 'average exit gradient', the author studied its variation for different ratios of width of floor to depth of media, and obtained finite values of exit gradient. But the author's conception of a finite value of exit gradient (at the downstream edge of floor) is wrong, when there is no cut off at downstream edge of floor. In such a case the exit gradient will be infinite under any conditions.

The author concluded praising the technique of investigation as very simple and easy. It may be helpful for those not experienced in seepage flow studies. The results of the study presented provide a basis for evaluating seepage flow through two layers of different permeabilities with upstream cut off.

### 3.7. TWO LAYERED MEDIA (FOUNDATION) WITH TWO CUT OFFS

The effect of foundation stratification on seepage under a hydraulic structure, on the underground contours and foundations of the spillways dams of the volga hydro electric stations named after V.I. Lenin was studied by Ronzhin (20). The foundation of the first dam was composed of three distinct layers and the second dam foundation of two layers. The underground contours comprised an upstream apron, two sheet piling walls and the spillway foundation slab.

The two layered foundation was tested by the electrical analogy method at different ratios of permeability coefficients of individual layers and at various permeabilities of sheet pile walls, but without considering the permeability of the upstream apron and that of concrete of body of dam. In the laboratory models, the upstream apron sheet piling and sheet piling under the dam were cut to the full depth of the first layer of the foundation like in the prototype. The test results showed that the diagram of

seepage uplift pressure acting on the underground contour changed with the increase in relative permeability of the lower layer in comparison with the permeability of the upper layer. Head losses on the sheet pilings decreased while those on the upstream apron increased. The same phenomenon took place by increasing the permeability of sheet pile, but the character of seepage pattern change was different. There was practically no change in the seepage pattern in the dam foundation even after increasing the permeabilities of sheet pile and lower soil layer from 0 to 0.002 . But only after further increasing the permeabilities of sheet pile under the dam or that of lower soil layer, a considerable change of seepage under dam occurred.

Ranzhin also studied the effect of the foundation consisting of three layers of different permeabilities. In the tests the permeabilities of upper and lower layers were assumed to be equal, with the middle layer having different permeabilities.

The elements of the dam underground were supposed to be impermeable in the tests. The first and the second layers were modelled to be traversed by the upstream apron cut off and cutoff under the dam. Under such conditions the

seepage uplift pressures on the upstream apron increased and that on the bas of the damspillway decreased with the increase of the middle layer permeability. However, the seepage uplift pressure on the upstream apron was found to be increasing with the increase in the relative permeability of the (soil foundation) middle layer from 0.05 to 1.

## C H A P T E R - I V

### ANISOTROPIC FOUNDATION

#### 4.0 GENERAL

Pervious soils may be subdivided into isotropic and anisotropic. In isotropic soils, the coefficient of permeability at any point is independent of direction of seepage velocity. Isotropic soils are further subdivided into homogeneous and non homogeneous soils. The permeability coefficient of homogeneous soils is independent of the coordinates of the seepage region and is constant throughout. In inhomogeneous soils the permeability coefficient depends on the coordinates of the seepage region. In anisotropic soils, the permeability coefficient is dependent on the direction of seepage velocity. The soil is said to be homogeneous and anisotropic if the permeability coefficient is dependent on the direction of velocity and if this directional dependence is the same at all points of flow region. In such a case the permeability coefficient is independent of coordinates of seepage region.

In nature, it is very difficult to get isotropic soils. Most soils are anisotropic to some degree and hence the isotropy of a soil is an ideal case and true for theoretical considerations only. One of the marked properties



found from the soil samples obtained from river bed is "transverse anisotropy" wherein the permeability coefficient parallel to bedding planes is different from that normal to it. The average permeability of a natural deposit of silt in the horizontal direction has been shown to be equal to 2 to 10 times that in the vertical direction (24). The ratio becomes larger than 10 for distinctly stratified soils. The ratio ( $k_x/k_y$ ) according to Justin may be 4 to 20 and in exceptional cases of horizontal seams, may even go upto 20 to 50. Generally, in natural deposits of homogeneous nature the permeability coefficient in horizontal direction is greater than that in vertical direction with one exception of Loess, where the opposite true.

If the direction of maximum permeability in the case of 'inclined anisotropy' caused by geological formations of bed, is inclined towards the river bed then it is of serious consequence to the stability of structure and cannot be overlooked.

The manner in which the permeability coefficient may vary at some point (say 'A') in an anisotropic soil is shown schematically in Fig. 4.1.

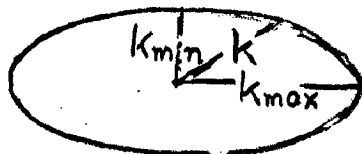


Fig. 4.1

The magnitude  $k$  of the radius vector is proportional to the value of the permeability coefficient and its direction coincides with that of the seepage velocity. There are two specific directions in which the permeability coefficient attains a least value of  $k_{\min}$  and greatest value of  $k_{\max}$ . as shown in Fig.4.1 These two directions together with a third one perpendicular to them are referred to as "principal directions of anisotropy of soil". A soil often proves to be anisotropic because it is made up of alternating layers having different permeabilities. If, in an anisotropic soil, the principal directions of anisotropy and the values of  $k_{\max}$  and  $k_{\min}$  are independent of the coordinates of the seepage region, then the soil is called "homogeneous anisotropic". On the other hand, if either the principal directions of anisotropy, or the values of  $k_{\max}$  and  $k_{\min}$ , or both characteristics, are functions of the coordinates, then the soil is said to be "inhomogeneous anisotropic".

In case the principal directions of anisotropic soil coincide with the coordinate axes of the physical plane i.e. the principal directions of permeability are horizontal or vertical, then seepage below a hydraulic structure can be analysed easily. The shape of the actual flow domain is similar to the shape of the transformed, fictitious, isotropic system. Let  $k_x, k_y$  and  $k_z$  be the principal values of coefficient of permeability in the

direction of coordinate axes. According to Darcy's law

$$\begin{aligned}v_x &= -k_x \frac{\partial h}{\partial x} \\v_y &= -k_y \frac{\partial h}{\partial y} \quad \dots(4.1) \\v_z &= -k_z \frac{\partial h}{\partial z}\end{aligned}$$

From continuity equation,

$$\frac{\partial v_x}{\partial x} + \frac{\partial v_y}{\partial y} + \frac{\partial v_z}{\partial z} = 0 \quad \dots(4.2)$$

From equations (4.1) and (4.2) we get,

$$k_x \frac{\partial^2 h}{\partial x^2} + k_y \frac{\partial^2 h}{\partial y^2} + k_z \frac{\partial^2 h}{\partial z^2} = 0 \quad \dots(4.3)$$

This equation (4.3) can be transformed by substituting

$$\bar{x} = \frac{x}{\sqrt{k_x}}, \quad \bar{y} = \frac{y}{\sqrt{k_y}}, \quad \bar{z} = \frac{z}{\sqrt{k_z}} \quad \dots(4.4)$$

The transformed differential equation is

$$\frac{\partial^2 h}{\partial \bar{x}^2} + \frac{\partial^2 h}{\partial \bar{y}^2} + \frac{\partial^2 h}{\partial \bar{z}^2} = 0 \quad \dots(4.5)$$

which is the Laplace's equation.

Thus the effect of anisotropy of the medium is obtained by transforming the coordinates system and solving Laplace's equation in the transformed plane.

The equivalent isotropic permeability of the transformed system is given by  $\sqrt[3]{k_x k_y k_z}$  for three dimensional flow or  $\sqrt{k_x k_y}$  for two dimensional flow.

#### 4.1 EQUATIONS OF MOTION IN HOMOGENEOUS ANISOTROPIC MEDIUM

When the principal directions of coefficient of permeabilities do not coincide with Horizontal or vertical directions the simple transformation described above is not applicable. In such a case the shape of the boundaries is also deformed.

For isotropic soil

$$V = -K \text{ grad } h$$

where  $K =$  seepage coefficient

...(4.6)

$$h = \frac{p}{\rho g} + y + \text{constant}$$

For homogeneous anisotropic soil, a symmetric seepage tensor may be written in the form

$$\begin{vmatrix} K_{11} & K_{12} \\ K_{21} & K_{22} \end{vmatrix}$$

Taking principal axes of this tensor along  $x_1, y_1$  axes of coordinate system, the tensor is

$$\begin{vmatrix} k_{x1} & 0 \\ 0 & k_{y1} \end{vmatrix}$$

where  $k_{x1}$  and  $k_{y1}$  are seepage coefficients in the direction of principal axes.

The equation of motion in  $x_1, y_1$  coordinate can be written as

$$0 = -\frac{1}{\rho} \frac{\partial p}{\partial x_1} - \frac{g}{k_{x1}} u_1 - g \sin \alpha \quad \dots(4.7)$$

$$0 = -\frac{1}{\rho} \frac{\partial p}{\partial y_1} - \frac{g}{k_{y1}} v_1 - g \cos \alpha$$

where  $\alpha$  is the angle measured from horizontal axis.

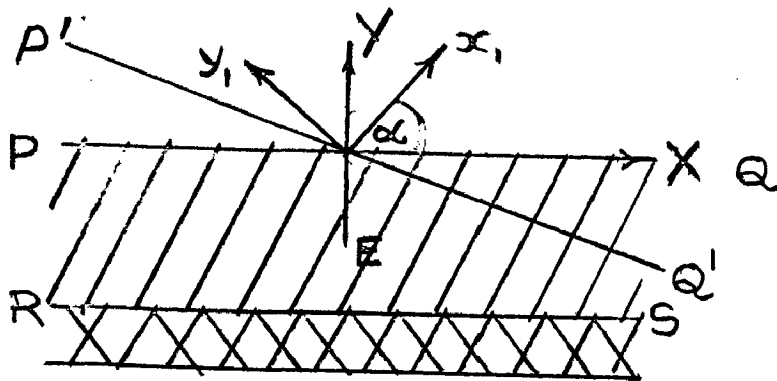


Figure 4.2.

Putting

$$\phi(x_1, y_1) = \frac{-p}{\rho g} - x_1 \sin \alpha - y_1 \cos \alpha \quad \dots(4.8)$$

where

$$u_1 = -k_{x1} \frac{\partial \phi}{\partial x_1} \quad \dots(4.9)$$

$$v_1 = -k_{y1} \frac{\partial \phi}{\partial y_1} \quad \dots(4.10)$$

$\phi$  may be called as the 'reduced head'.

A function  $\psi(x_1, y_1)$ , by means of equalities

$$u_1 = \sqrt{k_{x1} k_{y1}} \frac{\partial \psi}{\partial y_1}, \quad v_1 = -\sqrt{k_{x1} k_{y1}} \frac{\partial \psi}{\partial x_1} \quad \dots(4.11)$$

is herein introduced. Continuity equation gives

$$\frac{\partial u_1}{\partial x_1} + \frac{\partial v_1}{\partial y_1} = 0 \quad \dots(4.12)$$

from which it follows that  $\phi$  satisfies Laplace's equation

$$k_{x1} \frac{\partial^2 \phi}{\partial x_1^2} + k_{y1} \frac{\partial^2 \phi}{\partial y_1^2} = 0 \quad \dots(4.13)$$

With further transformation, i.e.  $x = x_1, y_1 = \sqrt{\frac{k_{y1}}{k_{x1}}} y$ ,

$\phi$  satisfies Laplace's equation in the new  $x, y$  coordinates

$$\frac{\partial^2 \phi}{\partial x^2} + \frac{\partial^2 \phi}{\partial y^2} = 0 \quad \dots(4.14)$$

The combination  $\phi + i\psi$  is a function of complex variable  $z = x + iy$ .

The rate of flow through the contour bounded by the arc AB is expressed by means of stream function as

$$Q = \sqrt{k_{x1} k_{y1}} (\Psi_A - \Psi_B) \quad \dots(4.15)$$

The three coordinate systems that were previously introduced are linked by the equations

$$X = x_1 \cos \alpha - y_1 \sin \alpha = x \cos \alpha - v y \sin \alpha \quad \dots(4.16)$$

$$Y = x_1 \sin \alpha + y_1 \cos \alpha = x \sin \alpha + v y \cos \alpha$$

$$x_1 = x = X \cos \alpha + Y \sin \alpha \quad \dots(4.17)$$

$$y_1 = v y = -X \sin \alpha + Y \cos \alpha$$

(here the notation  $v = \frac{\sqrt{k_{y1}}}{\sqrt{k_{x1}}}$  has been introduced)

In particular, the equations of the horizontal lines pQ, RS and of the vertical line MN in the x,y coordinate system are

$$y = -\frac{1}{v} x \operatorname{tg} \alpha$$

$$x \sin \alpha + v y \cos \alpha + h = 0 \quad \dots(4.18)$$

$$y = \frac{1}{v} x \operatorname{ctg} \alpha$$

In Fig. 4.2 p'Q' is the position of PQ in the x,y system.

In the x,y coordinate system, some fictitious flow in the region from that in X,Y plane through the transformation (Eq. 4.16) may be considered. The following conditions on the boundaries of flow region in x,y plane must be satisfied.

(1) On the boundary of water reservoir

$$\phi (x,y) = \text{constant}$$

On  $x_1, y_1$  plane,  $\phi (x_1, y_1) = \text{constant}$

(2) On impervious boundary

$$\psi (x,y) = \text{constant}$$

(3) On the free surface (when the pressure is constant)

$$\phi + x \sin \alpha + v y \cos \alpha = \text{constant} \quad \dots(4.19)$$

$$\psi(x,y) = \text{constant}$$

Differentiating equation(4.19) along S on the free surface (in x,y plane) and multiplying by  $\partial\phi / \partial s$

$$\left( \frac{\partial\phi}{\partial s} \right)^2 + \sin \alpha \frac{\partial\phi}{\partial s} \frac{dx}{ds} + v \cos \alpha \frac{\partial\phi}{\partial s} \frac{dy}{ds} = 0 \quad \dots(4.20)$$

$$\text{If } u = \frac{\partial\phi}{\partial s} \frac{dx}{ds}, \quad v = \frac{\partial\phi}{\partial s} \frac{dy}{ds}$$

$$u^2 + v^2 + u \sin \alpha + v u \cos \alpha = 0 \quad \dots(4.21)$$

which is the equation of a circle, in the plane of u,v (u, and v are the components of fictitious dimensionless velocity).

This circle passes through the origin of coordinates and has its center in the point  $(-1/2 \sin \alpha, -v/2 \cos \alpha)$ .

(4) The equation 4.19 holds good along seepage surface. Assuming that seepage segment to be a straight line, making an angle  $\beta$  with the x axis and differentiating equation



(4.19) with respect to 'S'

$$\frac{\partial \phi}{\partial s} + \sin \alpha \frac{dx}{ds} + v \cos \alpha \frac{dy}{ds} = 0$$

$$\begin{aligned} \frac{\partial \phi}{\partial s} &= \frac{\partial \phi}{\partial x} \frac{dx}{ds} + \frac{\partial \phi}{\partial y} \frac{dy}{ds} \\ &= \frac{\partial \phi}{\partial x} \cos \beta + \frac{\partial \phi}{\partial y} \sin \beta \\ &= u \cos \beta + v \sin \beta \end{aligned}$$

$$\text{Hence } u \cos \beta + v \sin \beta + \sin \alpha \cos \beta + v \cos \alpha \sin \beta = 0 \quad \dots(4.22)$$

which is the equation of a straight line .

This straight line passes through the point  $(-\sin \alpha, v \cos \alpha)$  and is perpendicular to the seepage surface.

Particular Case of Anisotropy: ( $\alpha = 0$ )

In this case for  $v < 1$  there will be horizontal stratification and for  $v > 1$  vertical stratification.

$$\text{Eq. 4.16 becomes } X = x_1 = x$$

$$Y = y_1 = vy$$

The directions of the coordinate system coincide, but in the region of fictitious flow  $(x,y)$ , this change in scale along the y axis holds good i.e the dam foundation preserves its length; but the vertical cut off is shortened

for horizontal stratification and stretched for vertical. The relationship between the reduced flow rate and the pressure according to Eq. 4.8 is

$$\phi(x_1, y_1) = \frac{p}{\rho g} - y_1 \quad \dots(4.23)$$

#### 4.2 FLOOR WITH A CUT OFF

Consider an impervious floor AB of length  $b_1 + b_2 = b$  founded on homogeneous anisotropic permeable soil extending upto infinite depth (Fig.4.3). The floor has a cut off CD of depth  $d$  at a distance  $b_1$  from the upstream end. On the upstream and downstream of the floor is pervious bed extending upto infinity. Along the upstream bed AF,  $\phi = -kH$  and along downstream bed BG,  $\phi = 0$ . The foundation profile AEDCB forms the inner boundary and can therefore be taken as a stream line  $\psi = 0$ .

Let  $\lambda (= k_2/k_1)$  be the coefficient of anisotropy and  $\alpha$  be the angle between x-axis and the principal seepage axis  $\mu$ . The relation between the physical z-plane and the  $\mu, \nu$  plane (where  $\mu$  and  $\nu$  are the directions of principal permeabilities) is given by

$$\begin{aligned} \mu &= x \cos \alpha + y \sin \alpha \\ \nu &= \frac{1}{\sqrt{\lambda}} (-x \sin \alpha + y \cos \alpha) \end{aligned} \quad \dots(4.24)$$

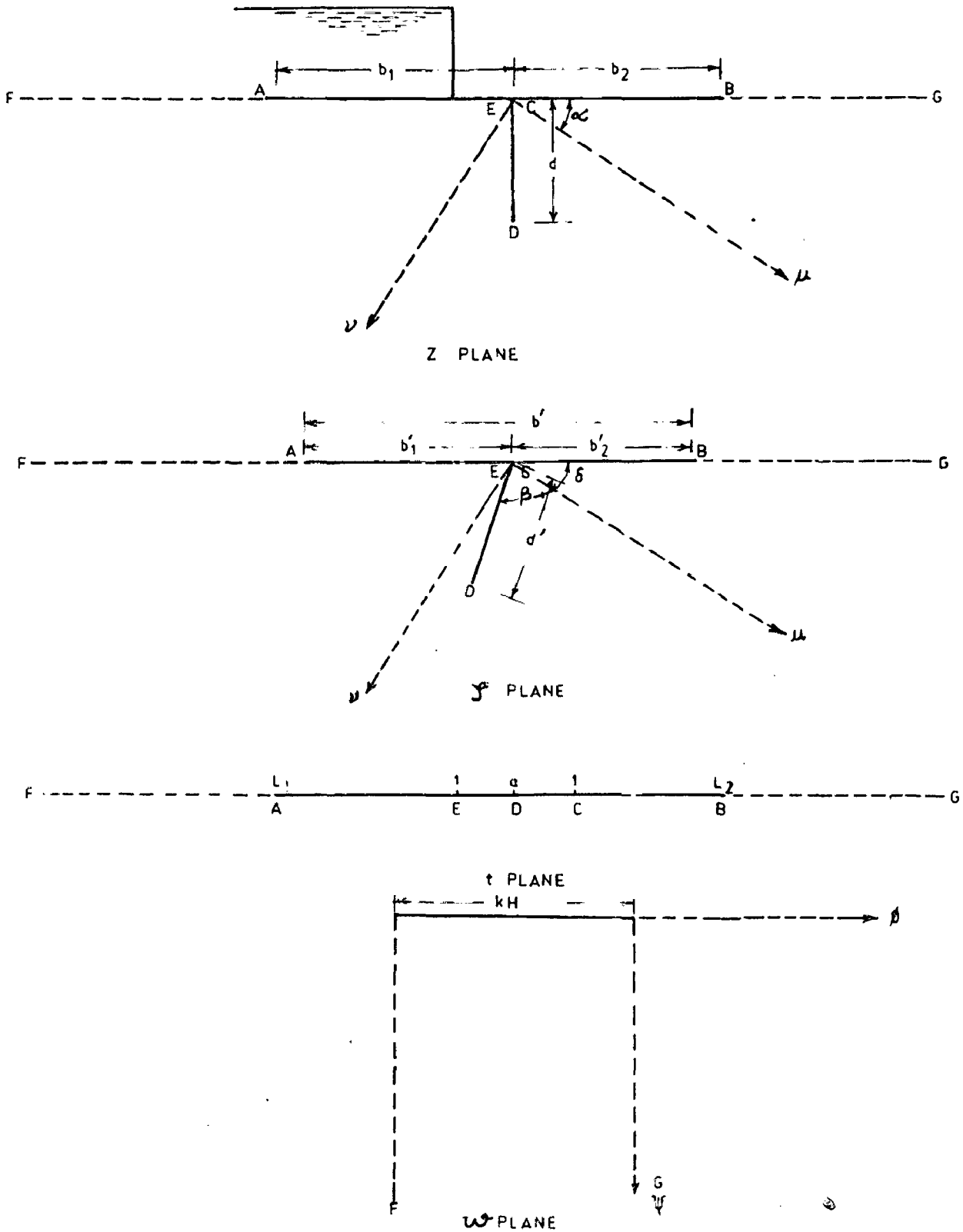


FIG. 4.3 - TRANSFORMATION LAYOUT.

The straight line  $y = 0$  (floor profile) becomes the straight line

$$\frac{v}{\mu} = - \frac{\tan \alpha}{\sqrt{\lambda}} \quad \dots(4.25)$$

Let  $\delta$  be the angle between the new straight line with the  $\mu$  axis

$$\tan \delta = - \frac{\tan \alpha}{\sqrt{\lambda}} \quad \dots(4.26)$$

In the same way the equation of cut off ( $x=0$ ) is transformed on to the straight line

$$\frac{v}{\mu} = \frac{\cot \alpha}{\sqrt{\lambda}} \quad \dots(4.27)$$

If the angle of the transformed cut-off with  $\mu$  axis is  $\beta$ , it is given by

$$\tan \beta = \frac{\cot \alpha}{\sqrt{\lambda}} \quad \dots(4.28)$$

From the Eqs 4.24 we can find the lengths of upstream and downstream aprons in  $\mu - v$  plane

$$b_1'^2 = b_1^2 \left( \cos^2 \alpha + \frac{\sin^2 \alpha}{\lambda} \right) \quad \dots(4.29)$$

$$b_2'^2 = b_2^2 \left( \cos^2 \alpha + \frac{\sin^2 \alpha}{\lambda} \right) \quad \dots(4.30)$$

The depth of cut off is given by ,

$$d'^2 = d^2 \left( \sin^2 \alpha + \frac{\cos^2 \alpha}{\lambda} \right) \quad \dots(4.31)$$

The relation between the ratio of  $b/d$  and  $b'/d'$  have been plotted against various values of  $\lambda$  and  $\alpha$  in Fig. 4.4.

The angle  $\pi\gamma$  between the downstream floor or bed and the cut off in fictitious  $\mu-v$  plane is given

by

$$\pi\gamma = \tan^{-1} \left[ \frac{2\lambda}{(\lambda-1)\sin 2\alpha} \right] \quad \dots(4.32)$$

The value of  $\pi\gamma$  have been plotted against the various values of  $\lambda$  and  $\alpha$  in Fig. 4.5. Transformation of  $\xi$  plane into  $t$ -plane is given by

$$\zeta = A \int (1+t)^{-\gamma} (t-a) (1-t)^{\gamma-1} dt \quad \dots(4.33)$$

Integration of this equation yields

$$\zeta = -A(1+t)^{1-\gamma} (1-t)^{\gamma} \quad \dots(4.34)$$

and  $a = 1 - 2\gamma \quad \dots(4.35)$

From the boundary conditions, we find

$$A = d' \frac{e^{-\pi\gamma i}}{(1+a)^{1-\gamma} (1-a)^{\gamma}} \quad \dots(4.36)$$

The transformation Eq. (4.34) reduces to

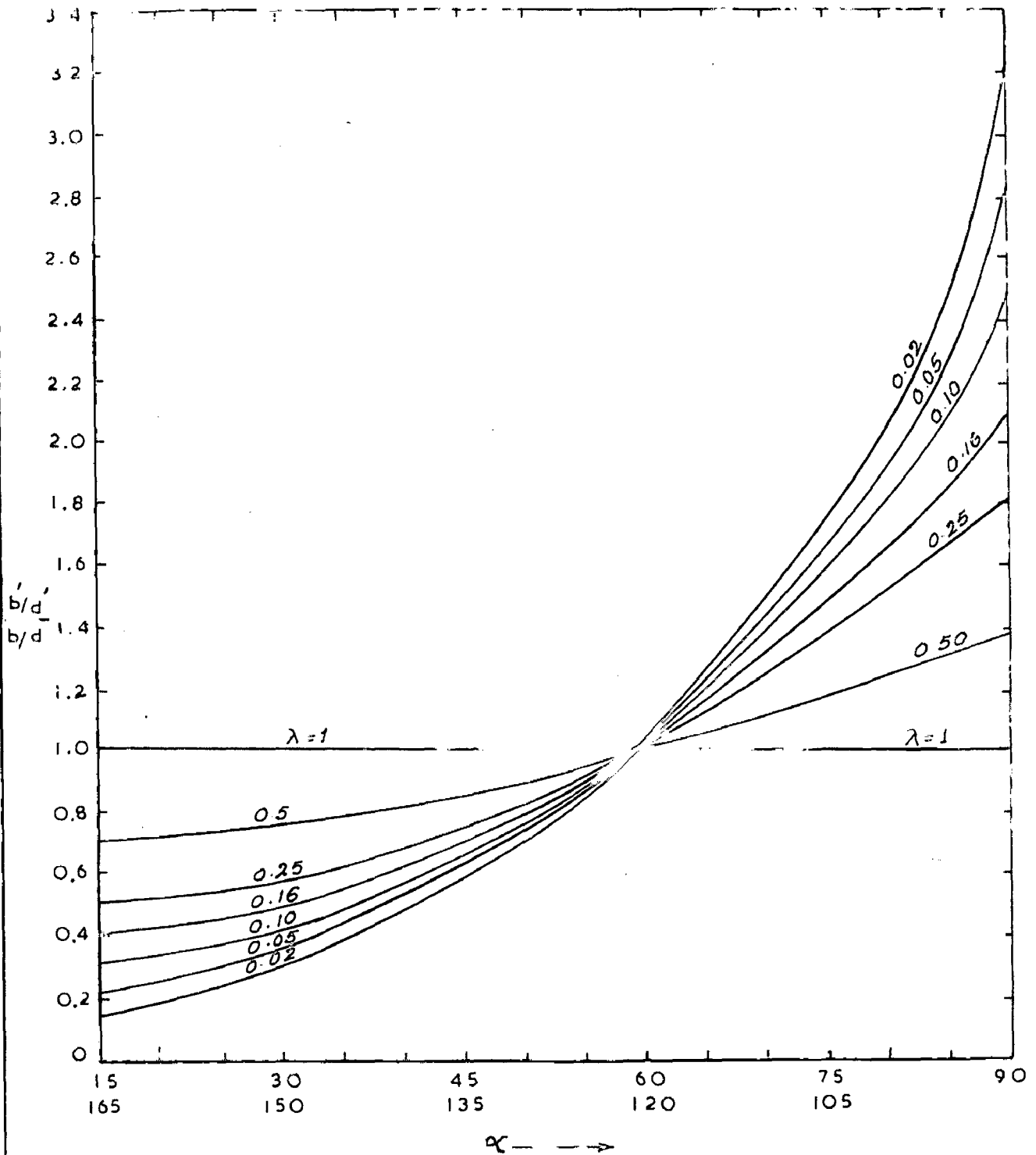


FIG 4 4 VALUES OF  $\frac{b'/d'}{b/d}$  FOR DIFFERENT  $\lambda$  AND  $\alpha$

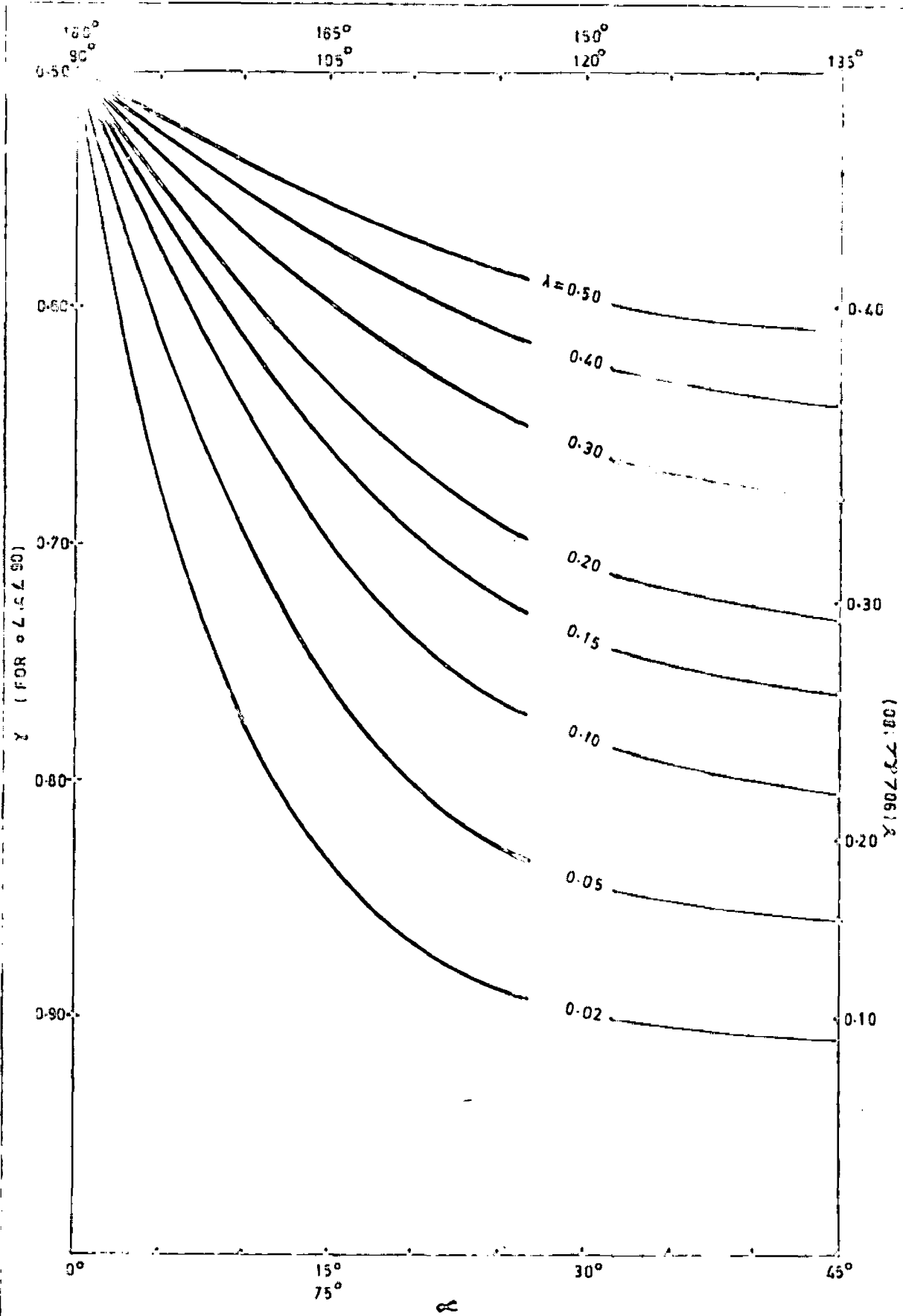


FIG. 4.5-VALUES OF  $r$  FOR VARIOUS VALUES OF  $\alpha$ .

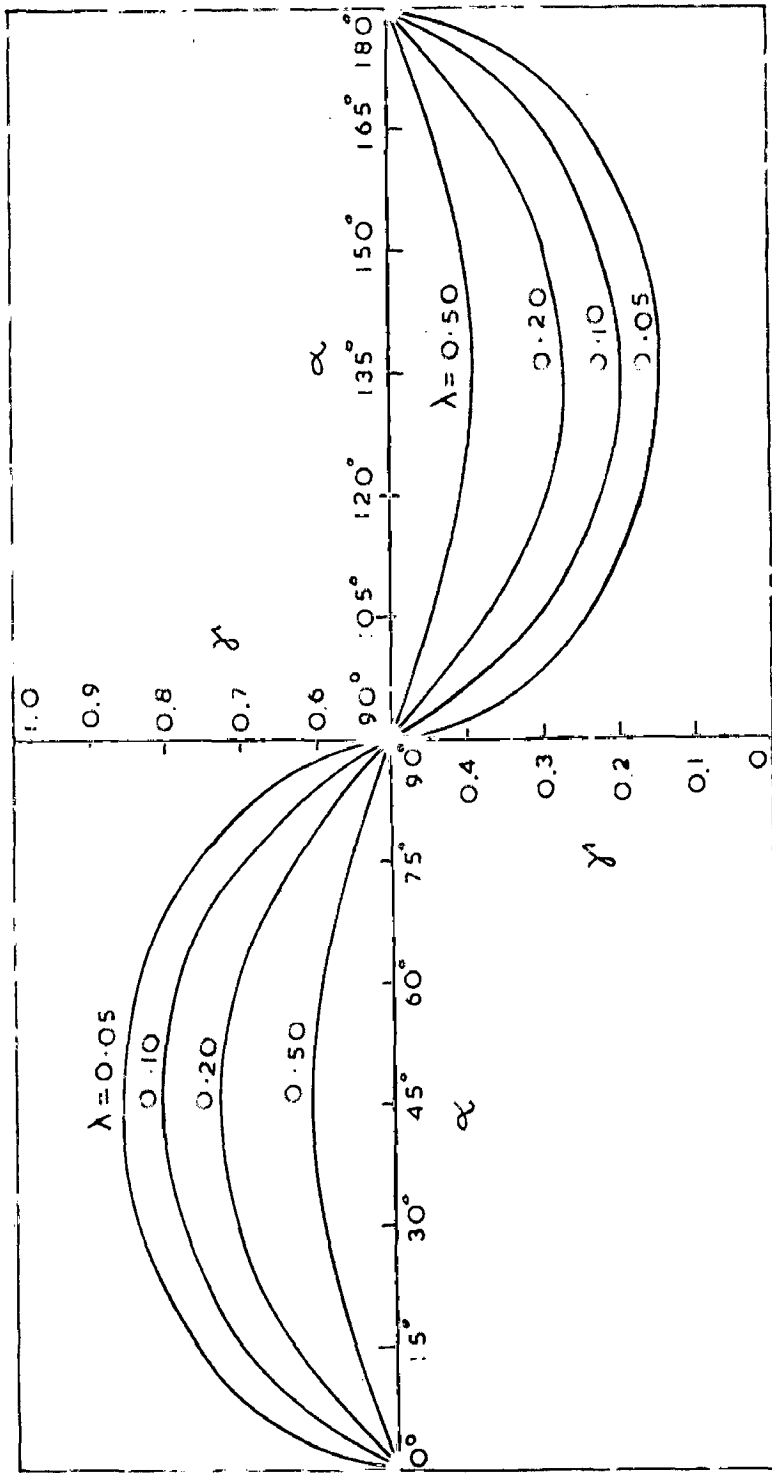


FIG 4.5 (a) VALUES OF  $\gamma$  FOR  $\alpha$  FROM  $0^\circ$  TO  $180^\circ$



$$\zeta = d' \left( \frac{1+t}{1+a} \right)^{1-\gamma} \left( \frac{t-1}{1-a} \right)^{\gamma} \dots(4.37)$$

This equation can be used to determine the values of  $L_1$  and  $L_2$  for the known values of  $b'_1$  and  $b'_2$ .

The transformation of  $w$ - plane onto the lower half of the  $t$  plane is given by

$$w = \frac{kH}{\pi} \sin^{-1} \left[ \frac{2t + L_1 - L_2}{L_1 + L_2} \right] - \frac{kH}{2} \dots(4.38)$$

The uplift pressures at D and E below a horizontal structure with an end cut off have been determined and plotted in Fig. 4.6 , 4.7 . These uplift pressures have been plotted against  $b'/d'$  values for various values of  $\gamma$  .

In order to determine the effect of the principal directions of anisotropy on uplift pressures at points D and E below floor with an end cut off, curves for  $b/d = 5, 10$  and  $15$  and  $\lambda = 0.5$  have been plotted in Fig.4.8 for various values of  $\alpha$  . Uplift pressures at these points for isotropic medium have also been plotted in this figure. A perusal of this figure indicates that value of  $\phi_D$  is minimum for value of  $\alpha$  around  $120^\circ$  and maximum at  $\alpha$  less than about  $30^\circ$  . The value of  $\alpha$  for maximum values of  $\phi_D$  varies with the value of  $b/d$  . A perusal of Fig.4.9

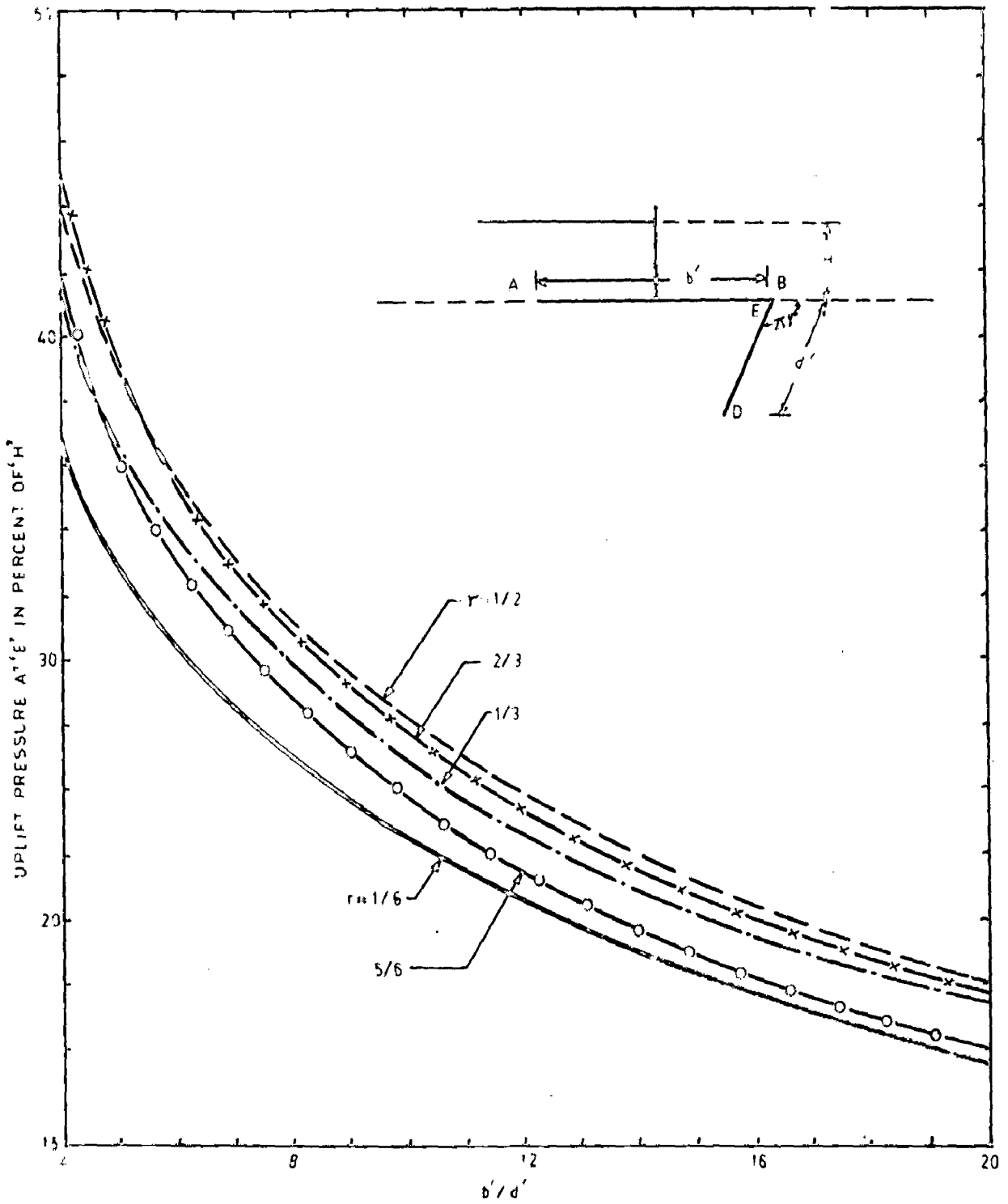


FIG.4.6-UPLIFT PRESSURE AT 'E'

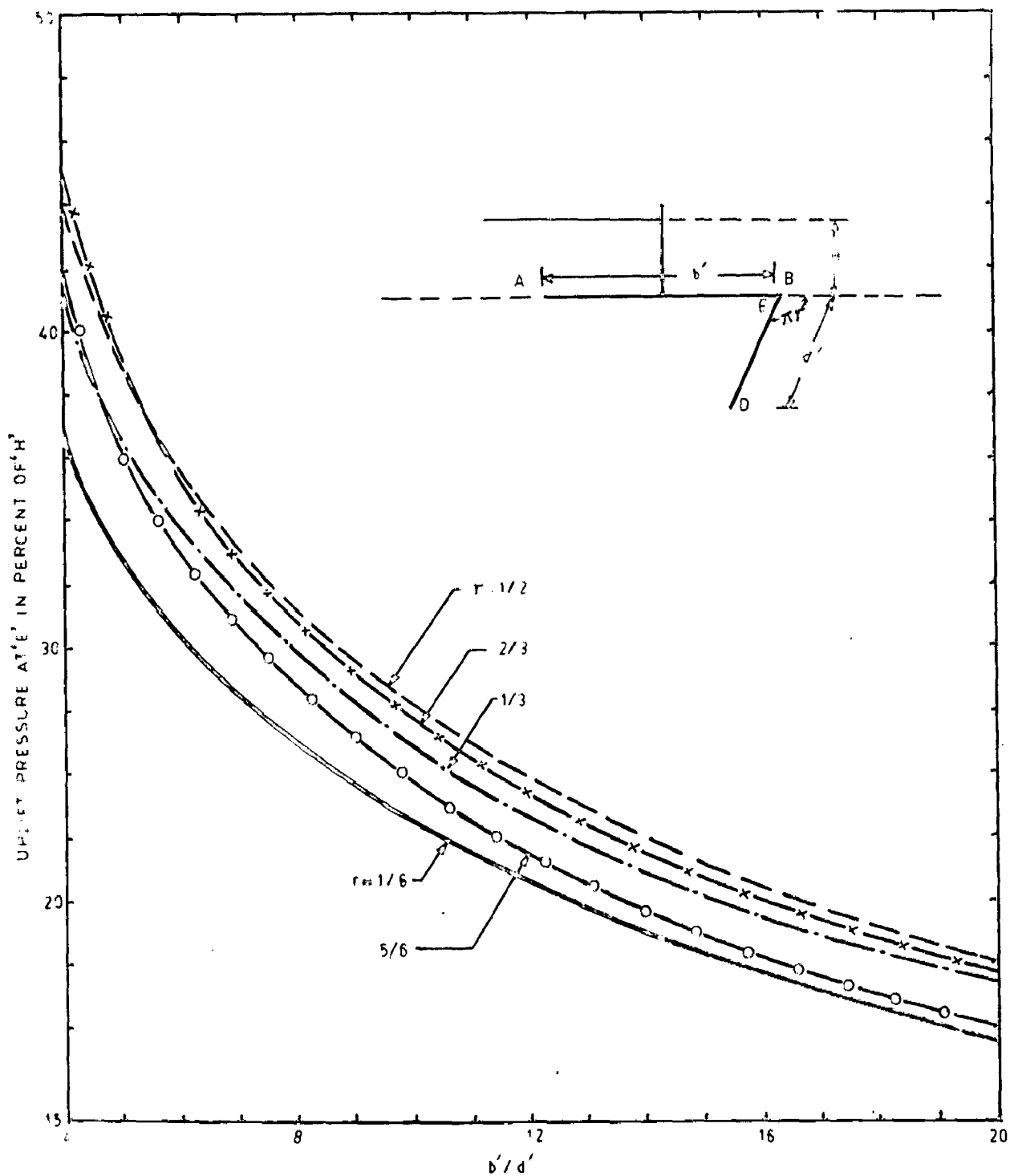


FIG.4.6-UPLIFT PRESSURE AT 'E'

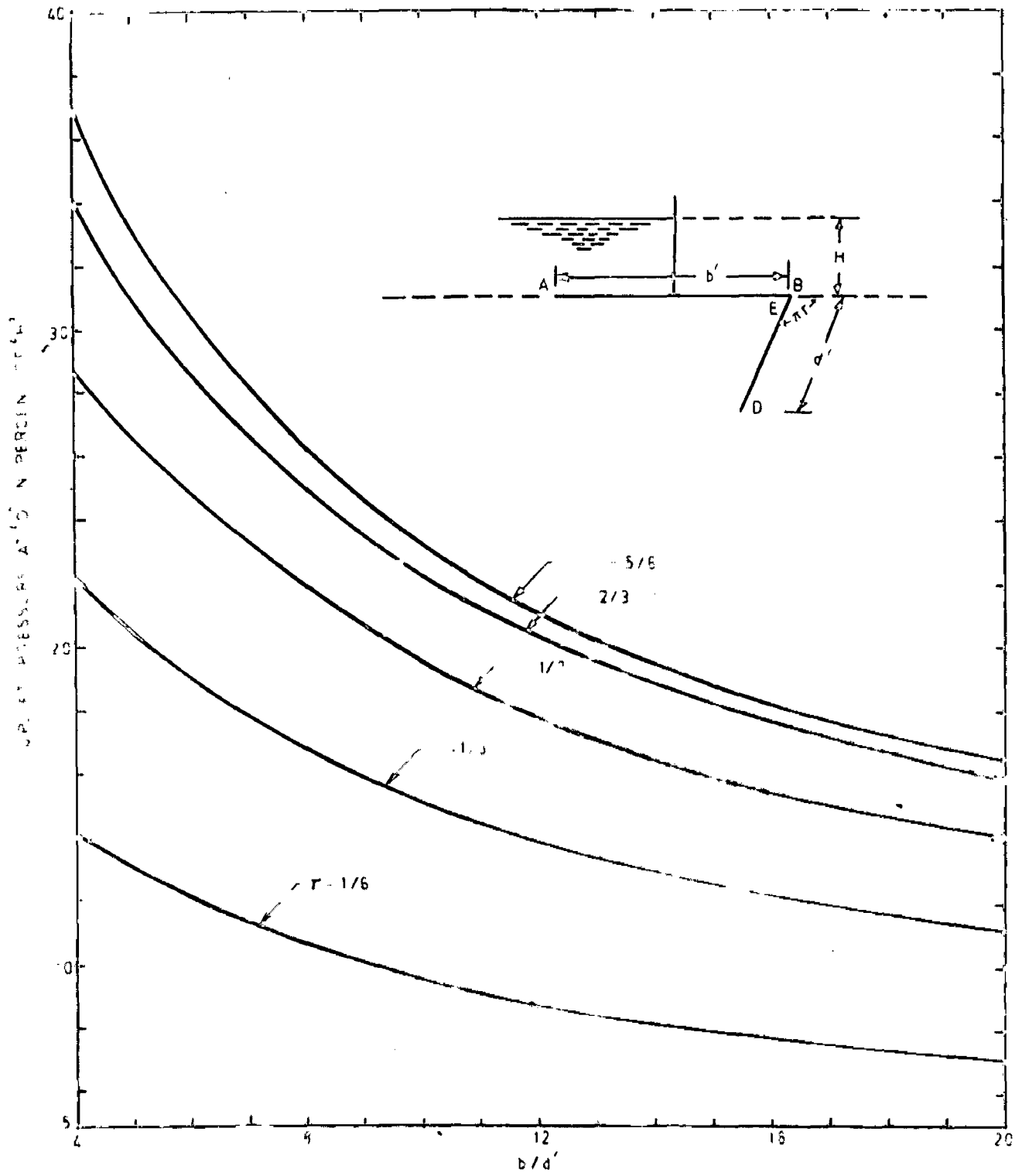


FIG. 4-7-UPLIFT PRESSURE AT 10'

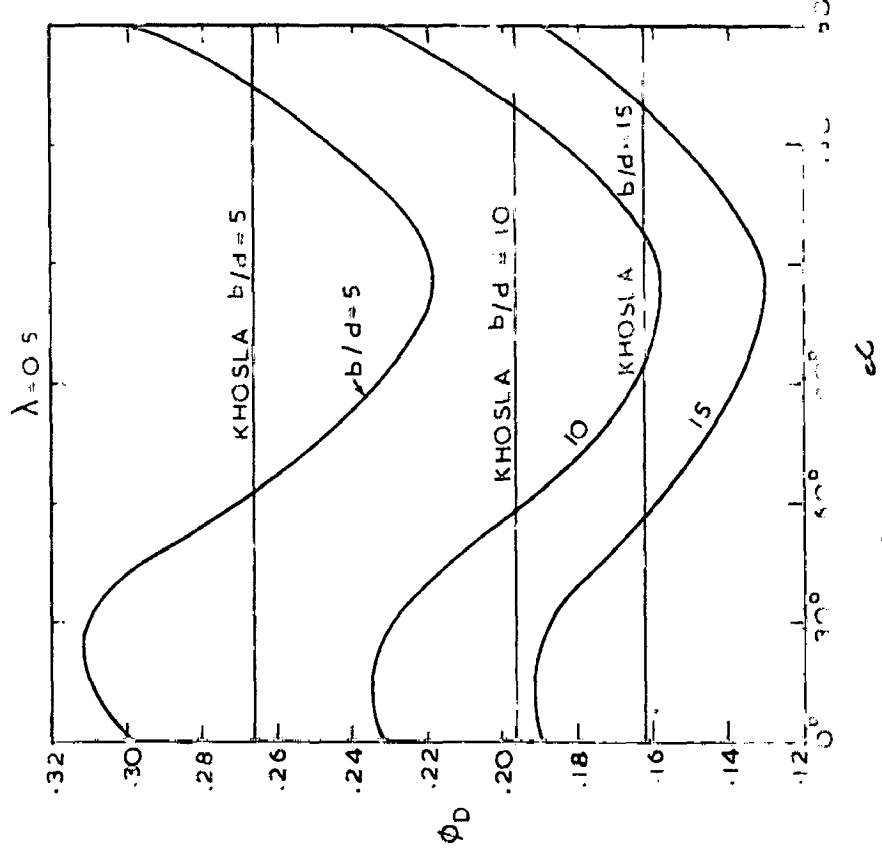
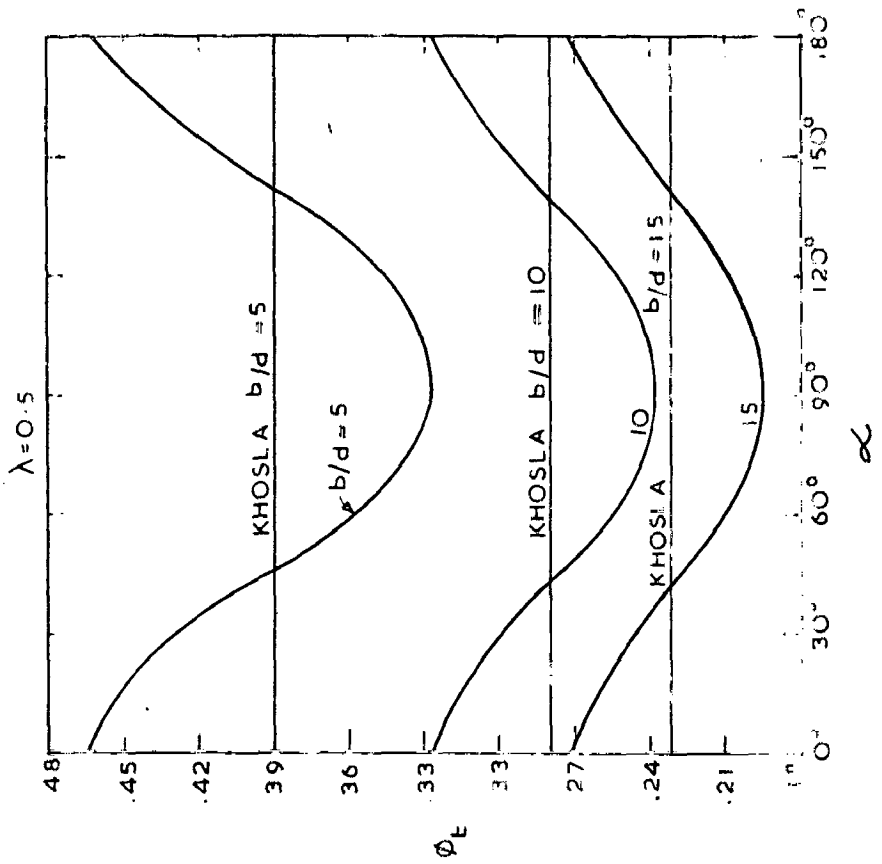


FIG. 4.8 VALUES OF  $\phi_D$  AND  $\phi_E$  FOR DIFFERENT VALUES OF  $b/d$  AND  $\alpha$  ( $\lambda = 0.5$ )

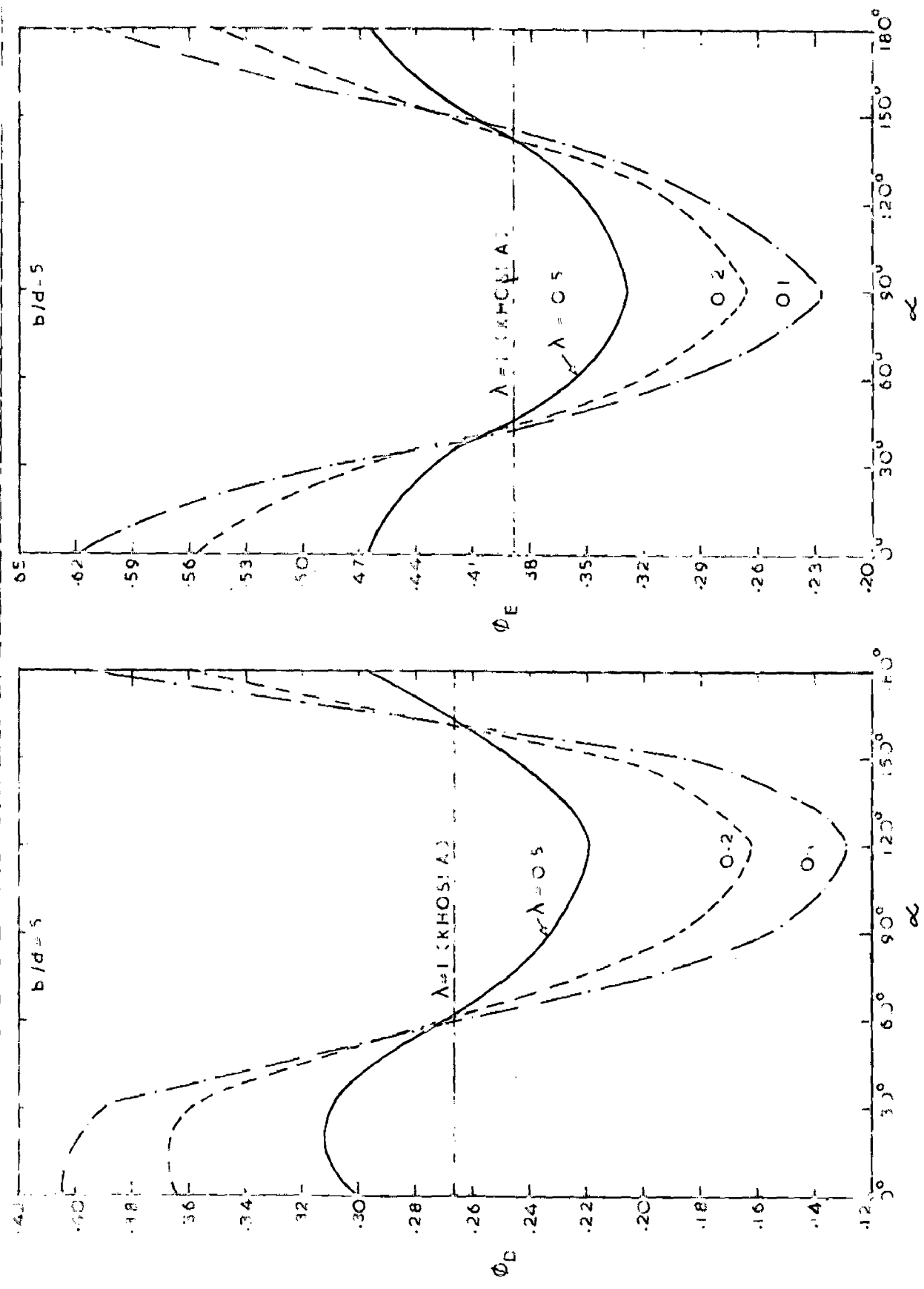


FIG. 4.9—VALUES OF  $\phi_D$  AND  $\phi_E$  FOR DIFFERENT VALUES OF  $\lambda$  AND  $\alpha$

in which values of  $\phi_D$  have been plotted against  $\alpha$  for values of  $\lambda = 0.5$ ,  $0.2$  and  $0.1$  and  $b/d = 5$  indicates that the values of  $\phi_D$  are maximum at  $\alpha = 0$ , for  $\lambda = 0.1$ , at  $\alpha$  equal to about  $15^\circ$  for  $\lambda = 0.2$  and  $\alpha$  equal to about  $20^\circ$  for  $\lambda = 0.5$ . A perusal of these figures also indicates that for value of  $\alpha$  ranging between  $60^\circ$  and about  $160^\circ$  the values of  $\phi_D$  are less than those for isotropic conditions. For values of  $\alpha < 60^\circ$  and greater than  $160^\circ$  the values of  $\phi_D$  are larger than those for isotropic conditions. The values of  $\phi_E$  have also been plotted in these figures for various values of  $\alpha$ ,  $\lambda$  and  $b/d$ . It is seen that the values of  $\phi_E$  are minimum for  $\alpha = 90^\circ$  and maximum for  $\alpha = 0^\circ$ . The values of  $\phi_E$  for anisotropic soil are less than those for isotropic soil for the values of  $\alpha$  ranging between about  $45^\circ$  and  $140^\circ$ . The minimum value of  $\phi_E$  and  $\phi_D$  decrease with decrease in the value of  $\lambda$  and their maximum values increase with increase in the value of  $\lambda$ .

The values of  $\phi_D$  and  $\phi_E$  have also been plotted in Fig. 4.10 against values of  $\lambda$ , for  $\alpha = 45^\circ$  and values of  $b/d = 5$ ,  $10$ ,  $15$  and  $20$ . A perusal of this figure indicates that values of  $\phi_D$  increase with decrease in the value of  $\lambda$  from  $1.0$  to about  $0.1$  and then decrease with further decrease in the value of  $\lambda$ . The value of  $\lambda$  for maximum value of  $\phi_D$  is not equal to  $0.1$ , for all values of  $b/d$ . It increases with increase in the value of  $b/d$ .

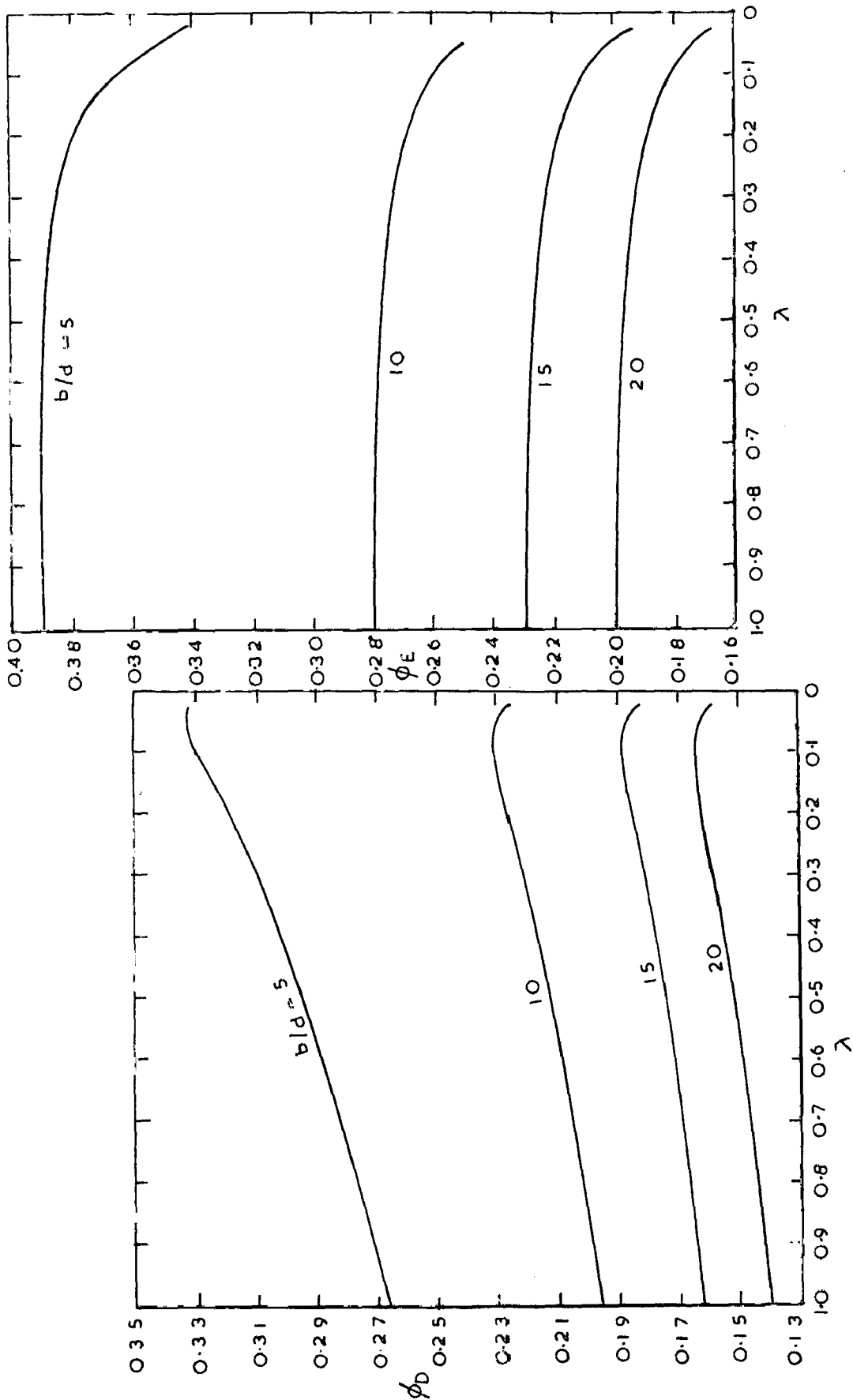


FIG. 4.10 - VALUES OF  $\phi_D$  AND  $\phi_E$  FOR DIFFERENT VALUES OF  $b/d$  AND  $\lambda$   
 (  $\alpha = 45^\circ$  )



in the values of  $\lambda$  and the decrease is rapid after  $\lambda = 0.2$ . The effect of  $\lambda$  on the values of  $\phi_E$  and  $\phi_D$  for  $b/d = 5$  and values of  $\alpha = 0^\circ, 30^\circ, 45^\circ, 90^\circ$  and  $135^\circ$  can be studied by the curves plotted in Fig. 4.11. A perusal of this figure indicates that values of  $\phi_D$  increase with decrease in the value of  $\lambda$  for the values of  $\alpha$  less than  $60^\circ$  and greater than  $160^\circ$  and decrease with the decrease in the value of  $\lambda$  for the range  $60^\circ < \alpha < 160^\circ$ . Similarly the values of  $\phi_E$  increase with decrease in the value of  $\lambda$  for  $\alpha$  less than  $45^\circ$  and greater than  $140^\circ$ , and decrease with decrease in the value of  $\lambda$  for  $45^\circ < \alpha < 140^\circ$ . The pressures at E for anisotropic conditions would therefore be more than those for isotropic condition when  $\alpha$  is less than  $45^\circ$  and greater than  $140^\circ$ , and the pressures at D for anisotropic conditions would be more than those for isotropic conditions when  $\alpha$  is less than  $60^\circ$  and greater than  $160^\circ$ .

#### 4.3 FLOOR WITH A CUT OFF FOUNDED ON ANISOTROPIC SOIL OF FINITE DEPTH

As indicated in para 4.1 and 4.2 the physical plane with inclined anisotropic soil can be transformed into a fictitious plane in which, the vertical cut off is transformed into an inclined cut off. Solution for inclined cut off with a step and apron on both sides founded on finite depth of permeable medium has been obtained by

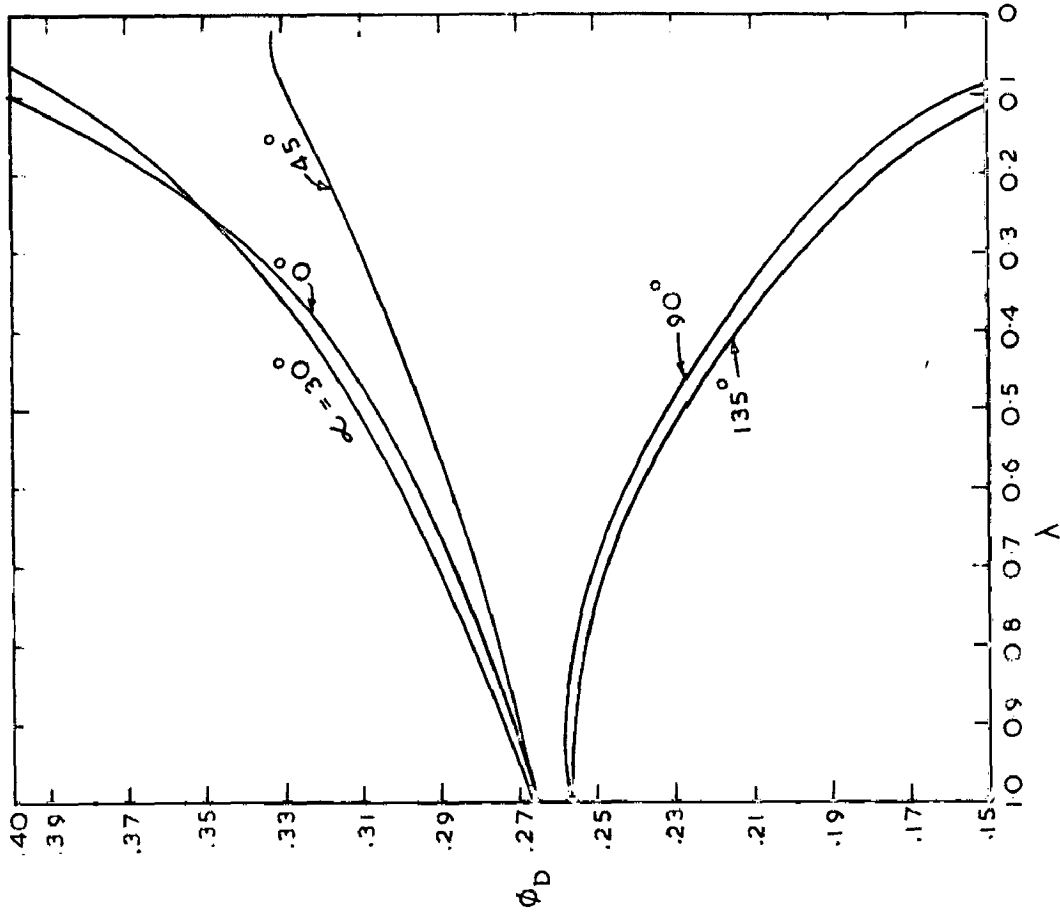
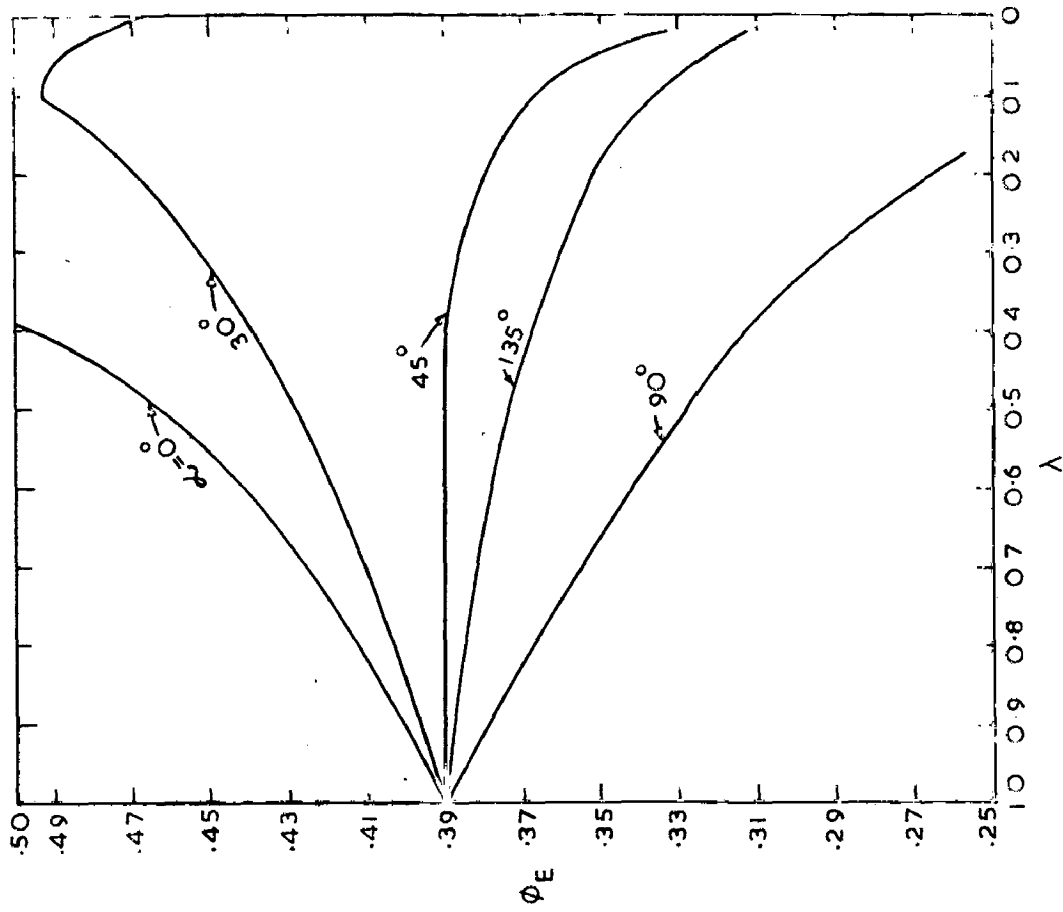


FIG 4.11 - VALUES OF  $\phi_D$  AND  $\phi_E$  FOR DIFFERENT VALUES OF  $\alpha$  AND  $\lambda$

Sivareddy et.al.(21). The transformation layout is shown in Fig. 4.12.

The relation between the physical plane and the fictitious  $z$  plane is given by Eqs 4.16 and 4.17. Transformation of the  $z$  plane into the intermediate  $t$ -plane is given by

$$z = M \int_0^t \frac{(t-\beta) dt}{t(t-\alpha)^{1-\gamma} (t-1)^\gamma} + Z_E \quad \dots(4.39)$$

where values of  $M$ ,  $\alpha$  and  $\beta$  can be evaluated from the following equations for known values of  $T$ ,  $Z_D$  and  $Z_E$ .

$$M = - \frac{T \alpha^{1-\gamma}}{\beta \pi} \quad \dots(4.40)$$

$$\frac{Z_D - Z_E}{T} = \frac{1}{\pi (-1)^\gamma} \left[ B_1 - B_2 \frac{\alpha^{1-\gamma}}{\beta} \right] \quad \dots(4.41)$$

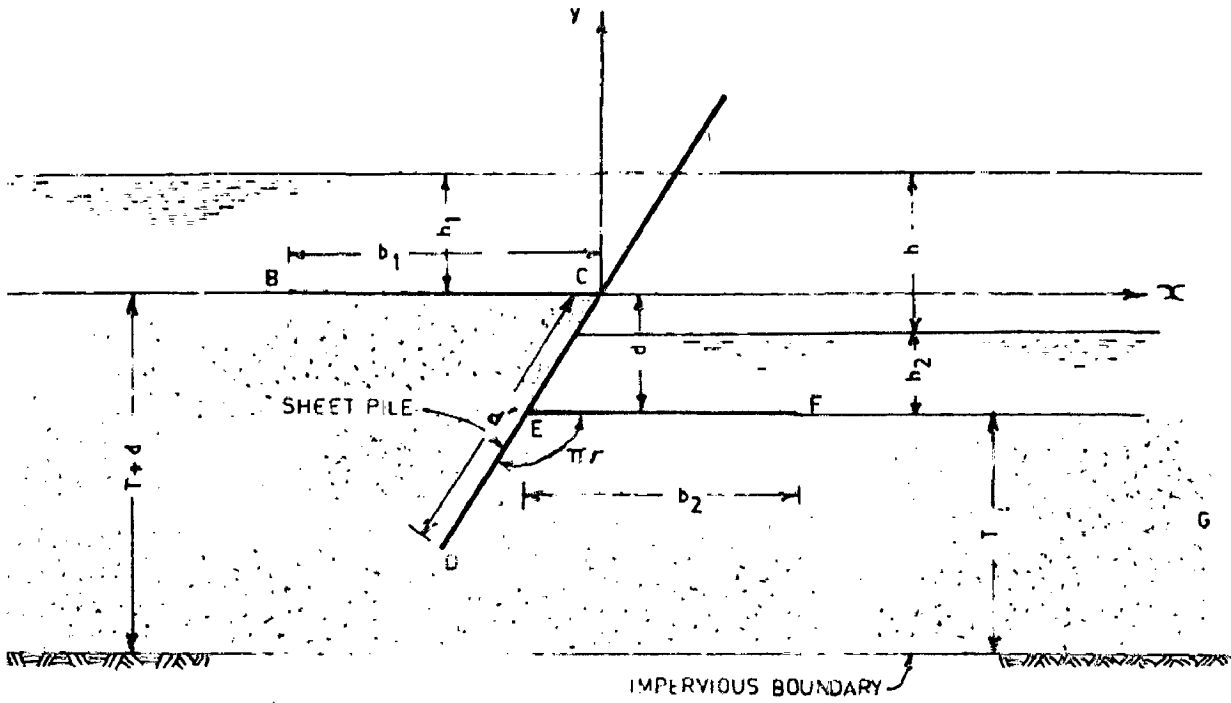
$$\frac{Z_E}{T} = \frac{(\beta - \alpha^{1-\gamma}) B(\gamma, 1-\gamma)}{(-1)^\gamma \beta \pi} \quad \dots(4.42)$$

where  $B_1 = B_{(\beta-\alpha)/(1-\alpha)}(\gamma, 1-\gamma)$  is incomplete beta function

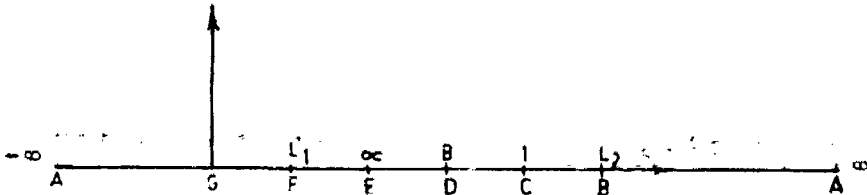
$B_2 = B_{(\beta-\alpha)/[\beta(1-\alpha)]}(\gamma, 1-\gamma)$  is incomplete beta function

$B(\gamma, 1-\gamma)$  is complete beta function

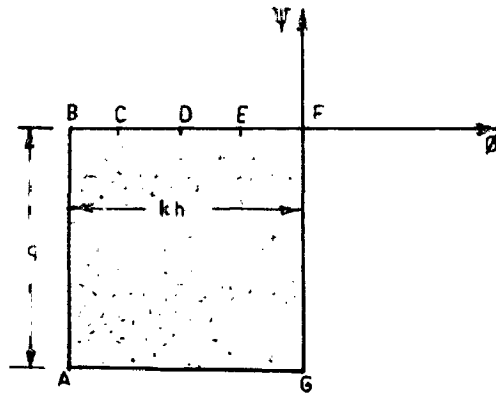
$\alpha$  and  $\beta$  are transformation parameters.



(a) z PLANE



(b) t PLANE



(c) w PLANE

FIG. 4-12-DIAGRAM OF PHYSICAL PROBLEM AND CONFORMAL MAPPING PLANES.

Eq 4.39 can then be used to evaluate the values of transformation parameters  $L_1$  and  $L_2$  for known values of  $b_1$  and  $b_2$ .

Transformation of w-plane into t-plane is given by

$$w = M' \int_{-\alpha}^t \frac{dt}{\sqrt{t(L_1-t)(L_2-t)}} + N' \quad \dots(4.43)$$

where  $M' = \frac{kH}{K} \sqrt{\frac{L_2}{4}} \quad \dots(4.44)$

$N' = -(kH + iq) \quad \dots(4.45)$

where  $K$  = complete elliptic function with modulus

$$= \sqrt{\frac{L_2 - L_1}{L_2}}$$

$q$  = Seepage discharge per unit length of the structure

$$= \frac{kH}{K} K'$$

$K'$  = complete elliptic function with modulus =  $\sqrt{\frac{L_1}{L_2}}$

Potential at any point along the floor is given by

$$\frac{\phi}{kH} = \frac{F(\theta, m)}{K} \quad \dots(4.46)$$

where  $F(\theta, m)$  = incomplete elliptic function

$$\theta = \sin^{-1} \sqrt{\frac{L_2(t-L_1)}{t(L_2-L_1)}} \quad \dots(4.47)$$

$$m = \sqrt{\frac{L_2 - L_1}{L_2}} \quad \dots(4.48)$$

Exit gradient at any point along the down-stream bed is given by

$$G_E \frac{T}{H} = \frac{\beta \pi \sqrt{L_2 t}}{2K (t-\beta)} \frac{\alpha^{\gamma-1} (t-\alpha)^{1-\gamma} (t-1)^\gamma}{\sqrt{t (L_1-t) (L_2-t)}} \quad \dots(4.49)$$

Seepage discharge and pressure at the tip of the cut off have been obtained for a cut off without a step and apron. The uplift pressures at D are shown in Fig. 4.13, and the seepage discharge in Fig. 4.14. Exit gradient at the end of the cut off are also plotted in Fig. 4.15, for various values of  $\gamma$ . A perusal of the figure indicates that the value of exit gradient just downstream of the cut off is zero for  $\gamma < 0.5$  and is infinite for  $\gamma > 0.5$ . For values of  $\gamma < 0.5$  the value of exit gradient first increases, reaches a maximum value and decreases as distance from the cut off increases. For  $\gamma > 0.5$  the value of exit gradient decreases with increase in distance from the cut off.

A perusal of Fig. 4.13 indicates that the value of  $\phi_D/kH$  is a linear function of  $d'/T$  in the range, these values have been plotted.

#### 4.4 EXPERIMENTAL STUDIES

In the previous sections cases of anisotropy where its principal directions do not coincide with coordinate axes

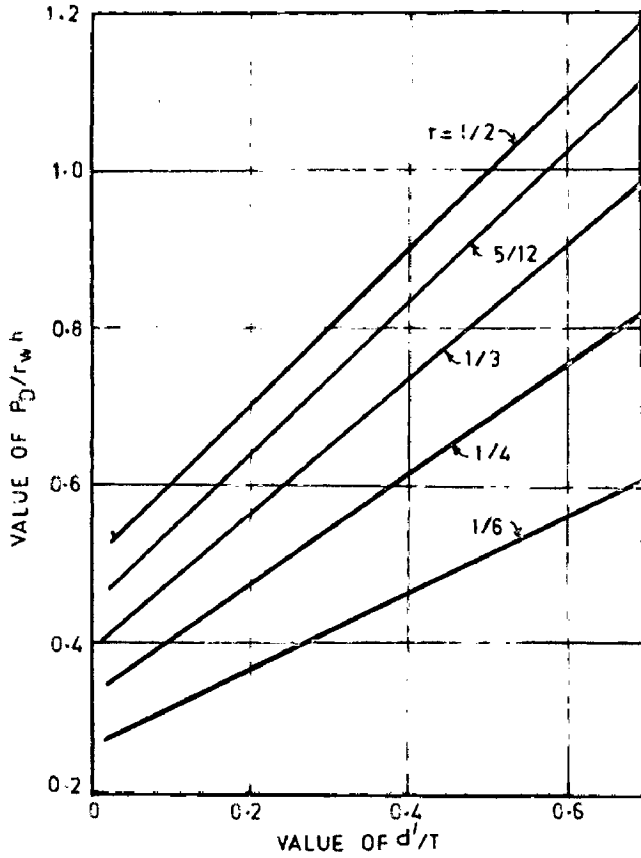


FIG.4.13-PRESSURE AT TIP OF SHEET PILE V/S LENGTH OF SHEET PILE FOR  $T=10$

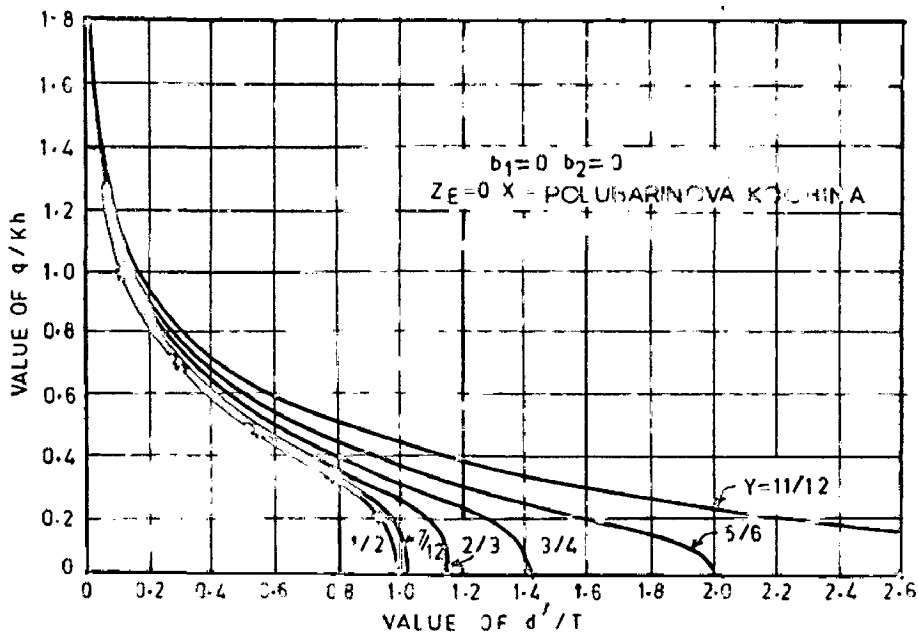


FIG.4.14-EFFECT OF LENGTH OF SHEET PILE ON QUANTITY SEEPAGE.

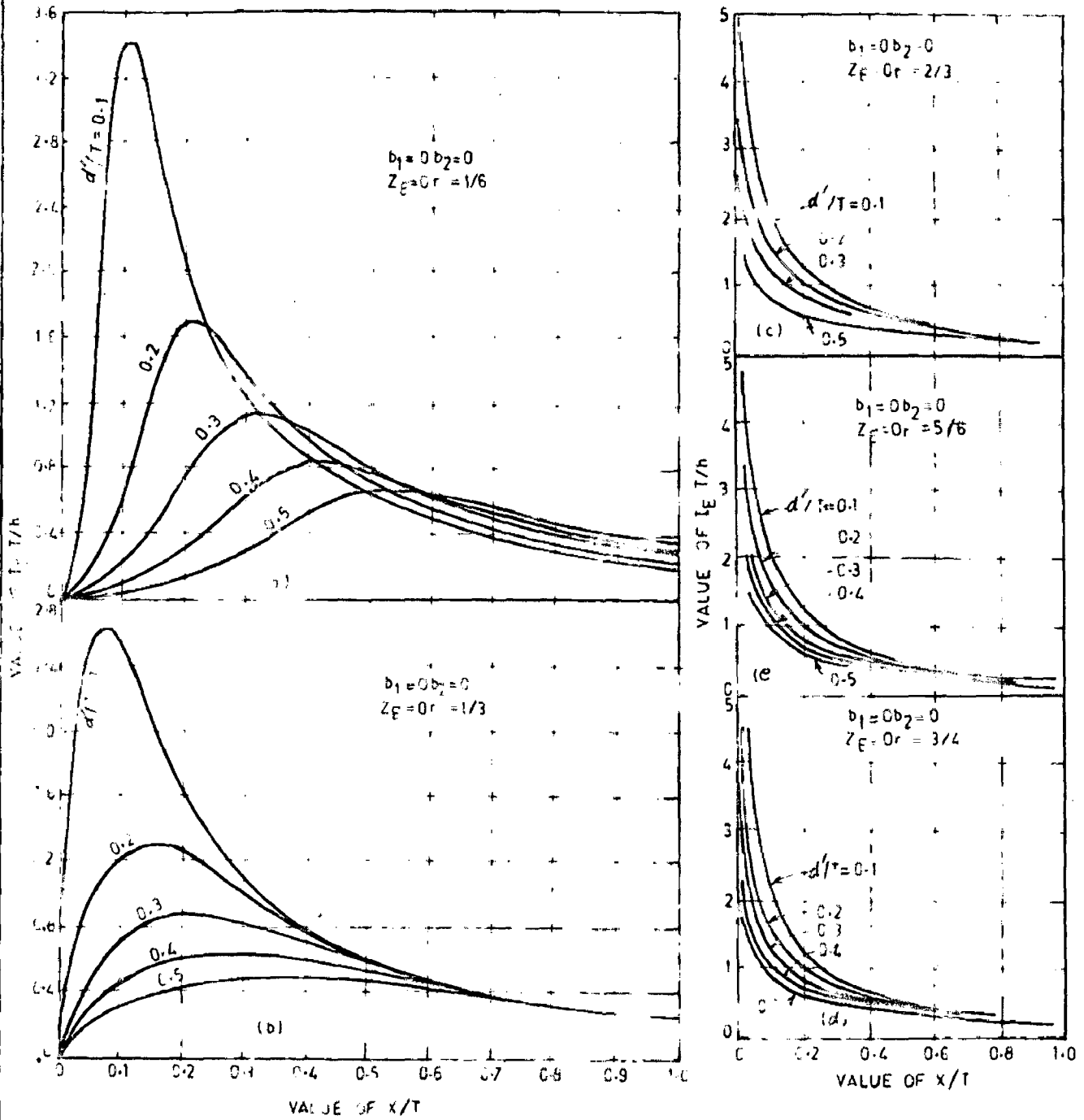


FIG.4.15-EXIT GRADIENT FOR SHEET PILE OF INCLINATION  
 (a)  $\pi/6$ . (b)  $\pi/3$ . (c)  $2\pi/3$ . (d)  $3\pi/4$ . (e)  $5\pi/6$ .



of physical plane were considered. The case of anisotropy with its principal directions parallel to the coordinate axes is simple to deal with. However earlier some experimental studies were conducted for this case based on electrical analogy method.

In the case of a depressed floor on infinite depth, P.V. Rao (19) opined that the uplift pressures increased in upstream half of floor length and decreased in downstream half with increase in anisotropic ratio. The maximum deviation in pressure was 8.5% from that of isotropic case, for a value of  $n$  ( $= K_x / K_y$ ) equal to 15.

The exit gradient was found to increase with 'n' value and this increase was found to be 50% of the pressures for isotropic case for  $n = 15$ . In the case of a flat floor with a cut off at either end, the author observed that maximum deviation of pressures from that of isotropic case to be  $\pm 28\%$  for  $n = 15$ .

The uplift pressure distribution below a floor on finite depth of anisotropic foundation for two cases viz. 1) downstream end cut off (2) intermediate cut off, were studied experimentally by Alamsingh et al (2) and Punmia et.al (18) respectively. The conclusions of the study were-

- (1) Pressure at any point under floor increased with increase in  $d/T$  ratio for a fixed  $b/T$  ratio (Fig.4.16)

- (2) For a given  $d/T$  ratio pressure at any point was larger for lesser values of  $b/T$  and decreased with increase in  $b/T$  ratio (Fig. 4.17).
- (3) The pressure at any point increased sharply with increase in anisotropic ratio (Fig. 4.18). The variation of pressure under floor was smaller for greater anisotropic ratios.
- (4) For given  $T/b$  and  $d/T$  ratios,  $\phi_E$  and  $\phi_D$  increased with increase in anisotropy (Fig. 4.19). Effect of anisotropy was more pronounced for lower value of  $T/b$ .
- (5) Both  $\phi_E$  and  $\phi_D$  decreased with increase in  $b/d$  ratio (Fig. 4.20 and 4.21).

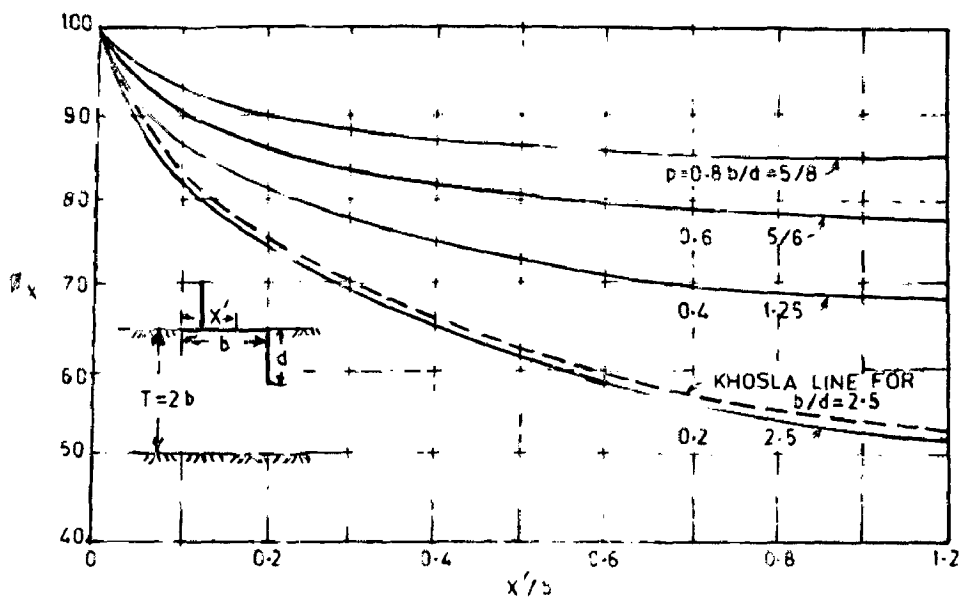


FIG.4.16-VARIATION OF  $\phi_x$  FOR VARIOUS VALUES OF  $d/T$  AND  $b/d$ ;  $b/T = 1/2$  (FIXED)

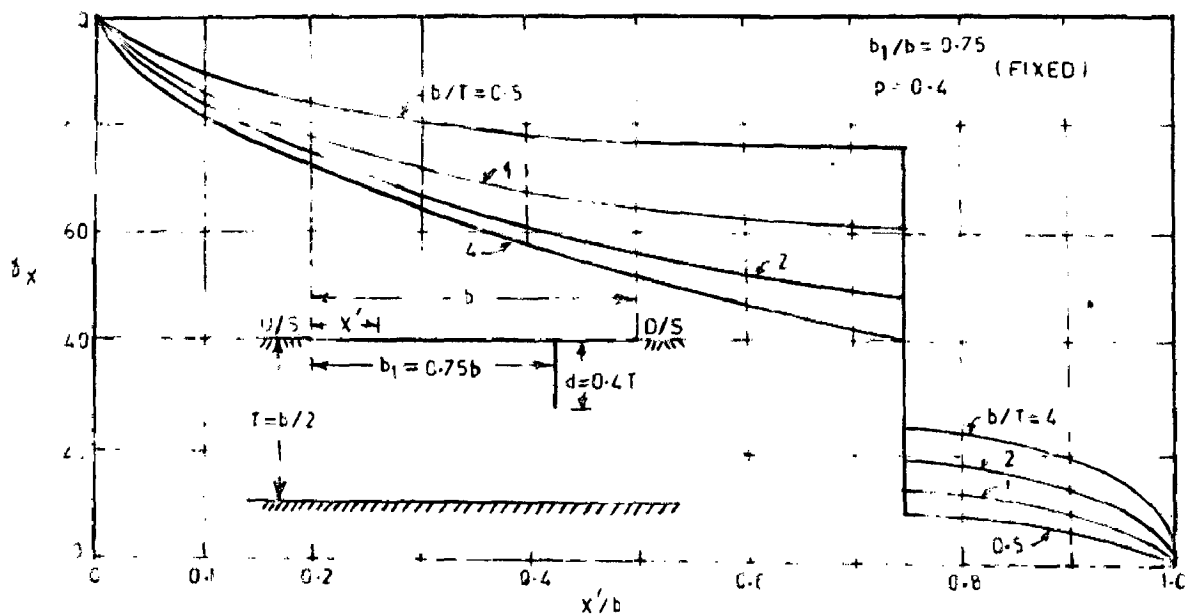


FIG.4.17-EFFECT OF  $b/T$  ON PRESSURE DISTRIBUTION.

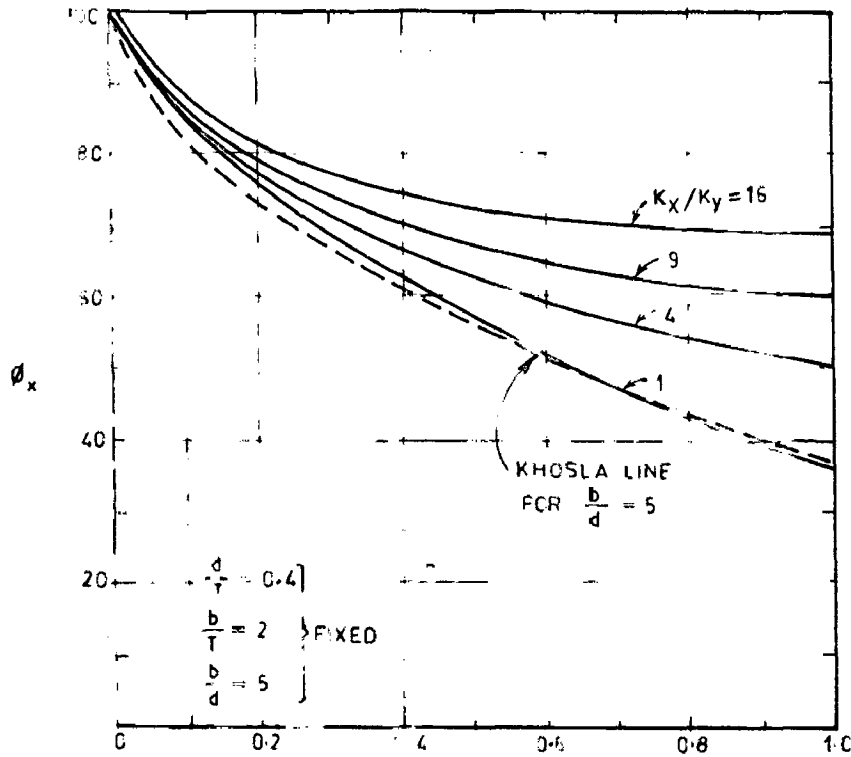


FIG.4-18-EFFECT OF ANISOTROPY ON PRESSURE DISTRIBUTION

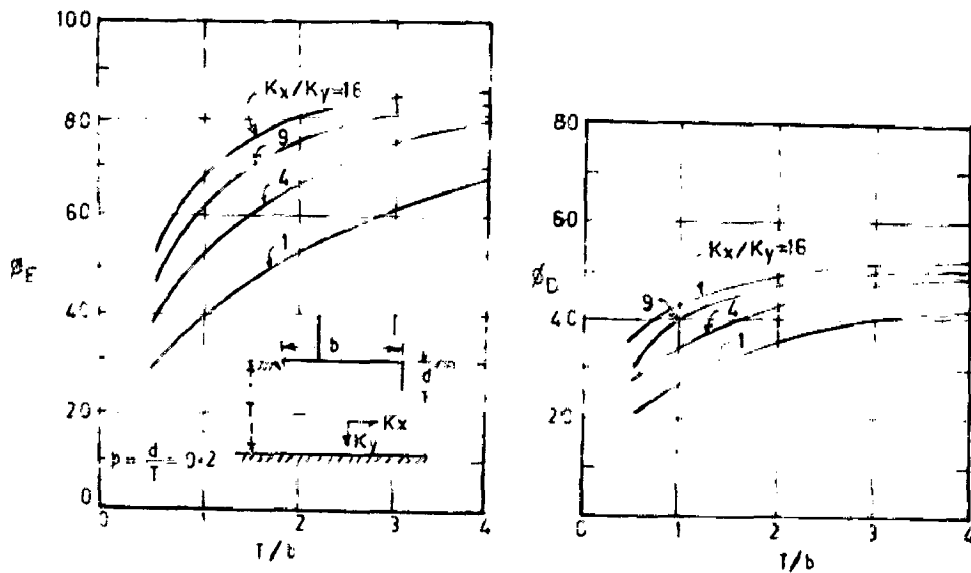


FIG.4-19-INFLUENCE OF T/b RATIO ON  $\phi_E$  &  $\phi_D$  ( $d/T=0.2$ )

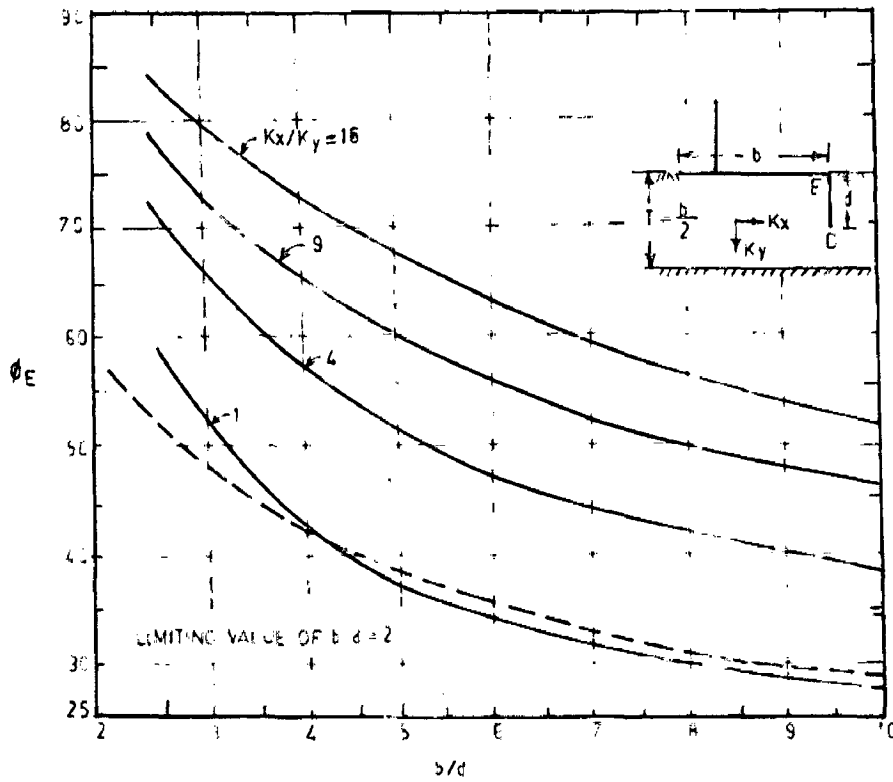


FIG. 20-VARIATION OF  $\phi_E$  WITH  $b/d$  AND ANISOTROPY ( $b/T=2$ )

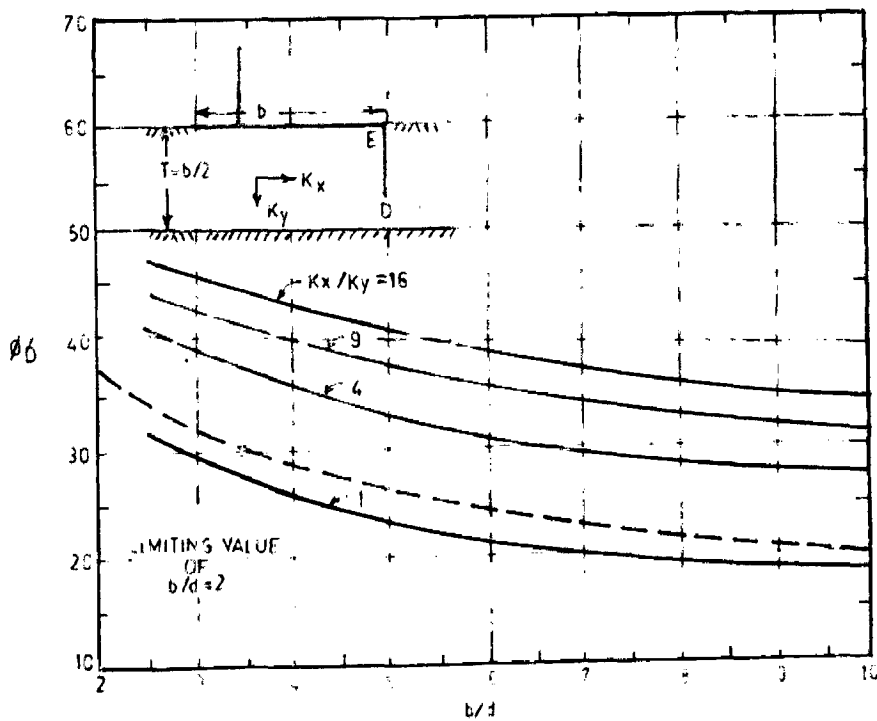


FIG. 21-VARIATION OF  $\phi_D$  WITH  $b/d$  & ANISOTROPY ( $b/T=2$ )

## C H A P T E R    V

### NUMERICAL METHODS FOR SOLUTION OF NON HOMOGENEOUS FOUNDATIONS

#### 5.1 GENERAL

The solution of seepage below hydraulic structures founded on homogeneous anisotropic medium can be obtained by the application of transformation that reduces the problem to that of a homogeneous isotropic medium (See Chapter IV). This method is however is not applicable when the subsoil comprises of several zones of different permeabilities or values of the permeability or its principal directions vary from point to point. Numerical methods could be applied to obtain an approximate solution for such problems.

#### 5.2 SOLUTION OF ANISOTROPIC SEEPAGE BY FINITE DIFFERENCE METHOD

5.2.1 The partial differential equation governing the steady state, two-dimensional flow in a homogeneous and isotropic medium is given by Eq.2.1

The medium is subdivided into squares of equal area,  $dx dy$ . The sides of the squares,  $\partial x$ , and  $\partial y$ , are equal and are of finite length  $\Delta x$ ,  $\Delta y$  respectively. The

square grid is shown in Fig. 5.1 . The intersections of grid lines are called nodes. The infinitesimal  $\Delta x \Delta y$  is approximated by  $a_g^2$  in which  $a_g$  is the width of grid interval. The area  $a_g^2$  , is small compared with the area of the medium.

The second differentials of head at node '0' can be approximated by

$$\frac{\partial^2 h}{\partial x^2} = \frac{h_2 + h_4 - 2h_0}{a_g^2} \quad \dots(5.1)$$

$$\frac{\partial^2 h}{\partial y^2} = \frac{h_1 + h_3 - 2h_0}{a_g^2} \quad \dots(5.2)$$

Substitution of Eqs 5.1 and 5.2 in Eq.2.1 results in

$$\frac{h_1 + h_2 + h_3 + h_4 - 4h_0}{a_g^2} = 0 \quad \dots(5.3)$$

or 
$$h_1 + h_2 + h_3 + h_4 - 4h_0 = 0 \quad \dots(5.4)$$

where  $h_0, h_1, h_2, h_3,$  and  $h_4$  are the heads at nodes 0,1,2,3,4 respectively.

The heads at every node except those at the up-stream and downstream boundaries are guessed initially, and then by the repeated use of equation (5.4) are adjusted towards their correct values.

Difficulties often arise from the presence of fractional spaces at boundaries of the mesh. These difficulties can be overcome by the use of triangular meshes. Suitable arrangement of the triangular meshes ensures that there are no fractional spaces at the boundaries.

G.R. Tomlin (25) has analysed seepage through soils that are zoned into areas of different permeability using the concept of triangular mesh and with the aid of a computer.

#### 5.2.2 Outline of the Method

The soil in each zone is assumed to be homogeneous. In general each zone can be anisotropic with the principal axes of permeability inclined at any angle. In applying the method, straight lines are substituted for curved zone boundaries and 'infinite' boundaries are reduced to some arbitrary finite length, so that the shape of each zone becomes a polygon.

The area within each zone is then divided into triangles by connecting selected pairs of vertices. Within each triangle, a fine-size triangular mesh is constructed with its axes parallel to the side of the triangle. The head at any node in this system of meshes is expressed in terms of heads at surrounding nodes. By the theory of finite differences, equations for the heads at various



types of nodes have been derived, and these equations are solved by iteration to obtain the values of head at every node. A standard computer programme has been used for the purpose.

### 5.2.3 Application

The method was tested using several problems which, by virtue of their regular boundary geometry, could be solved accurately by other methods. A close agreement was observed by the author between the solutions by the two methods.

The numerical method of analysis using a triangular mesh system, though mathematically approximate is extremely versatile. Anisotropic zoned soil sections with irregular boundary conditions can be as easily analysed by this method as a simple homogeneous section. Solutions of any desired accuracy can be obtained by increasing the number of iterations and by decreasing the mesh size. An obvious advantage in programming the method for a computer is that solutions can be obtained very quickly.

But the main disadvantage of the method is that it cannot be applied for the solution of seepage through non homogeneous and anisotropic soils. The method has thus limited applicability in the solution of field problems.

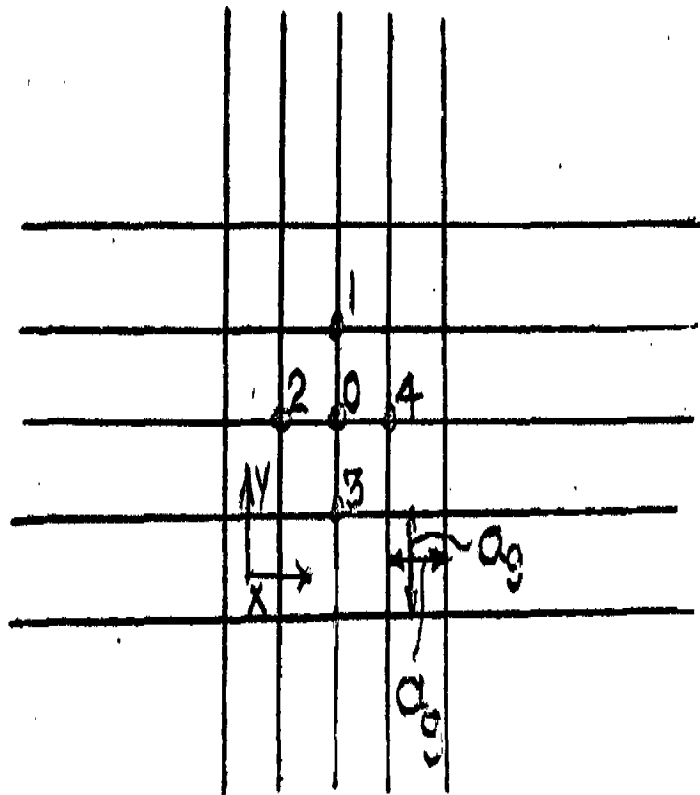


FIG. 5.1 Finite difference grid.

In contrast to this, finite element method is now-a-days very widely used in the solution of seepage through soils which are both anisotropic and nonhomogeneous. This method is very versatile in the sense it can be applied to all types of foundations (soils) irrespective of their character, and solutions can easily be got with the aid of a standard computer programme.

### 5.3 SOLUTION OF ANISOTROPIC SEEPAGE BY FINITE ELEMENT METHOD

A general numerical method of solution of two dimensional seepage problems in anisotropic media, particularly well suited for digital computation has been given by O.C. Zienkiewicz (26) This method is based on well known finite element method.

Ferrandon introduced the concept of a  $3 \times 3$  permeability matrix and showed that it is always symmetrical. Hence it is evident that in any anisotropic material three principal axes exist, in the direction of which the seepage velocity is always colinear with pressure gradient. These directions are known for the material at a particular point and the permeability can be described fully by three values of the permeability coefficients only.

#### 5.3.1 Theory of Flow in Anisotropic Media

The well known Darcy's law of seepage can be generalized to a  $n$ -dimensional situation as

the velocities along three orthogonal axes  $x, y$  and  $z$  can be designated by a column vector  $\{v\}$

and head gradients along these axes by another vector  $\{-\{\text{grad } H\}\}$  then by Darcy's law

$$\{v\} = -[K] \{\text{grad } H\} \quad \dots(5.1)$$

where  $k$  is a  $3 \times 3$  matrix of nine coefficients and since, it is symmetrical only six coefficients are needed to define it.

If the direction of the axes is changed to  $x', y'$  and  $z'$  then it can be shown (Appendix I) that the velocity vector in the new system is given by

$$v' = -[K'] \{\text{grad } H'\} \quad \dots(5.2)$$

$$\text{where } [K'] = [L][K][L^{-1}] \quad \dots(5.3)$$

where  $[L]$  is a transformation matrix of direction cosines.

$[K']$  can be reduced to a diagonal matrix, by suitably choosing the orthogonal directions, provided  $[K]$  is symmetrical. These directions are known as principal axes of the porous material and the particularly simple relationship (Eq. 6 Appendix 1) in the direction of these axes are obviously worth noting. The above transformation is identical to that used in

computing stress components where the existence of principal axes is well known.

### 5.3.2 Two Dimensional Seepage in Anisotropic medium

The continuity equation when the x and y directions coincide (locally) with principal axes of material is

$$\frac{\partial v_x}{\partial x} + \frac{\partial v_y}{\partial y} = 0 \quad \dots(5.4)$$

Substituting Eq. 8 (of appendix 1) in above equation,

$$\frac{\partial}{\partial x} \left( K_{xx} \frac{\partial H}{\partial x} \right) + \frac{\partial}{\partial y} \left( K_{yy} \frac{\partial H}{\partial y} \right) = 0 \quad \dots(5.5)$$

which is valid for both homogeneous and nonhomogeneous situations. The solution of Eq. 5.5 is equivalent to finding a function H, which minimizes the following integral taken over the whole region of solution (subject to specified boundary conditions).

$$E = \iint \left[ K_{xx} \left( \frac{\partial H}{\partial x} \right)^2 + K_{yy} \left( \frac{\partial H}{\partial y} \right)^2 \right] dx dy \quad \dots(5.6)$$

If the Euler conditions of minimization are applied to Eq. 5.6 then Eq. 5.5 will be obtained directly. This is valid whether  $K_{xx}$  and  $K_{yy}$  are constant or variable with the x and y coordinates.

The solution of this type of problem by finite element method is explained in Appendix II.

The procedure is identical with that of a structural analysis and standard computer programs have been used for both assembly and solution of examples. The program first converts the coordinates of the nodal points of each element to its appropriate principal direction and then computes 'stiffness matrices' (S). The assembly and solution follows a standard routine common to many stiffness analysis problems. The data necessary for computation programmed for a digital computer are -

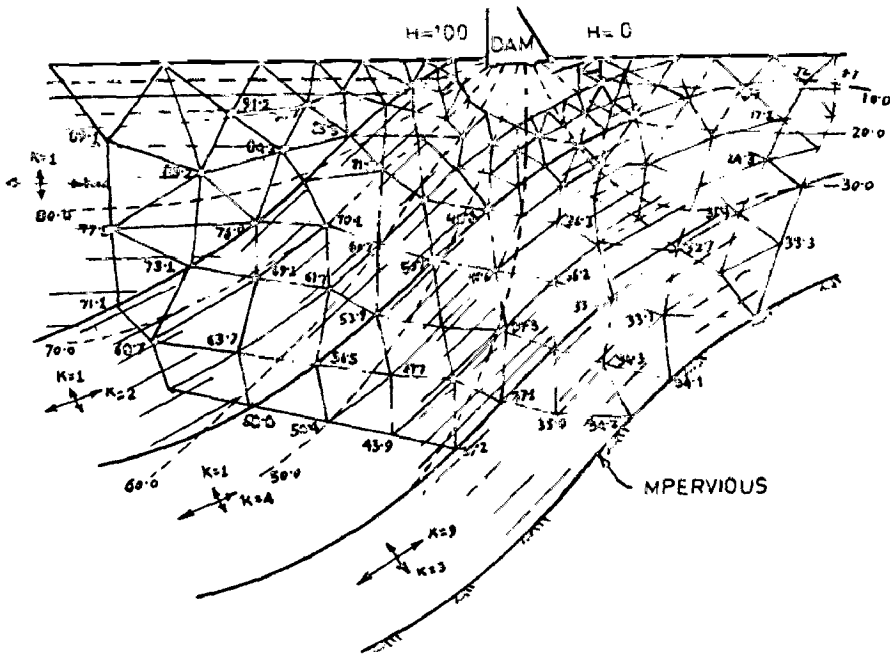
- (i) Coordinates of nodal points chosen in some common coordinate systems.
- (ii) Nodal numbers specifying the elementary triangles along with  $K_{xx}$  and  $K_{yy}$ , and
- (iii) A direction angle specifying the direction of the principal axes with reference to common coordinates.

### 5.3.3 Application

Two examples were chosen by Zienkiewicz(26) to illustrate the accuracy and wide range of applicability of the method, respectively. The first was the study of head distribution under an inclined layer of sheet piling on a stratified anisotropic foundation, for which analytical solution was known.

The equipotentials computed on the basis of exact solution and the number of values of heads computed at the nodes of triangles of finite element triangulation, on comparison were found to be in close agreement.

The second example is illustrated in Fig. 5.2 and 5.3 respectively, which is designed exclusively to illustrate the versatility of the computer programme and deals with the flow through a foundation of perhaps unusual complexity. But it should be noted that once the data pertaining to the characteristics of each element were specified no additional difficulty is presented by the computation.



5.2- FLOW UNDER A DAM THROUGH A HIGHLY NONHOMOGENEOUS ANISOTROPIC AND CONTORTED FOUNDATION.

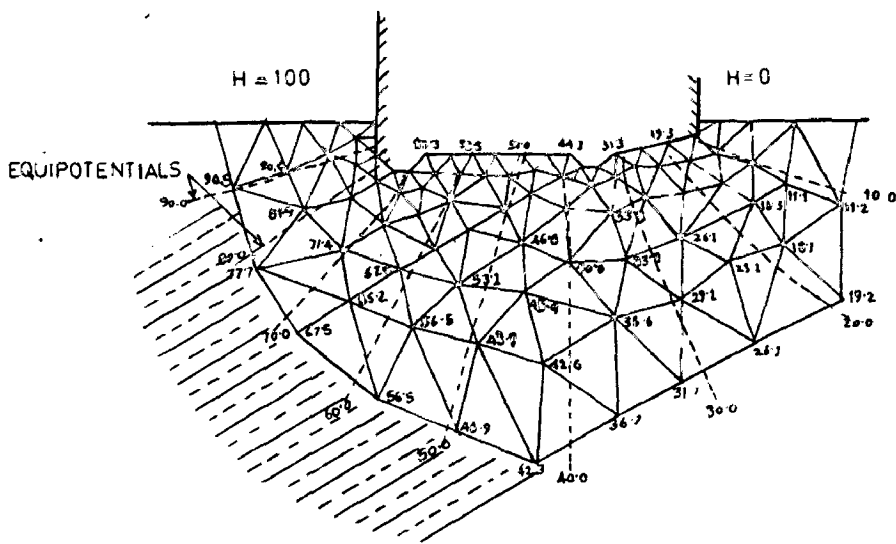


FIG. 5.3-DETAIL OF PROBLEM ILLUSTRATED.



C H A P T E R VI  
C O N C L U S I O N S

6.1 Closed-form or approximate solutions are available from the problem of seepage below the hydraulic structures founded on homogeneous and isotropic medium with various boundary conditions. But in practice the foundation material below the hydraulic structure is mostly non-homogeneous and anisotropic. The effect of finite depth, stratification, and anisotropic on the uplift pressures and finite element method for the solution of seepage below hydraulic structure founded on anisotropic and non-homogeneous mediums have been discussed. Following conclusions are drawn from these studies:

1. Design curves are given for determination of exit gradient and uplift pressures at key points below a flat floor with an end cut off founded on finite depth of permeable medium. The effect of impermeable layer is negligible for  $T/b \geq 5$  and  $d/b \leq 0.1$ .
2. With the increasing scour downstream of the end cut off founded on finite depth of permeable soil, the uplift pressures below the floor decrease but the value of exit gradient increases. The extent of increase in the value of  $G_E$  can be determined from Fig. 2.19. This information can also be used to determine the effect of the depth of the downstream filter on the exit gradient.

3. In case of hydraulic structures founded on stratified soils comprising two layers and  $k_2/k_1 > 1$ , the uplift pressures increase in the portion where pressures are less than 50% and decrease in the portion where pressures are more than 50%. When  $k_2/k_1$  is more than 1, the effect of the thickness of lower stratum on the uplift pressures is negligible. Pressures below the floor with  $k_2/k_1 > 10$  are not affected by  $b/d$  i.e. depth of cut off. The value of exit gradient increases with increase in the permeability of lower stratum. Increase in the length of the floor or depth of the downstream cut off, has practically no effect on the value of exit gradient for  $k_2/k_1 > 10$ .
4. Solutions based on conformal mapping has been obtained for determination of uplift pressures below floor with an asymmetric cut off founded on anisotropic soil with principal direction of permeability inclined to the coordinate axis of the physical plane. The results have been given in the form of design curves, to determine pressures at the junction of floor and end cut off (E) and at the tip of end cutoff (D)

It is seen that uplift pressures at E are maximum for anisotropic medium with  $\alpha = 0$  and decrease with decrease in the value of  $\lambda$ . The

pressures at E are minimum for  $\alpha = 90^\circ$ . The pressures at the point E with anisotropic conditions are more than those for isotropic conditions for the value of  $\alpha$  less than  $45^\circ$  and greater than  $140^\circ$ . The pressure at the point D with anisotropic conditions are less than those for isotropic condition for the value of  $\alpha$  between  $60^\circ$  and  $160^\circ$ .

The pressures at D increase with decrease in the value of  $\lambda$  for  $\alpha < 60^\circ$  and  $\alpha > 160^\circ$  and decrease with decrease in the value of  $\lambda$  for  $60^\circ < \alpha < 160^\circ$ .

5. Finite element method can be applied for obtaining the uplift pressure below structures founded on anisotropic and non homogeneous foundations. With the availability of the fast digital computer this method has wide applicability and can be used to obtain results to desired accuracy.

APPENDIX I

THEORY OF FLOW IN ANISOTROPIC MEDIA

If the velocities in the direction of three orthogonal axes, x,y and z are designated by a vector v or

$$\{v\} = \begin{Bmatrix} v_x \\ v_y \\ v_z \end{Bmatrix} \quad \dots(1)$$

and if the head gradient is defined similarly by its three components,

$$-\{\text{grad } H\} = \begin{Bmatrix} -\frac{\partial H}{\partial x} \\ -\frac{\partial H}{\partial y} \\ -\frac{\partial H}{\partial z} \end{Bmatrix} \quad \dots(2)$$

then the most general linear relationship that can exist between the two quantities is of the form (by Darcy's law)

$$\{v\} = -[K] \{\text{grad } H\} \quad \dots(3)$$

in which [K] is a 3 x 3 matrix defined by nine numerical coefficients.

It can , however be shown that matrix K must be symmetrical to satisfy conservation of energy and therefore

it appears that only six coefficients are necessary to define it.

If the direction of the axes is changed to  $x', y', z'$  then the velocity vector in the direction of the new axes can be found as

$$\{v'\} = \begin{Bmatrix} v'_x \\ v'_y \\ v'_z \end{Bmatrix} = [L] \{v\} \quad \dots(4)$$

where  $L$  is a transformation matrix of direction cosines.

Similarly the new vector of the head gradient

$$-\{\text{grad } H'\} = \begin{Bmatrix} -\frac{\partial H}{\partial x'} \\ -\frac{\partial H}{\partial y'} \\ -\frac{\partial H}{\partial z'} \end{Bmatrix} = -[L] \{\text{grad } H\} \quad \dots(5)$$

Combining equations 3,4 and 5 yields

$$v' = -[K'] \{\text{grad } H'\} \quad \dots(6)$$

in which the new permeability matrix is

$$[K'] = [L][K][L^{-1}] \quad \dots(7)$$

With this type of transformation of  $K$  is symmetrical it is always possible to find three orthogonal directions

for which  $[K']$  reduces to a diagonal matrix giving

$$\{v'\} = - \begin{bmatrix} k_{x'x'} & 0 & 0 \\ 0 & k_{y'y'} & 0 \\ 0 & 0 & k_{z'z'} \end{bmatrix} \{\text{grad } H'\}$$

....(8)

A P P E N D I X    I I

TWO DIMENSIONAL SEEPAGE IN ANISOTROPIC MEDIUM

The continuity equation, when the x and y directions coincide (locally) with principal axes of material is

$$\frac{\partial v_x}{\partial x} + \frac{\partial v_y}{\partial y} = 0 \quad \dots(1)$$

Substituting Eq. (8) (of appendix 1) in above equation,

$$\frac{\partial}{\partial x} \left( K_{xx} \frac{\partial H}{\partial x} \right) + \frac{\partial}{\partial y} \left( K_{yy} \frac{\partial H}{\partial y} \right) = 0 \quad \dots(2)$$

which is valid for both homogeneous and non homogeneous situation. The solution of Eq. 2 is equivalent to finding a function H, which minimizes the following integral taken over the whole region of solution (subject to specified boundary conditions).

$$E = \frac{1}{2} \iint \left\{ K_{xx} \left( \frac{\partial H}{\partial x} \right)^2 + K_{yy} \left( \frac{\partial H}{\partial y} \right)^2 \right\} dx dy \quad \dots(3)$$

If the Euler conditions of minimization are applied to Eq. 3, then Eq. 2 will be obtained directly. This is valid whether  $K_{xx}$  and  $K_{yy}$  are constant or variable with the x and y coordinates.

The solution of this type of problem by finite element method is explained as follows.

The seepage region is divided into arbitrary elementary triangular areas, or finite elements as shows in Fig. 1. If the unknown values of the function  $H$  at the nodes of the triangles, define the function throughout the entire region completely and uniquely, then differentiating the function  $E$  with respect to each of these nodal values and equating each of these differentials to zero will result in a series of simultaneous equations.

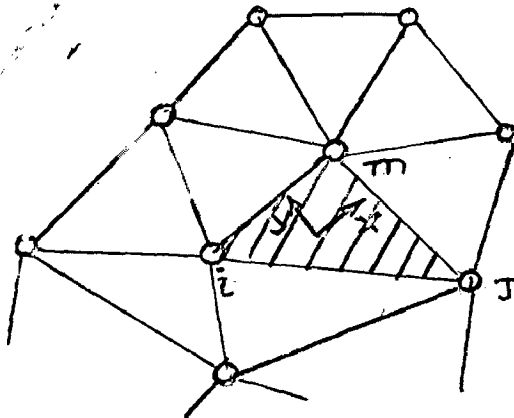


Fig.1 Division of Region into finite elements

From these the final, approximate solution can be obtained by feeding in the appropriate boundary values. If the nodal values define the function that is sought only in the element adjacent to a particular node, while fulfilling continuity requirements along lines separating the elements then each equation will contain only the contributions of these adjacent elements.

Considering a typical triangle  $i, j, m$  with a locally defined set of coordinate axes (coinciding with



the principal axes of the material) the simplest definition of the function H within the element will be obtained by taking a linear function.

$$u = A + Bx + Cy \quad \dots(4)$$

and evaluating the three constants in terms of coordinates of the nodes and the corresponding nodal values of the function. Performing the necessary algebra (in matrix language ) yields

$$H = \begin{bmatrix} (a_i + b_i x + c_i y) & , & (a_j + b_j x + c_j y) & , & \\ & & (a_m + b_m x + c_m y) & & \end{bmatrix} \begin{Bmatrix} H_i \\ H_j \\ H_m \end{Bmatrix} \quad \dots(5)$$

$$\text{or simply } H = [N_i, N_j, N_m] \{H^e\} \quad \dots(6)$$

where  $H^e$  stands for the values of the function characteristic of the element considered. The coefficients are defined as

$$\begin{aligned} a_i &= \frac{x_m y_j - x_j y_m}{2\Delta} \\ b_i &= \frac{(y_m - y_j)}{2\Delta} \\ c_i &= \frac{(x_j - x_m)}{2\Delta} \end{aligned} \quad \dots(7)$$

with others following a cyclic, anticlockwise, order in i,j,m. In Eq. 7 ,  $\Delta$  is the area of the triangle i,j,m.

The minimum of the functional  $E$  is obtained by first obtaining the contributions to the appropriate differentials for each element separately and then assembling the results for the whole region.

Thus terming  $E^c$  as the contribution of the element  $i, j, m$  yields

$$\frac{\partial E^c}{\partial H_i} = \iint \left[ K_{xx} \frac{\partial H}{\partial x} \frac{\partial}{\partial H_i} \left( \frac{\partial H}{\partial x} \right) + K_{yy} \frac{\partial H}{\partial y} \frac{\partial}{\partial H_i} \left( \frac{\partial H}{\partial y} \right) \right] dx dy \quad \dots(8)$$

With the integration limited to the area of the triangle  $i, j, m$ . This on substitution of Eq. 6 becomes

$$\begin{aligned} \frac{\partial E^c}{\partial H_i} = & \iint K_{xx} \left[ \frac{\partial N_i}{\partial x}, \frac{\partial N_j}{\partial x}, \frac{\partial N_m}{\partial x} \right] \{H^o\} \left( \frac{\partial N_i}{\partial x} \right) dx dy \\ & + \iint K_{yy} \left[ \frac{\partial N_i}{\partial y}, \frac{\partial N_j}{\partial y}, \frac{\partial N_m}{\partial y} \right] \{H^e\} \left( \frac{\partial N_i}{\partial y} \right) dx dy \quad \dots(9) \end{aligned}$$

Recognising that the element contributes only to the differentials with respect to the values at its three nodal points, assuming the permeability coefficients  $K_{xx}$  and  $K_{yy}$  to be constant within the element, then substitution of Eq. 7 yields simply,

$$\left\{ \frac{\partial E^e}{\partial H^e} \right\} = \left\{ \begin{array}{c} \frac{\partial E^e}{\partial H_1} \\ \frac{\partial E^e}{\partial H} \\ \frac{\partial E^e}{\partial H_m} \end{array} \right\} = [S_{ijm}] \left\{ \begin{array}{c} H_i \\ H_j \\ H_m \end{array} \right\} = [S_{ijm}] \{ H^e \} \quad \dots(10)$$

in which the  $[S]$  matrix has coefficients of the type

$$S_{ij} = \left\{ K_{xx}(y_m - y_i)(y_i - y_m) + K_{yy}(x_m - x_j)(x_i - x_m) \right\} / 4\Delta \quad \dots(11)$$

or explicitly

$$[S_{ijm}] = \left[ \begin{array}{ccc} K_{xx}(y_m - y_j)(y_m - y_j) & K_{xx}(y_m - y_j)(y_i - y_m) & K_{xx}(y_m - y_j)(y_j - y_i) \\ + & + & + \\ k_{yy}(x_m - x_j)(x_m - x_j) & k_{yy}(x_m - x_j)(x_i - x_m) & K_{yy}(x_m - x_j)(x_j - x_i) \\ & k_{xx}(y_i - y_m)(y_i - y_m) & K_{xx}(y_i - y_m)(y_j - y_i) \\ + & + & + \\ & k_{yy}(x_i - x_m)(x_i - x_m) & K_{yy}(x_i - x_m)(x_j - x_i) \\ & & K_{xx}(y_j - y_i)(y_j - y_i) \\ & & + \\ & & K_{yy}(x_j - x_i)(x_j - x_i) \end{array} \right]$$

Symmetrical.

... (12)

To assemble a typical equation for a differential of  $E$  with respect to any nodal value for the whole region, the contributions of elements adjacent to the node only are non zero and the assembly will clearly according to the pattern

$$\frac{\partial E}{\partial H_i} = \sum \frac{\partial E^e}{\partial H_i} = 0 \quad \dots(13)$$

$$\text{or } \sum H_n \sum s_{in}^e = 0 \quad \dots(13b)$$

The procedure is identical with that of structural analysis in which S matrix is a stiffness matrix of a structural component and Eq 13b represents the equation of equilibrium obtained on assembly of such elements . Standard computer programs have been used for both assembly and solution of examples.

## R E F E R E N C E S

1. Alamsingh et al., "Study of Uplift pressures below Apron with Downstream Cutoff founded on Two layered Media," Indian Geotechnical-Journal, Vol.2, No.4, Oct, 1972, pp 267-290.
2. Alamsingh, et al., " Seepage below Horizontal Apron with Downstream cutoff founded on Anisotropic pervious Medium of Finite depth", Indian Geotechnical Journal, Vol.3, No.3, July 1973, pp198-216.
3. Aravin V.I., Numerov S.N., "Theory of Fluid Flow in Undeformable Porous Media", Isreal Program for Scientific Translations, Jerusalem, 1965.
4. Chugaev R.R., " Design and Calculation of Underground Profile of Dams on Pervious Foundations", VI Congress on Large Dams, New York, 1958, Vol.II.
5. Gurudasram, et al., " Electrical Analogy studies for Stratified Foundation", Irrigation and Power, Vol.18, No.11, Nov, 1961, pp 988-1006.
6. Harr M.E., " Ground Water and Seepage" McGraw Hill, Book Co., New York, 1962.
7. Khosla A.N., et al., "Design of Weirs on Permeable Foundations", C.B.I.P., Publication, No.12, 1936.
8. Kulandaiswamy V.C., et al., "Design of Weirs on Pervious Foundations of Finite Depth", Journal of Institution of Engineers, (India), Vol. 52, No.5, Pt CI3, pp 129-136.

9. Lenau C.W., " Seepage under Structures on Stratified Soil", Journal of Engg. Mechanics Division, Proceedings, American Society of Civil Engineers, Vol.93, No.EM4, Aug., 1967, pp 39-53.
10. Lenau C.W., " Seepage under Structure on Four Soil Strata", Journal of Engg Mechanics Division, Proceedings, American Society of Civil Engineers, Vol97No3EM2April,1971,pp223-237
- 11., Luthra S.D.L., "Uplift Pressure below Hydraulic Structure on Stratified Permeable Foundation", IX Congress, International Association of Hydraulic Research, Belgrade, Sept., 1961. pp 279-286.
12. Muskat M., " The Flow of Homogeneous Fluids through Porous Media", J.W. Edwards Inc., Ann Arbor, Michigan, 1946.
13. Muthukumaran S., " Design of Weirs on Pervious Foundations", Proceedings, 43rd Symposium, Central Board of Irrigation and Power, (Annual Research Session), Dehradun, June 1973 Vol.I. Hydraulics.
14. Pavlovsky N.N., " The Theory of Ground Water Flow below Hydro technical Structures", Petersberg, 1922.
15. Polubarinova -Kochina, " Theory of Ground Water Movement", Princeton University Press, Princeton, New Jersey,1962.

16. Punmia B.C. et al., " Uplift Pressure below Apron founded on Pervious Medium of Finite Depth with Downstream cut off under scoured conditions" Journal of Institute of Engineers (India), Vol.53, Pt CI1, pp 34-40.
17. Punmia B.C. et al., "Uplift Pressure below Horizontal Apron with Intermediate Cut off founded on Two layered Media", Irrigation and Power, Vol.32, No.1, Jan., 1975 pp 69-79.
18. Punmia B.C. et al., "Uplift Pressure below Horizontal Apron with Cutoff at Intermediate points Founded on Anisotropic Pervious Medium of Finite Depth.", Irrigation and Power, Vol<sup>29</sup>No.4 Oct., 1972 . pp391-406
19. Rao P.V., " Effects of Anisotropy and Stratification of Sub Soil on Stability of Weirs", Master of Engineering, Thesis, Presented to Indian Institute of Technology, Kharagpur, Aug., 1957.
20. Ronzhin I.S., "On Water Seepage under Concrete Hydraulic Structures and Some of its Specific Features", XIII Congress International Association of Hydraulic Research, 1969.
21. Sivareddy A., et al., " Flow Around Inclined Sheet Pile", Journal of Engg. Mechanics Division, Proceedings, American Society of Civil Engineers, Vol. 97, No. Hy 7, July,1970, pp 1101-1115.

22. Sharma H.D., et al., "Stability of Structures founded on Stratified Soil", Publications, Uttar Pradesh Irrigation Research Institute, Roorkee
23. Stefan H., et al., "Seepage study using Electrical Analog", Journal of Hydraulics Division, Proceedings, American Society of Civil Engineers, Vol.96, No.HY2, Feb., 1970, pp 411-416.
24. Terzaghi, K., " Security from Under Seepage, Masonry Dams on Earth Foundations (by E.W. Lane), Transactions, American Society of Civil Engineers, paper 1919, 1935.
25. Tomlin G.R., "Seepage Analysis through Zoned Anisotropic Soil by Computer", Geotechnique, Vol.XVI, No.4, 1966, pp 220-230.
26. Zienkiewicz O.C., " Solution of Anisotropic Seepage by Finite Elements", Journal of Engg. Mechanics Division Proceedings, American Society of Civil Engineers, Vol. 92, No.EM 1, Feb, 1966, pp.111-120.